

**Climatology of warm season heat waves in Saudi Arabia:
A time-sensitive approach**

by

Ali Saeed Arifi Alghamdi

B.A., King Saud University, 2008

M.A., Towson University, 2014

AN ABSTRACT OF A DISSERTATION

submitted in partial fulfillment of the requirements for the degree

DOCTOR OF PHILOSOPHY

Department of Geography
College of Arts and Sciences

KANSAS STATE UNIVERSITY
Manhattan, Kansas

2018

Abstract

The climate of the Middle East is warming and extreme hot temperature events are becoming more common, as observed by the significant upward trends in mean and extreme temperatures during the last few decades. Climate modeling studies suggest that the frequency, intensity, and duration of extreme temperature events are expected to increase as the global and local climate continues to warm. Existing literature about heat waves (HWs) in Saudi Arabia provides information about HW duration using a single index, without considering the observed effects of climate change and the subtropical arid climate. With that in mind, this dissertation provides a series of three stand-alone papers evaluating temporal, geographic, and atmospheric aspects of the character of warm season (May-September) HWs in Saudi Arabia for 1985 to 2014.

Chapter 2 examines the temporal behavior(s) of the frequency, duration, and intensity of HWs under the observed recent climate change. Several issues are addressed including the identification of some improved methodological practices for HW indices. A time-sensitive approach to define and detect HWs is proposed and assessed. HW events and their duration are considered as count data; thus, different Poisson models were used for trend detection. Chapter 3 addresses the spatio-temporal patterns of the frequency and intensity of hot days and nights, and HWs. The chapter reemphasizes the importance of considering the on-goings effects of climate warming and applies a novel time-series clustering approach to recognize hot temperature event behavior through time and space. Chapter 4 explores the atmospheric circulation conditions that are associated with warm season HW event occurrence and how different HWs aspects are related to different circulation types. Further, possible teleconnections between HWs and sea surface temperature (SST) anomalies of nearby large bodies are examined.

Results from Chapters 2 and 3 detected systematic upward trends in maximum and minimum temperatures at most of the 25 stations, suggesting an on-going change in the climatology of the upper-tail of the frequency distribution. The analysis demonstrated the value of using a time-sensitive approach in studying extreme thermal events. Different patterns were observed over time and space not only across stations but also among extreme temperature events (i.e., hot days and nights, and HWs). The overall results suggest that not only local and regional factors, such as elevation, latitude, land cover, atmospheric humidity, and distance from a large body of water, but also large-scale factors such as atmospheric circulation patterns are responsible for the observed temporal and spatial patterns. Chapter 4 confirmed that as the Indian Summer Monsoon Trough and the Arabian heat low were key atmospheric features related to HW days. SST anomalies seemed to be a more important factor for HWs intensity. Extreme thermal events in Saudi Arabia tended to occur during regional warming due to atmospheric circulation conditions and SSTs teleconnections. This study documents the value of a time-sensitive approach and should initiate further research as some of temporal and spatial variabilities were not fully explained.

**Climatology of warm season heat waves in Saudi Arabia:
A time-sensitive approach**

by

Ali Saeed Arifi Alghamdi

B.A., King Saud University, 2008

M.A., Towson University, 2014

A DISSERTATION

submitted in partial fulfillment of the requirements for the degree

DOCTOR OF PHILOSOPHY

Department of Geography
College of Arts and Sciences

KANSAS STATE UNIVERSITY
Manhattan, Kansas

2018

Approved by:

Major Professor
John A. Harrington, Jr.

Copyright

© Ali Saeed Arifi Alghamdi 2018.

Abstract

The climate of the Middle East is warming and extreme hot temperature events are becoming more common, as observed by the significant upward trends in mean and extreme temperatures during the last few decades. Climate modeling studies suggest that the frequency, intensity, and duration of extreme temperature events are expected to increase as the global and local climate continues to warm. Existing literature about heat waves (HWs) in Saudi Arabia provides information about HW duration using a single index, without considering the observed effects of climate change and the subtropical arid climate. With that in mind, this dissertation provides a series of three stand-alone papers evaluating temporal, geographic, and atmospheric aspects of the character of warm season (May-September) HWs in Saudi Arabia for 1985 to 2014.

Chapter 2 examines the temporal behavior(s) of the frequency, duration, and intensity of HWs under the observed recent climate change. Several issues are addressed including the identification of some improved methodological practices for HW indices. A time-sensitive approach to define and detect HWs is proposed and assessed. HW events and their duration are considered as count data; thus, different Poisson models were used for trend detection. Chapter 3 addresses the spatio-temporal patterns of the frequency and intensity of hot days and nights, and HWs. The chapter reemphasizes the importance of considering the on-goings effects of climate warming and applies a novel time-series clustering approach to recognize hot temperature event behaviors through time and space. Chapter 4 explores the atmospheric circulation conditions that are associated with warm season HW event occurrence and how different HWs aspects are related to different circulation types. Further, possible teleconnections between HWs and sea surface temperature (SST) anomalies of nearby large bodies are examined.

Results from Chapters 2 and 3 detected systematic upward trends in maximum and minimum temperatures at most of the 25 stations, suggesting an on-going change in the climatology of the upper-tail of the frequency distribution. The analysis demonstrated the value of using a time-sensitive approach in studying extreme thermal events. Different patterns were observed over time and space not only across stations but also among extreme temperature events (i.e., hot days and nights, and HWs). The overall results suggest that not only local and regional factors, such as elevation, latitude, land cover, atmospheric humidity, and distance from a large body of water, but also large-scale factors such as atmospheric circulation patterns are responsible for the observed temporal and spatial patterns. Chapter 4 confirmed that as the Indian Summer Monsoon Trough and the Arabian heat low were key atmospheric features related to HW days. SST anomalies seemed to be a more important factor for HWs intensity. Extreme thermal events in Saudi Arabia tended to occur during regional warming due to atmospheric circulation conditions and SSTs teleconnections. This study documents the value of a time-sensitive approach and should initiate further research as some of temporal and spatial variabilities were not fully explained.

Table of Contents

List of Figures	xi
List of Tables	xv
Dedication	xvi
Chapter 1 - Introduction.....	1
1.1 Introduction	1
1.2 The Dissertation Outline	7
1.3 Study Area.....	8
Chapter 2 - Time-sensitive analysis of a warming climate on heat waves in Saudi Arabia:	
Temporal patterns and trends.....	10
Abstract.....	10
2.1 Introduction	11
2.2 Research Design and Methods	14
2.2.1 Study area and data	14
2.2.2 Quality control	16
2.2.3 Heat wave definition.....	18
2.2.3.1 Implications for Subtropical Arid Climates under warming effects.....	20
2.2.4 Heat Wave Intensity and Duration.....	24
2.2.5 Heat Wave Trend Analysis.....	26
2.3 Results and Discussions	28
2.3.1 Evaluation	28
2.3.1.1 Thirty-year trends in the upper-limits of Tmax and Tmin.....	28
2.3.1.2 Evaluation of the heat wave definition	31
2.3.1.3 Evaluation of duration metrics.....	33
2.3.2 Heat wave behavior.....	35
2.3.2.1 Frequency.....	35
2.3.2.2 Duration	37
2.3.2.3 Intensity.....	38
2.3.3 Trend analyses	40
2.4 Summary and Conclusions.....	42

Chapter 3 - Trends and spatial pattern recognition of warm season hot temperatures in Saudi Arabia	45
Abstract.....	45
3.1 Introduction	46
3.2 Research Design and Methods	50
3.2.1 Study area and data	50
3.2.2 WSHTIs for subtropical arid climates under changing climate effects	52
3.2.3 Temporal trends analysis	55
3.2.4 Spatial and temporal pattern recognition	57
3.3 Results and Discussions	59
3.3.1 Evaluation of trends in the upper-limits of Tmax and Tmin	59
3.3.2 Temporal trends in WSHTIs.....	62
3.3.3 Spatial pattern recognition of WSHTIs.....	65
3.4 Summary and Conclusions.....	73
Chapter 4 – A preliminary assessment on synoptic climatology and sea surface temperatures teleconnections for warm season heat waves in Saudi Arabia	76
Abstract.....	76
4.1 Introduction	77
4.2 Research Design and Methods	79
4.2.1 Study area and data	79
4.2.2 Heat Wave definition	81
4.2.3 Synoptic analysis	82
4.2.4 Circulation types, Heat Wave days frequency, intensity, and SSTs.....	84
4.3 Results	85
4.3.1 Circulation conditions.....	85
4.3.1.1 General synoptic conditions.....	85
4.3.1.2 Clustering.....	87
4.3.2 Heat Wave days frequency, intensity and circulation types	90
4.3.3 Analysis of SST Teleconnections	92
4.4 Discussion	94
4.5 Summary and Conclusions.....	97

Chapter 5 - Summary and Conclusions	100
References.....	104
Appendix A – Examples of different measurements and indices for extreme temperatures and heat waves.....	115
Appendix B – Statistical characteristics of maximum and minimum temperatures.....	118

List of Figures

Figure 1.1. Changes in the probability distributions with changes in mean and variance of Tmin air temperature at one of the Saudi Arabian stations (Gizan (25)). Simulations were prepared following Robeson (2002b). 4

Figure 1.2. Maps showing the topography (A) along with major cities, land cover (B) along with major geographical features, and administrative regions along with population (C) for the study area. Source: adapted from King Abdulaziz City for Science and Technology (A), modified after Broxton et al. (2014) (B), and Saudi General Authority for Statistics (C). 9

Figure 2.1. A map showing the study area and weather stations along with their names and IDs. Source: adapted from King Abdulaziz City for Science and Technology (KACST) and the GAMEP. * station was not included in this study. 15

Figure 2.2. Distributions of the probability density function (PDF) of daily temperatures at three stations for three decades using warm season months (May through September) Tmax, and Tmin along with their 85th and 90th percentiles (right). Bottom-right plot shows changes in the probability distributions and the 90th percentile in response to changes in mean and variance of Tmin at Gizan (25) station. Simulations were prepared following Robeson (2002b). Stations were selected as they represent different temporal patterns and climate types. 22

Figure 2.3. A hypothetical comparison between annual events count (bottom) and Annual count of days/WSDI (upper). 25

Figure 2.4. Heatmaps of decadal-based temporal trends in annual Tmin 85th (left) and Tmax 90th (right) percentile values ($^{\circ}\text{C}/\text{yr}^{-1}$) at monthly and warm season (x-axis) time scale for each station (y-axis). ***, **, *, and $+ \alpha = 0.001, 0.01, 0.05, 0.1$ level of significances respectively. Trends were computed by Kendall-tau and Sen’s slope estimator. For stations names and locations refer to Figure 2.1. 29

Figure 2.5. Monthly and warm season 90th percentile of Tmax thresholds at Al-Jouf (11) station determined on an annual basis. ***, **, and * $\alpha = 0.01, 0.05, 0.10$ level of significances respectively. Trends computed by Kendall-tau and Sen’s slope estimator..... 32

Figure 2.6. Annual count of heat waves per year at Al-Jouf (11) station using different time-
windows to estimate percentile, A and B constant (30-years) and C and D decade-sensitive
thresholds estimated on monthly (A and C) and warm season (B and D) bases. 33

Figure 2.7. Duration of the longest event or HWLD (green solid line), number of heat wave
events (blue long-dash line), and the annual count of days or WSDI₂ (red dashed line) at
four stations, representing different temporal patterns, elevation, and climate types..... 34

Figure 2.8. Classification of stations by the dominant month(s) of heat waves (A) and
proportional symbols for annual frequency (B). Land cover data was obtained and modified
after Broxton et al. (2014). Refer to Figure 2.1 for the elevation legend for (A) and for
stations names. 36

Figure 2.9. Number (upper) and percentage (bottom) of HWs based on three duration categories:
2-4-days, 5-7-days, and ≥8-days. For stations names refer to Figure 2.1 38

Figure 2.10. Two-dimensional (top) and three-dimensional (bottom) scatterplots of day of peak
(highest Tmean), duration (in day) and intensity (standardized Tmean with zero mean and
unit standard deviation at station level) at all the 25 stations. Coastal, Highland, and other
categories include stations (IDs): 21:25, 1:6, and 7:19, respectively. Refer to Figure 2.1 for
stations names and locations. 39

Figure 2.11. Temporal annual trends in frequency (left-top), intensity (right-top), and
duration/HWLD (bottom) aspects. ***, **, *, and + $\alpha = 0.001, 0.01, 0.05, 0.10$ level of
significances respectively. For stations names refer to Figure 2.1. 41

Figure 3.1. A map showing the study area and weather stations along with their names and IDs.
Source: adapted from King Abdulaziz City for Science and Technology (KACST) and the
GAMEP. * station was not included in this study. 51

Figure 3.2. Distributions of the probability density function of daily temperatures at Gizan (25)
for three decades using summer months (June-August) Tmean, Tmax, and Tmin (upper) and
for 30-years summer season months Tmean, Tmax and Tmin (bottom). Gizan was selected
as it exemplifies different temporal and shape changes found for many of the stations. 54

Figure 3.3. Heatmaps of decadal-based temporal trends in Tmin (left) and Tmax (right) 90th
percentile values ($^{\circ}\text{C}/\text{yr}^{-1}$) at monthly and warm season (x-axis) time scale for each station
(y-axis). ***, **, *, and + $\alpha = 0.001, 0.01, 0.05, 0.1$ level of significances respectively.

Trends were computed by Kendall-tau and Sen’s slope estimator. For stations names and locations refer to Figure 3.1.	60
Figure 3.4. Validity indices for the HD indicator (left) and cluster dendrogram (right) along with stations IDs.	66
Figure 3.5. Maps showing the clustering of stations of WSHTIs. For stations names refer to Figure 3.1.	67
Figure 3.6. Clustering stations using Distance of Mean Standardized Indicators (DMSI), A and Mean Indicators’ Distances (MID), B. Land cover data was obtained and modified after Broxton et al. (2014). For stations names refer to Figure 3.1.	70
Figure 3.7. Boxplots of Pearson correlations between each cluster’s stations and cluster average for each WSHTI and each distance method. DMSI: Distance of Mean of Standardized Indicators, MID: Mean Indicators' Distances.	71
Figure 4.1. A map showing the study domain (upper-right) and the topography of Saudi Arabia along with the used weather stations. Source: adapted from King Abdulaziz City for Science and Technology and GAMEP.	80
Figure 4.2. Annual (A) and monthly (B) heat wave days frequency using different minimum criterion.	83
Figure 4.3. Composite maps for MSLP- hPa (A shaded), geopotential height at 500- hPa (A contour), geopotential height at 850- hPa (C shaded) and T-850 (C contour) during warm season. Heat wave days (746 days) composite maps for MSLP- hPa (B shaded), geopotential height at 500- hPa (B contour), geopotential height at 850- hPa (D shaded), T-850 (D contour) and their anomalies (E for MSLP, shaded, and 500- hPa, contour, and F for 850- hPa, shaded, and T-850, contour). Anomalies are departures from 1985–2014 climatology.	86
Figure 4.4. Weather Type 1 composites for MSLP (A shaded and contours for anomaly); geopotential height at 500-hPa (B shaded and contours for anomaly); geopotential height at 850- hPa (C shaded, contour for anomaly); and T-850 (D shaded and contour for anomaly). Anomalies are departures from 1985–2014 climatology.	87
Figure 4.5. Monthly frequency of detected weather types during warm season months. Percentages inside bars are per weather type, that is 9.4%, 70.3%, and 20.3% of type 3 occurred in June, July, and August.	88

Figure 4.6. As in Figure 4.4 but for weather Type 2.	89
Figure 4.7. As in Figure 4.4 but for weather Type 3.	90
Figure 4.8. Correlation coefficients between anomalies of heat wave days frequency (A-C) and intensity (D-F) and anomalies of circulation Type 1 (A and D), 2 (B and E), and 3 (C and F). Refer to Figure 4.1 for station names. ** and * are statistically significant at the 95% and 90% levels, respectively.	91
Figure 4.9. SSTs anomalies composites of all heat wave days (upper-left), and circulation Types: 1 (upper-right), 2 (bottom-left), and 3 (bottom-right). Anomalies are departures from 1985–2014 climatology.	92
Figure 4.10. Specific humidity anomaly composites of circulation Type 1 (A), 2 (B), and 3 (C) and wind speed anomaly and mean direction composites of circulation Type 1 (D), 2 (E), and 3 (F). Anomalies are departures from 1985–2014 climatology.	95
Figure B.1. Multi-decadal variation in Tmax skewness at warm-season-monthly time scale. ...	118
Figure B.2. Multi-decadal variation in Tmax variance at warm-season-monthly time scale.	119
Figure B.3. Multi-decadal variation in Tmin skewness at warm-season-monthly time scale.	120
Figure B.4. Multi-decadal variation in Tmin variance at warm-season-monthly time scale.	121

List of Tables

Table 2.1. Weather stations with latitude, longitude, elevation, average maximum (Tmax) and minimum (Tmin) temperature of the studied warm season (May through September) for 1985-2014. Elevation data, provided by KACST, was used to number stations form high to low elevation.	17
Table 2.2. Definition of HW indices developed and used in this study.....	26
Table 2.3. Used framework for trend analysis of frequency and duration of heat waves. Modified after Yang et al. (2015).	27
Table 3.1. The definition of warm season hot temperature indicators (WSHTIs). Percentile values were estimated using a decadal time-window on a month-by-month basis. Tmean, Tmax, and Tmin are mean, maximum, and minimum temperatures respectively.....	53
Table 3.2. Used framework for trend analysis of WD, WN, and HWE indicators. Modified after Yang et al. (2015).	56
Table 3.3. Decadal-based temporal trends in annual warm season hot temperature indicators (WSHTIs). ***, **, *, and + $\alpha = 0.001, 0.01, 0.05, 0.1$ level of significance respectively..	63
Table 3.4. Heatmaps of descriptive statistics based on annual totals for the 30-year period 1985-2014.....	72
Table 3.5. Summary of WSHTs main characteristics of clustering. -, *, and +: low, moderate, and high year-to-year variability, respectively, SID: station ID.....	73
Table 4.1. Correlation coefficients between anomalies of local SSTs and different heat wave days characteristics for three detected weather types. ** and * are statistically significant at the 95% and 90% levels, respectively.....	93
Table A.1. List of commonly used extreme temperature indices of ETCCDI. Modified after Athar at al. (2013).	115
Table A.2. Definitions of heat wave indices (HI). ^b Apparent temperature is a function of air temperature, humidity, wind speed, and solar radiation. ^c The HI is a function of air temperature and humidity, parameterized to take account of other environmental factors. Modified after Kent et al. (2014).	116
Table A.3. Definitions of heat wave indices (HI). Modified after Smith et al. (2013).....	117

Dedication

To whom left while waiting for this moment, I promise to continue dad.

Chapter 1 - Introduction

1.1 Introduction

Warming of the global mean temperature (T_{mean}) of approximately $0.6\text{ }^{\circ}\text{C}$ over the last century is accompanied by changes in daily minimum (T_{min}) and maximum (T_{max}) temperatures (Easterling et al., 2000). According to the IPCC, the warming value is $0.85\text{ }^{\circ}\text{C}$ for the period 1880 to 2012 (IPCC Synthesis Report, 2014). One aspect of this change is that a large portion of the Earth's terrestrial area has experienced decreases in the number of cool nights and days and cold spells, and increases in the number of hot nights and days and heat waves/warm spells (Alexander et al., 2006). Heat waves (HWs), a period of consecutive days of hot temperature, are expected to get considerably worse later in the 21st century (Meehl and Tebaldi, 2004). HWs have significant impacts on people's health, the environment, and economic conditions worldwide (e.g., 1995 Chicago, 2003 and 2006 Europe, and 2010 Russia HWs) and are considered the top-ranked severe weather killer (Kousky, 2014). Recently, Guirguis et al. (2014) reported that during a HW event the hospital admissions in California increased by 7%, with a significant impact on cardiovascular disease, respiratory diseases, dehydration, acute renal failure, heat illness, and mental health. The July 1995 Chicago HW resulted in an estimated 718 deaths in 10 states (Changnon et al., 1996) whereas the August 2003 European HW (considered as one of the worst HWs in the last five decades) caused about 30,000 deaths across several European counties (COPA-COGECA, 2003).

In terms of social and economic effects, many types of livestock died during the August 2003 European HW while crops failed throughout Europe, costing European farmers about 13.1 billion euros (Met Office, 2013). This HW led to various transportation effects; for example, some railway tracks buckled and road surfaces melted (Met Office, 2013). Two nuclear power

plants closed down in Germany as well (Met Office, 2013). Recently, Eskey et al. (2015) studied the impact of HWs and extreme temperature on some tree species and found that several tree functions are significantly affected during HWs. For example, photosynthesis declines, leaf abscission increases, and the growth rate of remaining leaves is negatively affected; whereas photo-oxidative stress and stomatal conductance increase. Unfortunately, the health, environmental, and economic impacts of extreme weather events including HWs are still topics about which not much is known in Saudi Arabia.

A warming of 1.7°C over the Sahara and the Arabian Peninsula is predicted by the year 2050 (IPCC, 2001), where the continental interior is likely to warm at a higher rate than the coastal regions (Lioubimtseva, 2004). Nasrallah et al. (2004) reported that during the last decade of the 20th century HW events over Kuwait had become longer and more severe. In the case of Saudi Arabia, multiple recent studies have been dedicated to gaining a better understanding of mean and extreme temperature patterns and trends (e.g., Rehman, 2010; AlSarmi and Washington, 2011, 2013; Almazroui et al., 2012a, 2012b; Rehman and Al-Hadhrami, 2012, Almazroui et al., 2014; Athar, 2014). Previous studies have agreed that T_{mean} , and both T_{max} and T_{min} in their study areas have increased during the last few decades; consequently, the frequency of cool nights and days has decreased and the frequency of warm nights and days has increased. Almazroui et al (2012a), for example, reported a warming of 0.60°C decade⁻¹ in the T_{mean} over Saudi Arabia for 1978–2009, which was lower than that of the T_{max} (0.71°C decade⁻¹) and greater than T_{min} (0.48°C decade⁻¹).

Studies of the climatology of HWs in Saudi Arabia tend to not provide enough detail regarding data and methods, the HW definition used, and several questions about characteristics of HWs are not addressed. The recent studies of HW events in Saudi Arabia focus primarily on

duration using a single meteorological factor in their analyses, daily Tmax (e.g., Almazroui et al., 2014; Athar, 2014; Donat et al., 2014; Raggad, 2017a). This dissertation focusses on four main points including (1) developing a HW definition taking into account the on-going climatic change and the subtropical arid climate; (2) local spatial and temporal aspects of HWs; and (3) atmospheric circulation patterns that induce HWs, and (4) links to sea surface temperature anomalies.

Analysis of HWs in the prior research was based only on one HW criterion: the annual number for days of events that last at least 6 consecutive days wherein the Tmax exceeds the 90th percentile and this percentile is based on the period of record. It can be argued that the duration threshold of this HW definition (6 days) is too long and fails to include the shorter, and potentially high impact HWs. Based on the existing literature, a two- or three-day threshold is usually used as the minimum duration of a HW (e.g., Karl and Knight, 1997; Robinson, 2001; García et al., 2010; Smith et al., 2013; Perkins and Alexander, 2013). By using a shorter threshold (e.g., two- or three-days), longer HWs (e.g., six- or seven-days) would not be excluded (Russo et al., 2014). When both daytime and nighttime temperatures are used in defining HWs, Robinson (2001) suggested that 2-day threshold is an appropriate duration criterion as this requirement would not affect detecting extremely rare events. Heat-related health impacts of 2-day HWs on humans have been shown to be substantial (Perkins, 2015).

One of the main effects of climatic change is a shift or change in the mean climate. In addition, the shift in central tendency can be accompanied by changes in the characteristics of extreme weather events including their probability and intensity. As the climate warms the temperature frequency distribution shifts positively and thus new rare warm conditions emerge (Figure 1.1). Accordingly, use of a constant threshold, not varying corresponding to the

warming, would not correspond to the warming climate and would be more likely to be reached more often in the later years in the time series and ultimately the frequency of events will increase over time. Most of the previous extreme temperature studies have detected positive shifts in the frequency distribution of both the mean and high temperature values and year-to-year variability (e.g., Almazroui et al., 2013; Hansen and Sato, 2016), and yet such an aspect of change has not been considered in the operational definition of a HW. In fact, Raggad (2017a) showed that temporal patterns of extreme temperatures are better described by non-stationary models for most of the country. Important questions that have not been addressed include whether the warming climate has resulted in increases in average intensity and the duration of the HWs. Further, changes in the frequency of HWs are not fully explained by changes in mean climate, as the temporal patterns of extreme temperature events frequency are more sensitive to variance and other shape parameters (e.g., skewness) (Katz and Brown, 1992; Robeson, 2002b).

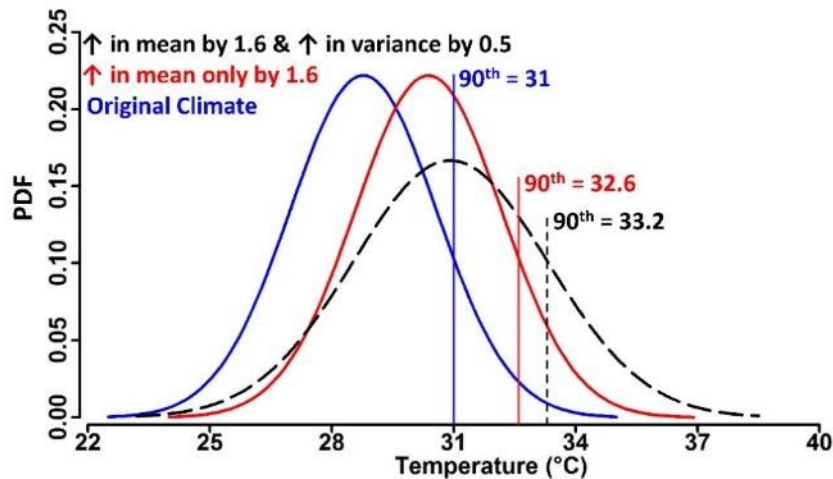


Figure 1.1. Changes in the probability distributions with changes in mean and variance of Tmin air temperature at one of the Saudi Arabian stations (Gizan (25)). Simulations were prepared following Robeson (2002b).

Although previous studies provided insights into the general changes in extreme temperatures, little has been done to address possible causes/factors. Further efforts are necessary to understand the changes in extreme climate and to overcome several open challenges. In fact,

the majority of previous studies are more focused on the temporal changes and little attention has been given to the spatial aspect. Understanding the spatial patterns and changes would help to recognize the geography of change and also it will help to speculate on some possible local factors that may have influence on changes in extreme temperature such as topography, water bodies, and vegetation cover. This also would help provide insights into how spatial factors could relate or influence the atmospheric circulation at different levels (e.g., micro-, local-, and meso-scales) that induce extreme temperatures. Topography and distance from a coastline can impact HW events by influencing extreme temperature event patterns at local and regional levels (Kenawy et al., 2012). Thus, detailed studies are needed that investigate the spatial changes in extreme temperatures and whether or not some spatial factors help explain important aspects of HWs. Frequency of hot days/nights are changing and intensity and duration of the spatial patterns should be linked to variations in atmospheric circulation.

A few studies have given attention to atmospheric circulation conditions (i.e., synoptic patterns) leading to some extreme weather phenomena, such as precipitation events (i.e., heavy rain, cyclones, and winter storms) in the Middle East (e.g., Lee et al., 1988; Dayan et al., 2001; Tsvieli et al., 2005). A very limited number of detailed studies has been conducted concerning HWs (e.g., Nasrallah et al., 2004), especially in Saudi Arabia. Synoptic studies examine weather components to identify the meteorological conditions for a given event; these conditions are then linked to atmospheric circulation at different scales (Harman and Winkler, 1991). Synoptic studies tend to explore how variations in the properties and behavior of the atmospheric circulation induce particular weather conditions (e.g., HWs, sand storms, or hurricanes) over and around a given area in order to better understand and predict the weather events at the earth's surface. The benefit of synoptic studies is not only found in diagnosing climate and weather and

how an individual synoptic system works, but also in detecting changes in frequency, forecasting, and in empirical and numerical modeling (Yarnal et al., 2001).

In addition to synoptic conditions, studies have shown several factors contribute to the formation, intensity and persistence of HWs including soil moisture (e.g., Ferranti and Viterbo, 2006; Fischer et al., 2007b), drought (e.g., Vautard et al., 2006) and anomalies in sea surface temperature (SST) (e.g., Feudale and Shukla, 2007; Carril et al., 2008; Feudale and Shukla, 2011). During the European 2003 HW, SSTs over the Mediterranean and the Black Sea were the warmest on record (Feudale and Shukla, 2007) and it was suggested that they might have intensified the HW due to atmosphere-ocean interaction (Feudale and Shukla, 2011). Feudale and Shukla (2007) modeled the contribution of SSTs to the European 2003 HW and showed that the warm SSTs contributed to increased heating of the atmosphere over the Mediterranean basin and the surrounding regions. This low level heating helped to form an upper level anticyclone over the region. The influence of SSTs on HW events in the Arabian Peninsula has not been addressed.

Therefore and building on the previous research, the main goal this dissertation seeks to accomplish is to gain a better understanding of the climatology of warm season (May-September) HWs in Saudi Arabia, considering the on-goings effects of climate warming within a subtropical arid climate. More specifically, a statistical climatology of recent HWs for Saudi Arabia is presented in Chapter 2. The analysis uses a definition of a HW designed with the regional subtropical climate in mind. This was done by lowering the nighttime temperature (Tmin) threshold (i.e., using the 85th percentile). Given the ongoing upward trend of air temperatures for the region, the analysis uses and demonstrates the value of thresholds using a time-sensitive approach in studying extreme thermal events.

For chapter 3, objectives were to (1) detect temporal changes in the frequency and intensity in six warm season hot temperature indicators (WSHTIs) using the time-sensitive approach to account for the ongoing regional warming trend; and (2) recognize the spatiotemporal character of warm season hot thermal events with an emphasis on event behavior through time and space using a time-series clustering approach. In chapter 4, the objectives were to (1) identify the general synoptic situations that are associated with the occurrence of warm season HW days in Saudi Arabia; examine how different aspects of HWs (e.g., frequency and intensity) are related to different circulation types; and (3) assess possible links/associations between HW events and SST anomalies of nearby large bodies of water (i.e., Mediterranean Sea, Black Sea, Caspian Sea, Arabian Gulf, Arabian Sea, and Red Sea).

1.2 The Dissertation Outline

This dissertation was prepared as a series of three stand-alone but interrelated research efforts. The first paper, which has been published in the *International Journal of Climatology*, is presented in Chapter 2 and establishes the development of a time-sensitive HW definition and its suitability. The second and third papers build on the first paper and explore in greater detail some important spatial, temporal, and atmospheric aspects of HWs in Saudi Arabia. The second paper, which has been submitted to *Theoretical and Applied Climatology*, explores spatiotemporal aspects of warm season hot thermal events. Chapter 4, the third research effort which has been submitted to *Atmospheric Research*, takes on a further step by analyzing the atmospheric circulation conditions and SST anomalies during selected HW days. This component of the research has an applied aspect addressing which of these two factors might help in event forecasting. Chapter 5 brings all these papers together to summarize their main findings, implications and conclusions.

1.3 Study Area

Saudi Arabia is located in southwestern Asia and occupies 80% of the Arabian Peninsula with a total area of around 2,000,000 km² (Almazroui et al., 2013; Saudi General Authority for Statistics, 2018). Saudi Arabia lies between the Red Sea (west) and Arabian Gulf (east) and is bordered by Kuwait, Iraq and Jordan (north), Bahrain, Qatar and United Arab Emirates (east), and Oman and Yemen (south) (Figure 1.2). According to 2010 census, the country has a population of 27,136,977 (Saudi General Authority for Statistics, 2010). The Kingdom has 13 administrative/province regions (Figure 1.2 C), where Riyadh, Makkah, and Eastern are the top 3 provinces for population (Figure 1.2 C). Riyadh is the location of the capital (Riyadh City), Makah is where the holy mosque and the Hajj (pilgrimage) takes place, and oil and gas are produced and exported from the Eastern province.

The topography for much of Saudi Arabia is characterized by low-elevations. Elevation gradually increases toward the more mountainous southwest region (Figure 1.2 A). The highest peak, Jabal Al-Sawda (Al-Sawda Mountain), approaches 3,000 m in elevation and is located within the Sarawat Mountains. Generally, most of the landscape is barren land except for portions of the southwestern mountains. About 33% of the landscape cover is sand desert, where the Al-Rub Al-Khali Desert (Empty Quarter), the Al-Nefud Desert, and the Ad-Dahna Desert constitute 85% of the sand desert areas (Saudi Geological Survey, 2012). Most of the vegetation cover is located within southwestern mountains (Figure 1.2 B). *Juniperus phoenicia*, *Juniperus excelsa*, *Olea Africana*, and *Acacia - Commiphora* scrub are the common vegetation types within southwestern mountains (Saudi General Authority for Meteorology and Environmental Protection, 2016).

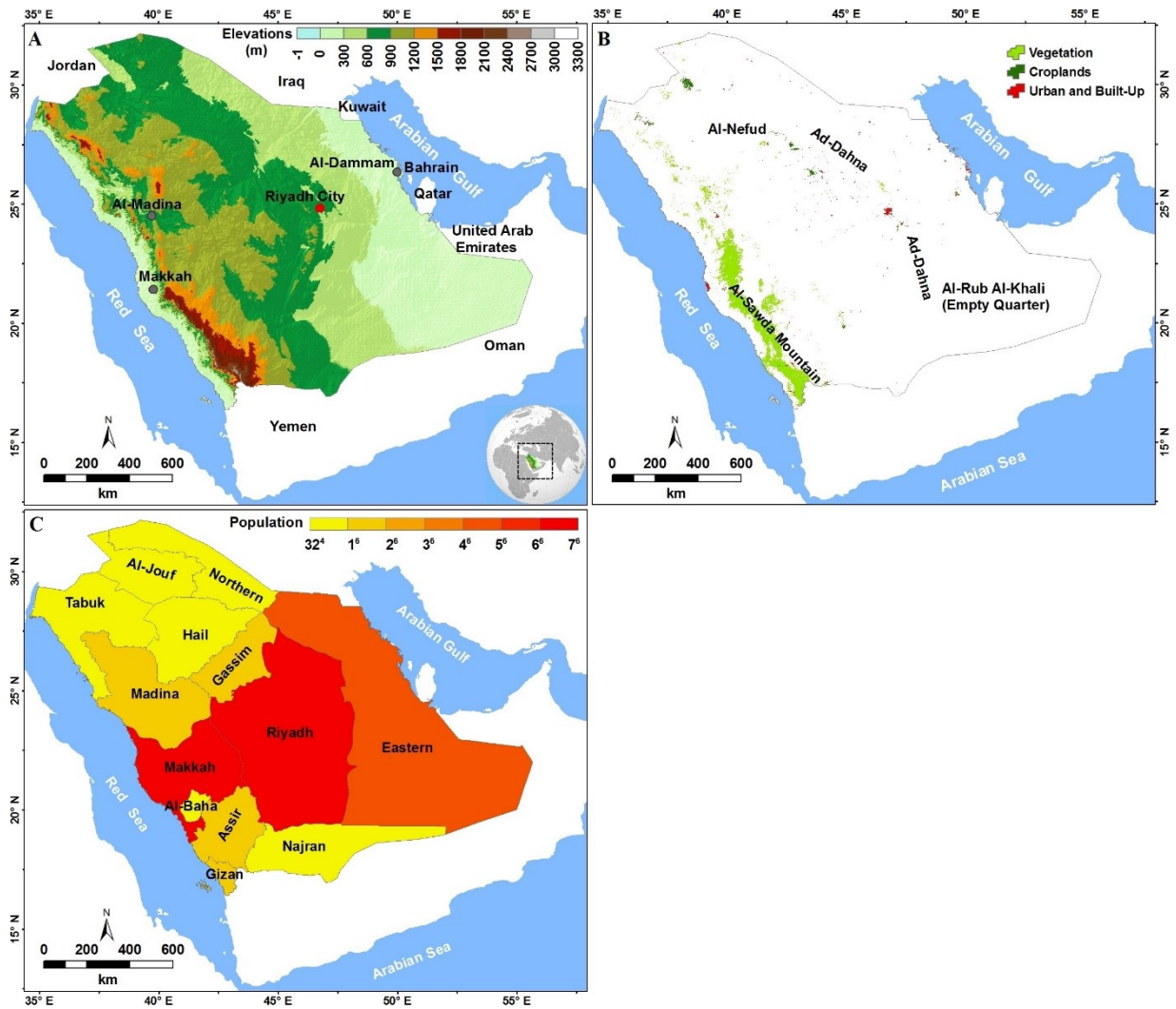


Figure 1.2. Maps showing the topography (A) along with major cities, land cover (B) along with major geographical features, and administrative regions along with population (C) for the study area. Source: adapted from King Abdulaziz City for Science and Technology (A), modified after Broxton et al. (2014) (B), and Saudi General Authority for Statistics (C).

Chapter 2 - Time-sensitive analysis of a warming climate on heat waves in Saudi Arabia: Temporal patterns and trends

Abstract

Most of the literature about HWs in Saudi Arabia provides information about the duration aspect using a single index, with no detailed information about frequency and intensity aspects. To help establish a baseline for understanding past and future change, this study explored the temporal behavior(s) of the frequency, duration, and intensity of HWs in Saudi Arabia under the observed recent climatic change. Several issues are addressed including some methodological concerns associated with the commonly used HW index, data quality control and statistical analysis. A new definition and method to detect HWs and their changes is proposed, considering the on-goings effects of climate warming and the subtropical arid climate.

A HW event is defined as a period of two or more consecutive days (i.e., at least 48 hours) with a daily maximum and minimum temperature exceeding the 90th and 85th percentiles of the maximum and minimum, respectively. Threshold percentiles were calculated monthly and adjusted for each decade of analysis. For temporal trend analyses, we consider HW events and their duration as count data using different Poisson models for analysis. HW frequency, intensity, and duration across Saudi Arabia were found to behave geographically and temporally differently across the 25 stations studied. Distinct temporal and geographical patterns were observed indicating a confounding interplay of regional and local factors, such as urbanization, elevation, latitude, and distance from a large body of water.

2.1 Introduction

Under the effects of climate warming, the global pattern of the occurrence of extreme weather events such as HWs, a period of consecutive days with hot temperatures, is expected to increase significantly (Tebaldi et al., 2006), suggesting an increase in the risk of more severe and longer HW events (Kent et al., 2014). Extreme high temperatures directly affect human health (Souch and Grimmond, 2004) and energy consumption (IPCC, 2007). HWs increase energy consumption for air-conditioning, which has environmental impacts (e.g., pollution) and economic effects (e.g., increasing energy cost). During late July 2016, large parts of the Middle East were under a major HW and a Tmax of 54°C in Mitrabah, Kuwait, could be the newest Asian highest temperature (WMO, 2017). During the summer of 2010, eight power plants throughout Saudi Arabia were forced to shut down due to the extreme heat (Alghamdi and Moore, 2014), with Tmax reaching 52°C in Jeddah City (Almazroui et al., 2014). This was an extraordinary temperature event as it was 7°C higher than the 45°C summer Tmax 99th percentile of 1985-2014. Loss of power left people in several cities exposed and vulnerable (Alghamdi and Moore, 2014).

Within the Middle East, changes in extreme temperature have been considered at different spatial scales including the Arab region (e.g., Donat et al., 2014), the Arabian Peninsula (e.g., AlSarmi and Washington, 2011, 2013), Saudi Arabia (e.g., Almazroui et al., 2012a, 2012b, Almazroui et al., 2014; Athar, 2014), and even at the individual city level (e.g., Rehman, 2010; Rehman and Al-Hadhrami, 2012; Alghamdi and Moore, 2014). These studies indicate that during the last few decades the Tmean, and both the Tmax and Tmin in the region have increased. Consequently, the frequencies of cool nights and cool days have decreased and the frequencies of warm nights, warm days, and warm spells/HWs have increased.

Most of the previous extreme temperature studies have detected a positive shift in the frequency distribution of both the mean and high temperature, suggesting that HWs would not only be expected to become more frequent, but also more severe. It is clear from the previous research that HWs have exhibited their maximum frequency during the last few decades. Important questions that have not been addressed include whether this shift has resulted in increases in average intensity and the duration of the HWs. Further, changes in HW frequency are not fully explained by changes in mean climate, as the character of extreme temperature events frequency is more sensitive to variance and other shape parameters (e.g., skewness) (Katz and Brown, 1992; Robeson, 2002b). Recent studies of HW events focus primarily on the duration aspect by using a single meteorological factor in their analyses, daily Tmax (e.g., Almazroui et al., 2014; Athar, 2014; Donat et al., 2014; Raggad, 2017a).

Climatological studies of HWs in Saudi Arabia tend to not provide enough detail regarding data and methods and several questions are not addressed. Analysis of HWs in this prior research was based only on one HW criterion: the annual number of days of events that last at least 6 consecutive days wherein the Tmax exceeds the 90th percentile and this percentile is based on the period of record. It can be argued that the duration threshold of this HW definition (6 days) is too long and fails to include the shorter, and potentially high impact HWs. Based on the existing literature, a two- or three-day threshold is usually used as the minimum duration of a HW (e.g., Karl and Knight, 1997; Robinson, 2001; García et al., 2010; Smith et al., 2013; Perkins and Alexander, 2013). By using a shorter threshold (e.g., two- or three-days), longer HWs (e.g., six- or seven-days) would not be excluded (Russo et al., 2014). When daytime and nighttime temperatures are used in defining HWs, Robinson (2001) suggested that 2-day threshold is appropriate as this requirement would not affect detecting extremely rare events.

Heat-related health impacts of 2-day HWs on humans have been shown to be substantial (Perkins, 2015).

Use of the 90th percentile threshold is commonly based on data for the period of record. Use of such a time window to determine the threshold would not incorporate climate changes in the occurrence of HWs if there is a trend (either positive or negative) in the thermal climate because the threshold would remain constant over the analysis period (Radinovic and Curic, 2012). This concern is critical since studies document a positive shift in the frequency distribution of air temperature for Saudi Arabia. Recently, Raggad (2017a) showed that temporal patterns of extreme temperatures are better described by non-stationary models for most of the country. Thus, under the ongoing change a constant threshold determined from the entire period-of-record would assume a stationary climate and ignore any temporal variability in the probability distributions of extreme temperatures. For instance, under a warming climate a constant threshold would identify more HWs for the more recent period and detect fewer events for the earliest period.

In these previous studies, the temporal trend analyses were based on the annual count of days of HWs and not on the number/frequency of events. Use of this duration metric is arguable and it cannot be used alone since it does not reflect the full picture of the heat hazard. As such, past research may provide a misleading assessment. In fact, the sum of days using the 6-day or longer metric only provides count information about the number of participating HW days (Perkins and Alexander, 2013) rather than frequency, intensity, or other duration aspects. Moreover, the quality of observation data for stations in Saudi Arabia has received limited attention in previous studies. Further details regarding these critical points are presented and discussed in Section 2.

A statistical climatology of recent HWs for Saudi Arabia is presented in Section 2.3. The analysis uses a definition of HWs designed with the subtropical climate of the region under consideration. This was done by lowering the T_{min} threshold to 85th percentile. Given the ongoing upward trend of air temperatures for the region, the analysis demonstrates the value of using a time-sensitive approach in studying extreme thermal events.

2.2 Research Design and Methods

2.2.1 Study area and data

Saudi Arabia (Figure 2.1) occupies a large part of the Arabian Peninsula. Except for the southwestern mountain area, Saudi Arabia has a tropical/subtropical climate that is a low-latitude warm desert (BWh) according to the Köppen climate classification. The southwestern mountains lie in an area of low-latitude semi-arid steppe (BSh). The climate of the country can be described as continental, a result derived from the geographical location of the country in the subsidence part of the Hadley Cell (Alkolibi, 1995). Sinking and warming aspects of the Hadley circulation restricts the sources of water vapor for rainfall over the Arabian Peninsula to be from Red Sea and Arabian Gulf (Almazroui et al., 2013).

Daily maximum and minimum surface air temperature data for the warm season months, were obtained from the Saudi General Authority for Meteorology and Environmental Protection (GAMEP). Spring and autumn seasons in the study area are short compared to summer season (Alkolibi, 1995). Spring occurs for approximately one month (in March or April), autumn in October and November, and winter for three months (December, January, and February) (Ali, 1994). In Kuwait, May HWs were reported to be equivalent to other summer months and they could be more severe (Nasrallah et al., 2004). Given the timing and acclimatization related to heat events, the early season and late season HWs are important in terms of health outcomes,

e.g., heat-related morbidity and mortality (Hajat et al., 2002). Thus, the data obtained for this study are for the months of May through September and this period was considered as the summer or warm season.

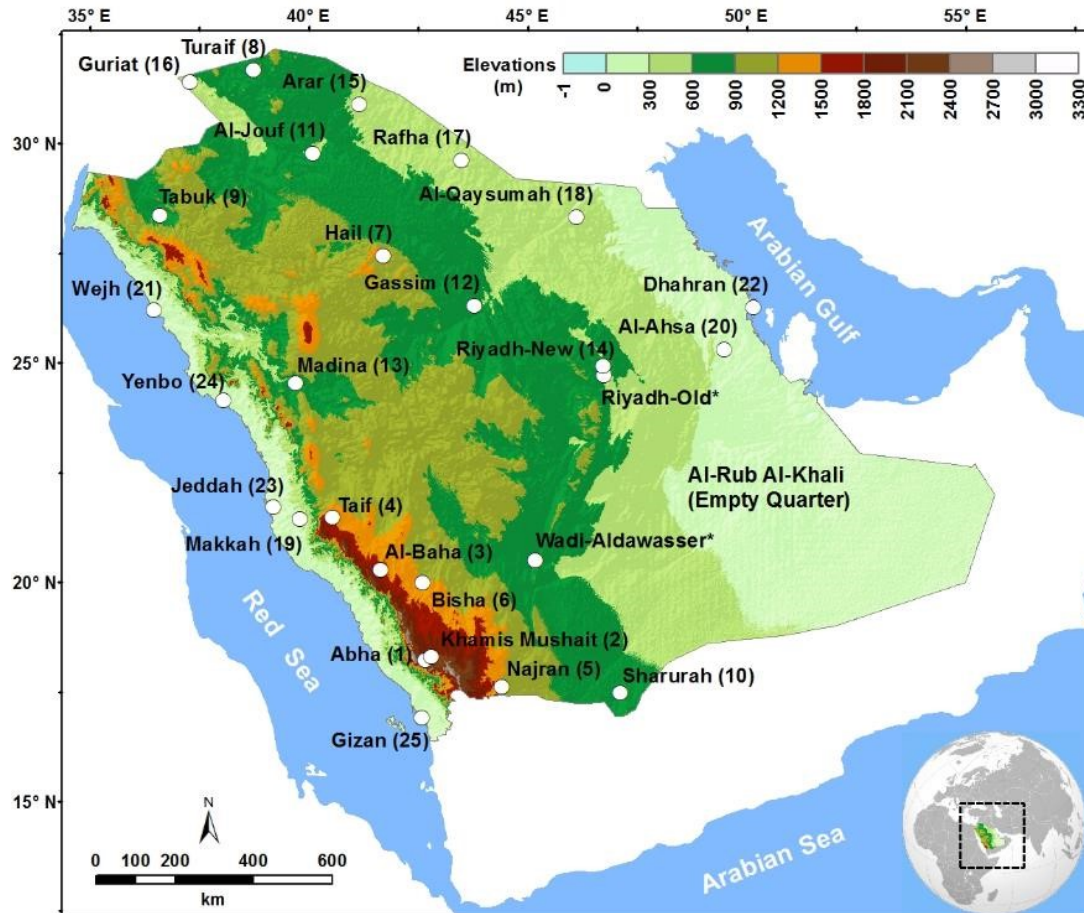


Figure 2.1. A map showing the study area and weather stations along with their names and IDs. Source: adapted from King Abdulaziz City for Science and Technology (KACST) and the GAMEP. * station was not included in this study.

Data were obtained for 25 weather stations across Saudi Arabia (Figure 2.1 and Table 2.1). The selected weather stations provide adequate spatial coverage and offer high-quality and a relatively long-term series for temporal trend analysis. Data from these stations have been found to be homogeneous (e.g., AlSarmi and Washington, 2013). The period of record for this study begins in 1985 due to issues in the station metadata including inhomogeneity, missing data, and the limited amount of data available prior to 1985. Six stations began recording observations

in 1985 (Al-Baha (6), Sharurah (10), Riyadh-New (14), Guriat (16), Makkah (19), and Al-Ahsa (20)) and examination of their locations (Figure 2.1) indicates that these stations can provide important spatial insights about within country variations. Some stations started collecting data earlier than 1985 and previous studies have used 27 stations (e.g., Almazroui et al., 2012a, 2012b), two of which were excluded in this study because the records have large gaps of missing data in 2011-2013 for Riyadh-Old and in 1985-1990 for Wadi-Aldawasser (Figure 2.1). An attempt was made to use additional stations from the Arab Gulf States to cover the spatial gaps in the north-east and south-east parts of the study area, but near-border stations were found to have both short temporal coverage and poor data quality.

2.2.2 Quality control

Prior to statistical analysis, the quality of the air temperature data was carefully assessed. Two quality control (QC) procedures, which are commonly applied, were used: (1) when a daily T_{min} is higher than the T_{max} , it is marked as unreasonable/error and replaced by NA and (2) observations that are ± 4 standard deviations (SD) greater or lesser than the T_{min} and T_{max} are identified as possible outliers and marked as errors and replaced by NA. Further, diurnal temperature ranges that are greater than ± 4 SD were assessed for possible errors. Instead of maintaining the marked errors by NA, which is a common practice in previous local studies, a further step of exploring if there was an obvious reason for these NA observations was taken. A quality controlled dataset from the U.S.A. NOAA/NCEI was used to inspect these observations. Transposition of digits and misplacement of decimal points were found to be the causes of most the errors and they were fixed accordingly. This step allowed the overall quality to be increased by 3-5%, on average, at the station level. To maximize the quality of the data, QC was applied

twice as the mean and standard deviation statistics change due to changes in the number of acceptable observations.

Table 2.1. Weather stations with latitude, longitude, elevation, average maximum (Tmax) and minimum (Tmin) temperature of the studied warm season (May through September) for 1985-2014. Elevation data, provided by KACST, was used to number stations from high to low elevation.

ID	Station name	Latitude (°N)	Longitude (°E)	Elevation (m)	Tmax (°C)	Tmin (°C)
1	Abha	18.23	42.66	2096	30.08	16.21
2	Khamis Mushait	18.29	42.8	2057	34.49	21.91
3	Al-Baha	20.29	41.64	1653	31.31	17.18
4	Taif	21.48	40.55	1455	35.05	21.93
5	Najran	17.61	44.41	1217	38.39	22.95
6	Bisha	19.99	42.61	1182	38.97	23.06
7	Hail	27.44	41.69	972	38.04	22.15
8	Turaif	31.68	38.73	846	35.20	19.23
9	Tabuk	28.37	36.6	800	37.55	21.88
10	Sharurah	17.47	47.12	740	41.91	25.22
11	Al-Jouf	29.78	40.10	668	38.27	22.97
12	Gassim	26.30	43.77	646	41.94	24.76
13	Madina	24.54	39.70	636	42.30	28.28
14	Riyadh-New	24.92	46.72	614	42.02	25.02
15	Arar	30.90	41.14	544	39.57	23.47
16	Guriat	31.40	37.28	507	37.02	18.42
17	Rafha	29.62	43.49	449	40.91	23.73
18	Al-Qaysumah	28.33	46.12	362	42.92	26.54
19	Makkah	21.43	39.79	249	42.96	28.89
20	Al-Ahsa	25.30	49.49	181	43.99	27.31
21	Wejh	26.20	36.47	21	33.46	24.25
22	Dhahran	26.26	50.16	17	37.02	18.42
23	Jeddah	21.71	39.18	16	38.25	26.07
24	Yenbo	24.14	38.06	10	39.79	25.80
25	Gizan	16.90	42.58	6	38.07	29.32

2.2.3 Heat wave definition

Due to the fact that extreme weather events, including HWs, have geographic relativism (i.e., impacts are a function of culture and social practices), scholars have developed a wide range of HW definitions and indices (e.g., basic indices, which use air temperature or apparent temperature are common; more complex indices use physiological reactions of humans or other organisms under extreme conditions) (Souch and Grimmond, 2004). In addition, HWs are of interest to diverse stakeholders, including health researchers, agricultural producers, energy providers, climatologists, and meteorologists due to the diversity of impacts (Smith et al., 2013). For such reasons, it has been concluded that there is no single perfect standard method or definition for a HW that works for all applications (e.g., Perkins and Alexander, 2013; Smith et al., 2013; Kent et al., 2014).

Scientific literature has established that HWs can be defined broadly as a period of consecutive days, including daytime and/or nighttime, where perceived thermal conditions are well above normal. This involves three aspects that should be determined appropriately (Smith et al., 2013): (1) relevant meteorological metrics (e.g., Tmax alone or plus any one of or a combination of Tmin, humidity, wind speed, and solar radiation); (2) a type of threshold value that the relevant metric should exceed (i.e., an absolute or relative value), and (3) a duration aspect, (e.g., up to several days).

Although Tmax is the commonly used meteorological metric, it is often combined with Tmin as warm nighttime temperature can further intensify the impact of weather conditions because organisms may not experience a period of stress relief (Perkins and Alexander, 2013). Relative humidity is another meteorological metric that has been used mostly in assessing the impacts of HWs on human and other organism health as high temperature and high humidity

combined (e.g., apparent temperature or Temperature Humidity Index (THI)) have significant effects on heat wave-related mortality (Tong and Kan, 2011). Commonly, humidity is combined with temperature and then a resulting index, such as apparent temperature or the heat index, is used. Because of some limitations that relate to availability and quality of relative humidity observations (Perkins and Alexander, 2013), T_{min} has been used to infer the weather conditions during a HW as low humidity tends to lead to lower T_{mins} and high humidity to higher minima (Nairn and Fawcett, 2015). Thus, combining T_{max} and T_{min} in a definition allows the health impact to be assessed implicitly (Nairn and Fawcett, 2015). It is also possible to assess other aspects such as climatic and agriculture impacts. Indices, such as the THI and the Comprehensive Climate Index (CCI), are used to address environmental stresses on livestock (Mader et al., 2010).

Several studies have been conducted to compare different measurements and indices, Appendix A (e.g., Perkins and Alexander, 2013; Smith et al., 2013; Kent et al., 2014) and it has been concluded that there is no single perfect standard method or definition for a HW that works for all applications; this is due to the different aims or purposes of the different studies. Perhaps the most common extreme temperature indices that have been used extensively, especially in the Middle East region, are those of the WMO Expert Team on Climate Change Detection and Indices' (ETCCDI) of the Commission for Climatology/Climate Variability and Predictability/ Joint Technical Commission for Oceanography and Marine Meteorology (see Appendix A). Such indices, however, have been reported to have limitations. They do not capture all the aspects of a HW in a single measurement (Perkins and Alexander, 2013). Some of ETCCDI indices rely on fixed or absolute thresholds, which may indicate extremes in particular

homogeneous climates or particular applications, e.g., the effects on a particular type of crop or livestock (Folland et al., 1999).

Percentile based thresholds, above which a relevant metric should exceed and are relative to the area of consideration (i.e., a place-specific metric that allows for spatial comparisons), are commonly used and considered more appropriate (Klein Tank et al., 2009; Perkins and Alexander, 2013). Yet selecting the appropriate percentile threshold (e.g., 95th, 90th or 85th), the estimating time scale (e.g., monthly, seasonally, or annual), and the period of analysis (e.g., a decade, 30 years, the period of record) become critical decisions. Perkins and Alexander (2013) reported that the 90th percentile (for both maxima and minima) is an appropriate threshold as it optimizes the balance of extreme versus other temperature events. However, the relevance of such a threshold may differ from one climate type to another depending on the physical nature of the temperature regime along with cultural and social practices.

2.2.3.1 Implications for Subtropical Arid Climates under warming effects

In arid climates, the diurnal temperature range is usually large as T_{min} tends to drop quickly due to the nature of radiational cooling in dry environments (Oke et al., 1998). Thus, in common situations, i.e., no HW, T_{min} tends to be low. Thus, a lower threshold value (e.g., the 85th percentile) might be a more suitable HW criterion for subtropical desert environments. An implication of using the 85th percentile is that temperatures remain warm enough to limit the amount of stress relief. Since high humidity tends to lead to higher T_{min} , incorporating T_{min} in a definition allows the humidity effect to be assessed implicitly (Nairn and Fawcett, 2015). The 85th percentile has been established as a suitable threshold for heat and humidity-related health outcomes as it reflects population acclimatization (see Habeeb et al., 2015 for references). The difference between 85th and 90th percentiles of T_{min} during HWs could be more related to local

factors (e.g., urbanization) than to the prevailing synoptic conditions. Furthermore, within such an arid climate type, the nighttime summer temperature is already warm, stress relief is limited, and a small increase in temperature could be significant.

Defining what constitutes above normal conditions is a critical aspect since long-term warming or cooling trends and short-term variability of temperatures impact the statistics from which normal/abnormal conditions are determined. Under the effect of a multi-decadal warming trend, the threshold(s) above which a heat extreme is identified are expected to shift to warmer values over time. A warming climate could, also, result in both a large year-to-year fluctuation in climate and an increase in the length of a thermally defined season (e.g., a longer summer) (Hansen and Sato, 2016).

The pace of climate change is an important factor in defining HWs, where evolving climatic conditions and time frames should be reflected in any metric (Perkins and Alexander, 2013). By definition, HWs are rare events and by the end of this century, the extreme high temperature events of today are projected to become the norm (Mora et al., 2017) and new rare events will emerge in several places in the Arabian Gulf States (Pal and Eltahir, 2015). During the summer of 1987, the Tmax during a 7-day HW at Riyadh-new station (14) recorded its highest temperature of 47.4 °C for the period of 1985-1997. During 1998-2014 that 47.4 °C temperature was exceeded several times, suggesting a change in the character of extreme conditions.

As the mean climate frequency distribution shifts (to the left or right), the probability of an extreme event would not necessarily change without changes in the other characteristics of the distribution such as variance and skewness. Figure 2.2 indicates observed differences in the probability distributions and 85th percentile of Tmin and 90th percentile of Tmax at three stations

over different decadal and period of record time scales. These three stations represent and summarize different temporal patterns and climate types for Saudi Arabia. The Tmin percentiles of the 30-year period were higher than the first decade and lower than the third decade at these stations (Figure 2.2). The Tmax percentiles of the 30-year period, were lower than second and third decades at both Madina (13) and Al-Jouf (11).

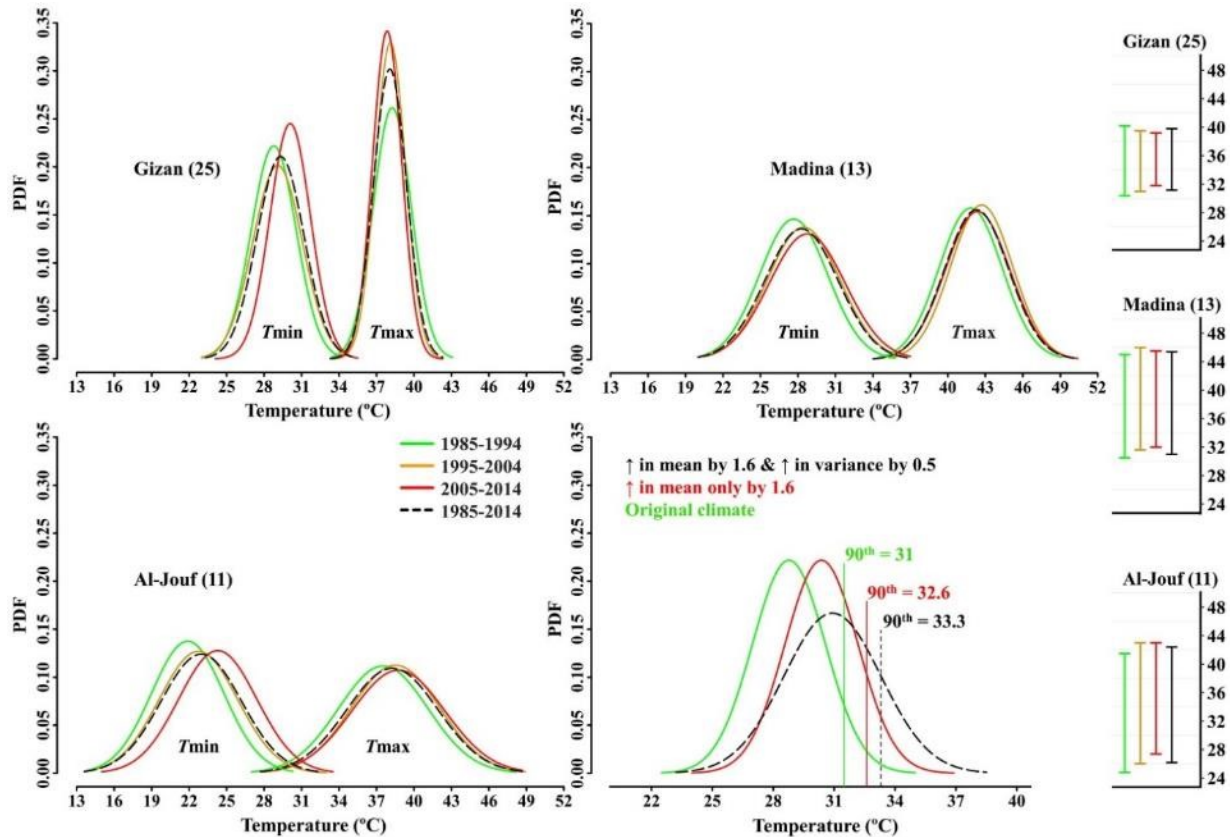


Figure 2.2. Distributions of the probability density function (PDF) of daily temperatures at three stations for three decades using warm season months (May through September) Tmax, and Tmin along with their 85th and 90th percentiles (right). Bottom-right plot shows changes in the probability distributions and the 90th percentile in response to changes in mean and variance of Tmin at Gizan (25) station. Simulations were prepared following Robeson (2002b). Stations were selected as they represent different temporal patterns and climate types.

Thus, using the entire 30-year period to estimate the 90th percentile would not highlight decadal variability and omit the impact of a trend in the climate. At Al-Jouf and Madina stations, constant percentiles based on the period of record would result in fewer detected HWs in the first decade and more HWs in the last two decades. At the coastal station, Gizan, the Tmax 90th of

the period-of-record was higher than the second and third periods. As such, use of that threshold would detect fewer hot day events in second and third periods and more in the first decade.

Differences in decade-to-decade percentiles do not have to be very big to result in large changes in the probability of extreme temperature events due to the nonlinear relationship between mean climate and extreme event probabilities (Mearns et al., 1984). Temporal patterns in the frequency of extreme temperature events are more related to variance characteristics than to the mean, as extreme events are more sensitive to variance (Katz and Brown, 1992).

In this work percentiles were determined on a month-by-month basis (e.g., Pezza et al., 2012; Cowan et al., 2014) using a decadal time-window (Robeson, 2002a). By estimating percentiles on a monthly basis, the effects of extreme values and annual and seasonal cycles can be minimized and the percentile threshold becomes more representative (Robeson, 2004; Pezza et al., 2012). If percentiles are calculated using a seasonal or annual basis, the warmer months will dominate the determination of the heat extremes that comprise the upper-tail. Percentiles could be also calculated using a centered window (e.g., 5-days, Klein Tank et al. (2009), 15-day, Perkins and Alexander (2013), or 31-days, Russo et al. (2015)). Cowan et al. (2014) compared monthly and 15-days centered window thresholds regarding their biases and reported no substantial differences. Thus, a HW event for Saudi Arabia was defined herein using the following criteria:

A period of two or more consecutive days with a daily maximum temperature exceeding the 90th percentile of the monthly maximum and the minimum temperature exceeding the 85th percentile of the monthly minimum for the decade in question (1985-1994, 1995-2004 and 2005-2014).

Following Hyndman and Fan's (1996) recommendation, the R8 method was used to estimate percentiles, as the method provides unbiased estimates and requires no distribution assumptions. Given the length of available data (30 years), a 15-year, 10-year, or 5-year time-window could be used. To balance between relatively long and short-term climate variability, a 10-year time-window was selected (e.g., Robeson, 2002a).

HWs can be continuous phenomena that extend over the transition between two adjacent months (Folland et al., 1999). Since HWs were defined and studied on a monthly scale, the definition has to be an operational one. Therefore, in the case that a HW extends into the next month, the percentiles (of T_{min} and T_{max}) of the month in which the event started were used to track the event into the next month, since the relevant synoptic weather system often moves slowly and can remain quasi-stationary for days. A HW is then reported for the month in which it lasts the longest.

2.2.4 Heat Wave Intensity and Duration

In defining what constitutes a HW event, there are no standard criteria for defining HW intensity and/or duration. The intensity of a HW should be defined in such a way that intensity is independent of event duration. This way the separate effects of duration on HW intensity can be explored. Intensity of a HW in this study was assessed using the T_{mean} of the hottest day, which is considered the peak of the HW (e.g., Perkins and Alexander, 2013). Thus, intensity is not a metric of the cumulative stress for the duration of the event. T_{mean} was used since both T_{max} and T_{min} are used to characterize a HW.

For duration, many local studies have used the Warm Spell Duration Indicator (WSDI), a metric from the ETCCDI, where WSDI is the annual count of days within events of at least six consecutive days when the T_{max} exceeded the 90th percentile. WSDI provides a general

assessment that could lead to a misleading conclusion. WSDI relies on the total number of days that result from lengthy events. With the use of a shorter duration criterion (e.g., 2-days or more), individual years could have an equal total of HW days but with different HW event counts and different durations (Figure 2.3). For instance, all the four years in Figure 2.3 have an equal total annual count of days, but individual events are different in duration across the four years. Year 1 has 3 HWs which last for 3, 4, and 5 days, respectively, which results in a total of 12 for the annual count of HW days. Year 2, on the other hand, has 4 HWs which last for 2, 3, 3, and 4 days, respectively.

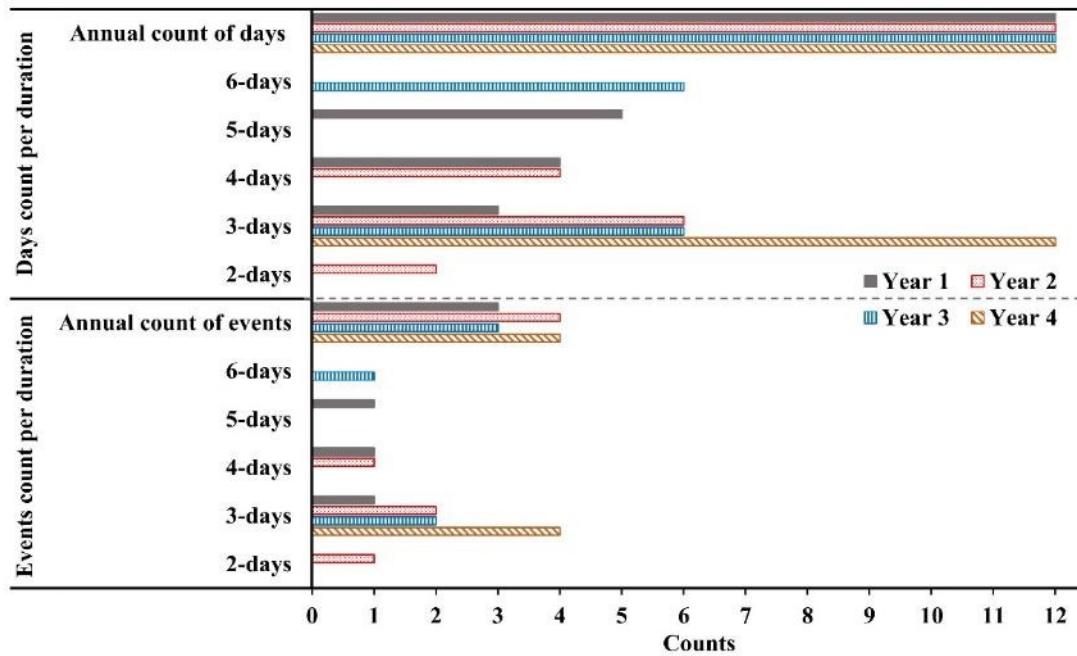


Figure 2.3. A hypothetical comparison between annual events count (bottom) and Annual count of days/WSDI (upper).

Similarly, years could have a similar annual count of days and annual event count but different durations. For example, both years 1 and 3 have an annual count of days (12 days) and annual count of events (3 events). Nevertheless, events of each year have different duration. It is important to note that, for any selected duration threshold, length, (e.g., 2, 6, or 7-day) in defining WSDI, similar observations are still existing as WSDI relies on the total count of HW

days, not on the duration threshold. In fact, the WSDI is more suitable for providing a measurement about trends in annual sum of participating days in lengthy HWs rather about the cumulative duration of multiple individual events.

A temporal trend in event duration can be assessed by using the length of the longest HW (HWLD) during the year in question (e.g., Perkins and Alexander, 2013; Cowan et al., 2014). This index was selected for use in this work as it relies on the greatest length of an individual HW; thus, it can be understood as an indicator about change in the upper limits of event duration. Table 2.2 summarizes all the HW indices developed for use in this study.

Table 2.2. Definition of HW indices developed and used in this study.

Indices	Definitions	Units
Heat wave frequency	A period of at least 2 consecutive days with a daily $T_{max} \geq$ the 90th percentile of the monthly maximum and the $T_{min} \geq$ the 85th percentile of the monthly minimum for the decade in question (1985-1994, 1995-2004 or 2005-2014)	Events
Heat wave intensity	Annual average of mean temperatures of the hottest days of heat waves	°C
Heat wave duration	The longest heat wave duration (HWLD) during the year in question	Days

2.2.5 Heat Wave Trend Analysis

Trend analysis was applied to the three aspects of HWs: frequency, duration, and intensity. For intensity, Kendall-tau and Sen’s slope estimator methods were used as they do not require a normal data distribution. From a statistical perspective, use of a trend analysis technique that addresses count data is appropriate (Ryden, 2016). HW frequency and duration indicators are count indicators rather than a ranking (i.e., number of events or length per unit time) and thus event-count time series techniques are most suitable. One option is to use ordinary least squares regression analysis; but for that technique, the data need to be normally distributed.

More importantly, both the frequency and duration indicators are count variables that can only be non-negative values. Consequently, using a linear regression model is not appropriate as negative estimated mean responses are not possible (Chatterjee and Simonoff, 2013).

An alternative is the Poisson regression model, and it has been used in HW studies (e.g., Bishop-Williams et al., 2015; Ryden, 2016). Unlike a linear regression model, a count regression model provides slope coefficients of the mean relative change (not the absolute change) in the expected response/occurrence associated with a unit change in the predictor variable. Event count time series approaches are not free of challenges and three main features should be addressed: autocorrelation, over-dispersion (variance is greater than the mean), and zero-inflation (an excess number of zeros, i.e., no event observations) (Zeileis et al., 2008; Yang et al., 2015). Autocorrelation, was found to not be an issue for the data used in this work. For the other two challenges, a straightforward framework (Table 2.3) provided by (Yang et al., 2015) was used. For example, when over-dispersion is present, a negative binomial regression model should be applied whereas a zero-inflated negative binomial regression model is more appropriated when over-dispersion and zero-inflation exist. To compare and select models, the Vuong’s test (Vuong, 1989) was applied. For theory and implementation, one can refer to Yang et al., (2015) and Zeileis et al., (2008).

Table 2.3. Used framework for trend analysis of frequency and duration of heat waves. Modified after Yang et al. (2015).

Over-dispersion	Zero-inflation	Model
No	No	Poisson regression
Yes	No	Negative binomial regression
No	Yes	Zero-inflated Poisson regression
Yes	Yes	Zero-inflation negative binomial regression

2.3 Results and Discussions

2.3.1 Evaluation

2.3.1.1 Thirty-year trends in the upper-limits of Tmax and Tmin

For evaluation and further investigation, the 90th and 85th percentiles of Tmax and Tmin, respectively, were estimated for each of the warm season months on a yearly basis for the period 1985-2014. Temporal trends in percentile values were selected for evaluation due to the possible unscaled relationship between changes in mean climate and climate extremes and because hot temperatures and upper-tail variations in Tmax and Tmin are closely coupled (Seneviratne et al., 2012). Generally, thirty-year warming trends were detected in both Tmax and Tmin percentile values across the warm season months with a few downward trends in Tmax percentiles values (Figure 2.4). The Tmin percentile values showed more pronounced increases than those of Tmax not only in the 85th percentile but also for the 90th percentile. These trends in the thresholds for HW events and multi-decade variations in the shape parameters of Tmin and Tmax distribution (i.e., variance and skewness, Appendix B- Figures 1-4) suggest changes in the climatology of the upper-tail conditions have occurred (i.e., events are getting hotter, and new norms are emerging).

Thus, using decadal time windows rather than the entire 30-year period for determining HW thresholds can help adjust for these trends and for multi-decade variations in variance and skewness of related distributions (Appendix B- Figures 1-4). It is likely that by using the entire period of record to estimate thresholds values that the role of rarity of a HW event would be violated. This would result in mis-detecting some possible rare events, particularly for short and low intensity hot events during early years in the data record. Small hot events (with respect to duration and intensity) can be of high importance locally. Particularly for the vulnerable populations (e.g., elderly, and children) that are already at higher risk. In arid environments,

these events could have significant effects such as in managing large electricity demands and limited water resources. Therefore, a time-sensitive approach for detecting threshold statistics recognizes the ongoing change and adjusts exceedance thresholds accordingly.

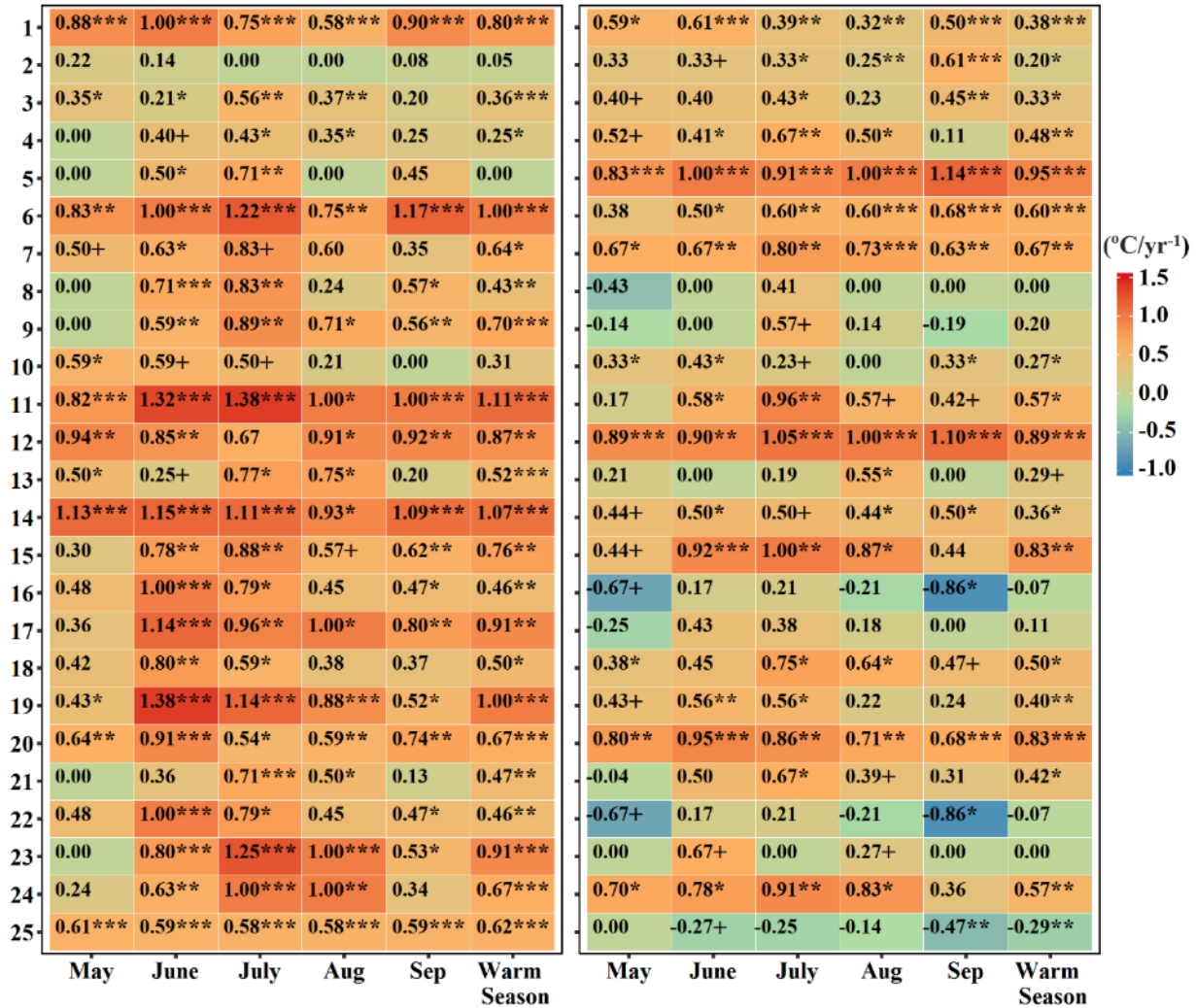


Figure 2.4. Heatmaps of decadal-based temporal trends in annual Tmin 85th (left) and Tmax 90th (right) percentile values ($^{\circ}\text{C}/\text{yr}^{-1}$) at monthly and warm season (x-axis) time scale for each station (y-axis). ***, **, *, and + $\alpha = 0.001, 0.01, 0.05, 0.1$ level of significances respectively. Trends were computed by Kendall-tau and Sen’s slope estimator. For stations names and locations refer to Figure 2.1.

A few individual stations differ from the national pattern and seven of 25 stations had declining trends in some of their monthly Tmax values (Figure 2.4). Such downward trends do not suggest absences of HW events, but a rather lower probability of events. Differences in the

heatmap patterns (Figure 2.4) of Tmax and Tmin thresholds (at monthly and seasonal scales) indicate that using a single atmospheric factor (e.g., Tmax) would omit important aspects of the climatology of HWs. A time-sensitive approach (monthly and decadal) has been established to be more suitable for low-probability climate events and their long-term change (e.g., Robeson, 2002a, 2002b, 2004; Robeson and Doty, 2005). Many terrestrial ecosystem processes are affected by short-term variations of hot temperatures (Suseela et al., 2012).

Several studies have reported reductions in heat-related mortality risk as populations adapted/acclimatized over time due to increased use of air conditioning, warning systems, improved health-care, and improved public awareness (e.g., Davis et al., 2003a; Davis et al, 2003b; Carson et al., 2006; Kysely and Plavcova, 2012). From 1990 to 2010, summer electricity consumption in Saudi Arabia increased by 35% as a result of the use of air conditioning (Alrashed and Asif, 2012). Air conditioning usage in the country consumes 60% of summer electricity (Alrashed and Asif, 2012). Kysely and Plavcova (2012) showed that a population's vulnerability to heat is influenced relatively little by climate change when other factors, such as socioeconomic developments, advance substantially. However, the population's ability to acclimatize to heat could be affected by temperature variability, even when populations of hot-cities become more adapted to high temperatures (Braga et al., 2001). Higher year-to-year variability in the temperature of warm months increases heat-related mortalities, due to sudden changes in temperature (e.g., Braga et al., 2001; Medina-Ramón and Schwartz, 2007). Thus, a monthly and decadal time-dependent approach can help to account not only for interdecadal variations and changes in extreme temperatures, but also for possible changes in population vulnerability to heat.

2.3.1.2 Evaluation of the heat wave definition

Frequency of count data on HWs detected using both a constant and a changeable threshold determined on monthly and seasonal bases are presented in Figure 2.4. Clearly different statistics were obtained as constant thresholds tended to detect more (fewer) events in the later (earlier) years. Higher frequencies of events in 1987 and 1989 are evident when a decade-sensitive approach is used. Due to the upward trend in the upper limit of T_{max} and T_{min} and thus in hot/warm days and nights in later years (e.g., Almazroui et al., 2014; Athar, 2014; Donat et al., 2014), a constant threshold is likely to be reached/exceeded more often in the later years; this choice influences the relative number of HWs and the rate/slope of change in HW events over time. A decade-sensitive determination of threshold percentile values resulted in a higher total number of events. This is due to the more equal representation of HWs across years, by taking into the account the warming trend and year-to-year variabilities (Figure 2.5).

Figure 2.5 provides the time series of the 90th percentile of T_{max} estimated on monthly and warm season bases at Al-Jouf. It is clear that the rate of warming and year-to-year variabilities were not the same across months. While the 90th percentile is increasing, the inconsistent temporal patterns among months impact detecting HWs as warm days and nights were found to be less detected in months with a low rate of warming along with those that had no significant warming trends. The full warm season's change was found to be more driven by the warmest months, which is consistent with Robeson's (2004) argument. Using a seasonal basis to determine the threshold would emphasize HWs in the warm months and vice versa since all months are not represented equally. For example, from late 80s to early 90s, the 90th percentile of the warm season, had a decreasing trend for July and August, which was not the case for the other months. Using a seasonal basis did not detect early and late warm season events (i.e., May

and September) as the threshold was derived from mid-season (i.e., warmer months). Use of the full warm season to establish a threshold would also affect the HW duration and intensity aspects as the warming trends are more pronounced in the later years. HW duration was found to decrease, generally, when the threshold was estimated using warm season data.

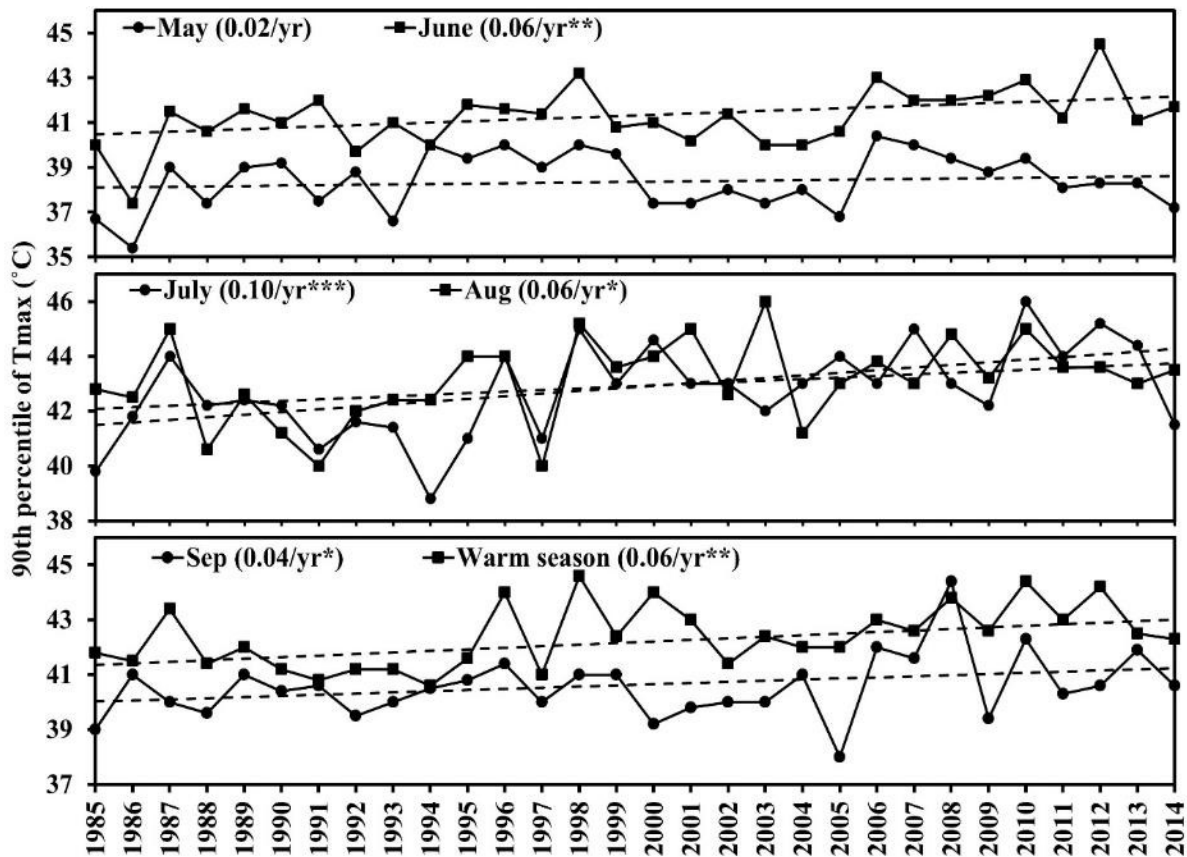


Figure 2.5. Monthly and warm season 90th percentile of Tmax thresholds at Al-Jouf (11) station determined on an annual basis. *, **, and * $\alpha = 0.01, 0.05, 0.10$ level of significances respectively. Trends computed by Kendall-tau and Sen's slope estimator.**

A constant 30-year threshold percentile approach detected 11 HWs during 2010 whereas the decade-sensitive approach detected six HWs (Figure 2.6A and C). Seven different HW events were found to have daily Tmeans less than 1 SD of the respective 2010 monthly Tmean, suggesting unreasonable over detection when using 30-years to define the relevant threshold. Using 30 years and the full warm season to determine the threshold, results in a period, 1989-1994, when no events are detected (Figure 2.6B). This period had lower values for the 90th

percentile statistics of both Tmin (not shown) and Tmax during the warm season months of July and August (Figure 2.5). From a meteorological perspective, such an observation does not necessarily suggest absences of HWs. In fact, the events identified by using a decade-sensitive percentile for this period (Figure 2.6D) were found to have Tmax values above 1.50 SD of the 1985-2014 warm season mean Tmax.

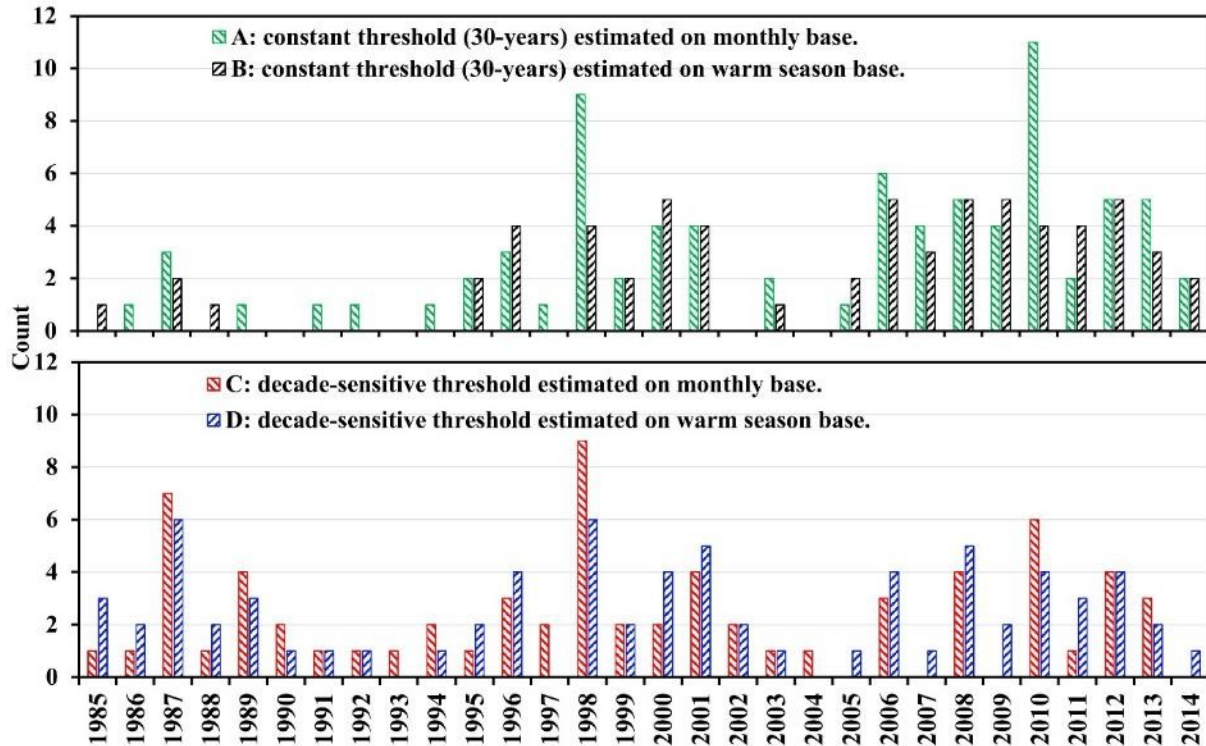


Figure 2.6. Annual count of heat waves per year at Al-Jouf (11) station using different time-windows to estimate percentile, A and B constant (30-years) and C and D decade-sensitive thresholds estimated on monthly (A and C) and warm season (B and D) bases.

2.3.1.3 Evaluation of duration metrics

Using a duration metric that is similar in design to ETCCDI, WSDI₂, the annual count of HWs days of events that are two days or longer, and HWLD, the duration of the longest HW each year, showed relatively similar overall patterns across Saudi Arabia with greater differences in their magnitudes and substantially different details for a few years (Figure 2.7). Both indicators were calculated using the HW definition established in this manuscript. WSDI₂ and

HWLD showed similar temporal patterns during years with a small range of HW durations that have low frequency and exact patterns were found during years with one HW. For instance, at Rafha (17) (Figure 2.7) from 1985 to 1988 both indices followed each other in their temporal pattern due to small range of durations that also had low frequencies. The data had an identical pattern from 2002 to 2006 as these years each had one event. During years with a wide range of HW durations or small range with high frequencies (i.e., a duration occurs several times in a given year), the curves deviated and sometimes showed inverse patterns. At Rafha (17) and Al-Baha (3) stations, different patterns between the two indices were found in 1998 and 2011 due to the greater number of events in these two years.

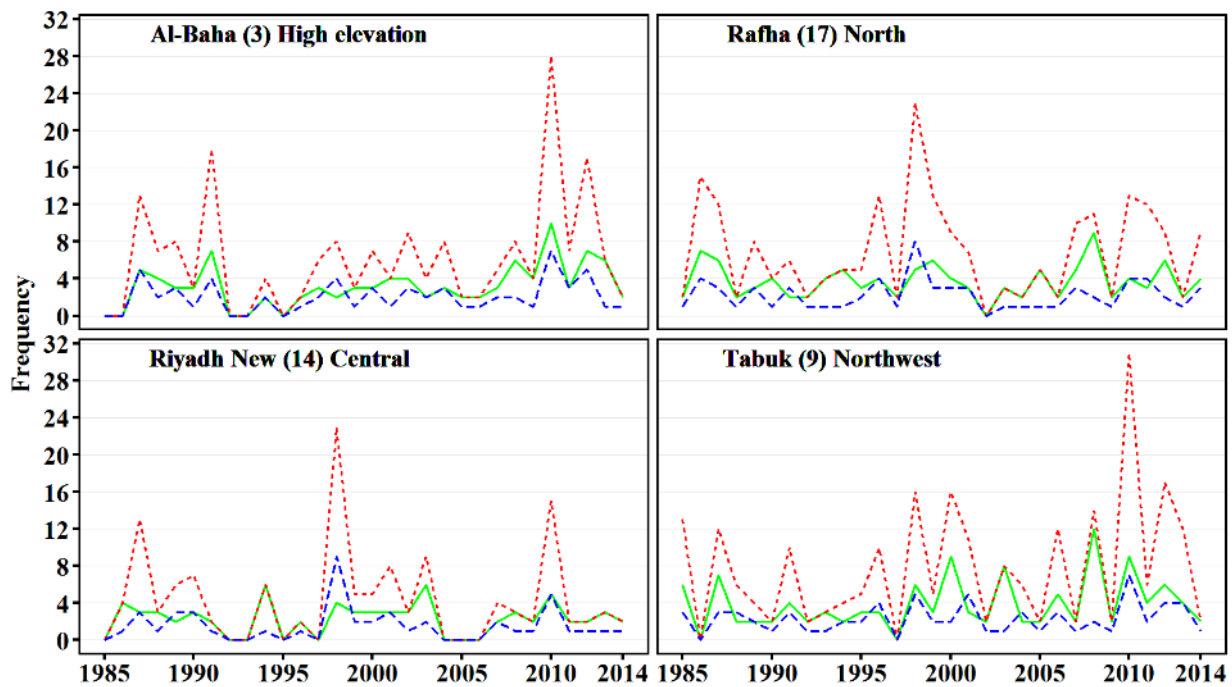


Figure 2.7. Duration of the longest event or HWLD (green solid line), number of heat wave events (blue long-dash line), and the annual count of days or WSDI₂ (red dashed line) at four stations, representing different temporal patterns, elevation, and climate types.

It is also clear from Figure 2.7 that years with a similar WSDI₂, did not have a similar range of durations nor similar magnitudes of duration. At Tabuk (9), WSDI₂ had a value of 12 days in 1987, 2006 and 2013 whereas the longest durations for these years were 7, 5 and 4 days

respectively. $WSDI_2$ did not significantly distinguish among the magnitudes of different durations, as $WSDI_2$ does not directly consider individual event length. At Tabuk (9), $WSDI_2$ had values of 8 and 11 days in 2003 and 2001 whereas the longest duration was 8 days in 2003 and only 3 days in 2001. A similar issue can be seen across all four stations in Figure 2.7. Such a difference in metric values will highly impact the rates and magnitudes of trends, negatively in the case where there is a positive trend in duration over time. This analysis raises similar concerns about another ETCCDI, the cold spell duration indicator (CSDI), the annual count of days with consecutive days when $T_{min} < 10$ th percentile.

Clearly, findings on the number, intensity, and duration of HWs will change depending on the threshold selected for an extreme event. Use of a time-sensitive metric (monthly rather than seasonal or annual) is helpful in examining the multiple types of HWs that occur during the extended five month period of ‘summer’ in Saudi Arabia. And, as regional temperatures continue to warm, the use of decadal rather than the period of record data for threshold determination will provide findings that better represent the changing warm season climate.

2.3.2 Heat wave behavior

2.3.2.1 Frequency

Classifying the 25 stations into groups based on the dominant month(s) of HW occurrence resulted in eight categories (Figure 2.8A). HWs during May were found to be more frequent at 9 stations (36%) followed by September and July (each 20%) (Figure 2.8A). Stations with more frequent events during May were those located at higher elevation (Abha (1), Khamis Mushait (2), Al-Baha (3), and Taif (4)) and in coastal areas (Dhahran (22), and Jeddah (23)), except Makkah (19) and Al-Ahsa (20). May-event-stations were characterized by a low number of annual HWs, except station Al-Baha (3) (Figure 2.8B). Most of May-event stations were

dominated by short-lived events (i.e., 2-days) and half of these stations recorded their maximum durations during May. May's events tended extended over into June for a few days, yet not to the extent that they were recorded as June events. The tendency for May HWs to extend into the next month was more frequent than events from other months. HWs occurring during the months of June through September showed a more random geographical distribution as there was not a common elevation, longitude or latitude pattern (Figure 2.8A). Some stations showed unique monthly frequency maxima (e.g., Bisha (6), Turaif (8), and Wejh (21)) and Gizan (25) had nearly equal frequency across all months.

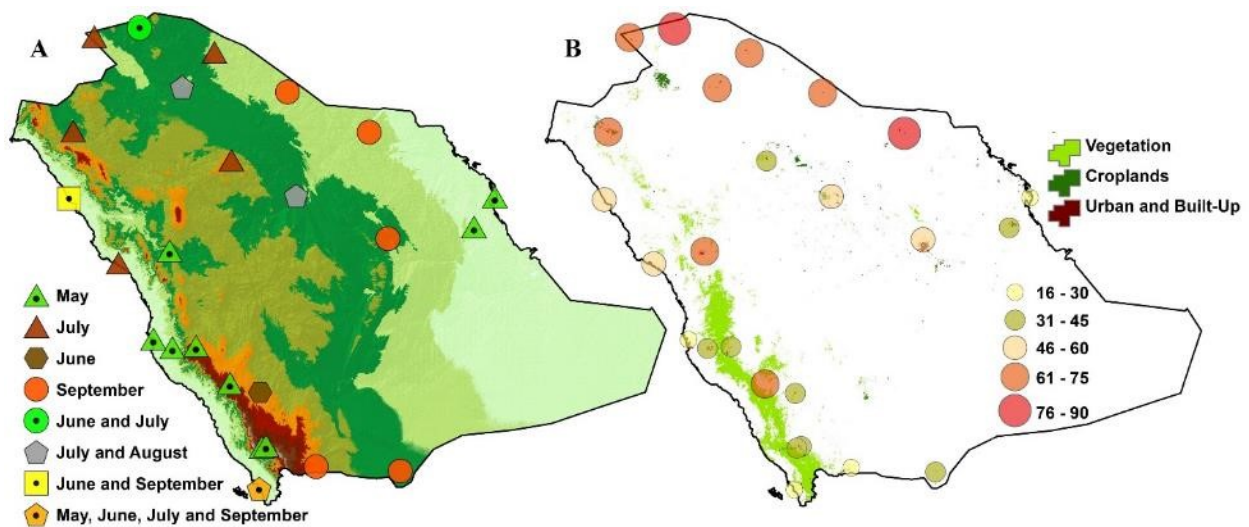


Figure 2.8. Classification of stations by the dominant month(s) of heat waves (A) and proportional symbols for annual frequency (B). Land cover data was obtained and modified after Broxton et al. (2014). Refer to Figure 2.1 for the elevation legend for (A) and for stations names.

Stations along the northern borders of Saudi Arabia had the highest HW frequency (Figure 2.8B) with events more often occurring in mid-to-late summer. Coastal and higher elevation stations had low event frequency, except two stations (Wejh (21) and Yenbo (24)) on the north-west coast. These latter stations and internal stations (Hail (7), Gassim (12), and Riyadh-New (14)) showed moderate HW frequency (Figure 2.8B). Such a spatial pattern may indicate that HWs in the north part of Saudi Arabia are induced by a similar and relatively

frequent synoptic weather pattern. Local factors may play a more important role in interacting with regional weather patterns for the other stations. Stations at a higher elevation (excluding Al-Baha (3)), those with a more dense vegetation cover (Abha (1), Khamis Mushait (2), Taif (4), and Bisha (6)), and those with more moist air present (coastal stations (Dhahran (22), Jeddah (23), and Gizan (25)), tend to have a low frequency of HWs (Figure 2.8B).

2.3.2.2 Duration

To map the 25 stations based on HW duration, three-categories were selected (Figure 2.9) due to the low frequency (<6%) of long-lived events (≥ 6 -days) at 56% of stations. Long-lived HWs (≥ 6 -days) constituted 9-16% at only 7 stations. The vast majority of stations had more of their events as short-lived or 2-4 day events (>85%). Events of this duration are missed by the ETCCD heat wave duration metric (WSDI). Specific locations where short events dominate were those stations clustered on the coast or at high elevation (Figure 2.9). Three other stations (Hail (7), Riyadh-New (14), and Al-Ahsa (20)) also had more than 90% of their events fall in the 2-4-day category. These stations were found to have a higher frequency with more events occurring at the boundary of the warm season (i.e., May and September). Perhaps, local factors (e.g., vegetation, topography or a sea breeze) help control the duration of events in these areas. Almazroui et al., (2015) showed that often extreme high temperature events (warm days and nights) did not result from just a single weather circulation type within a subclimate type.

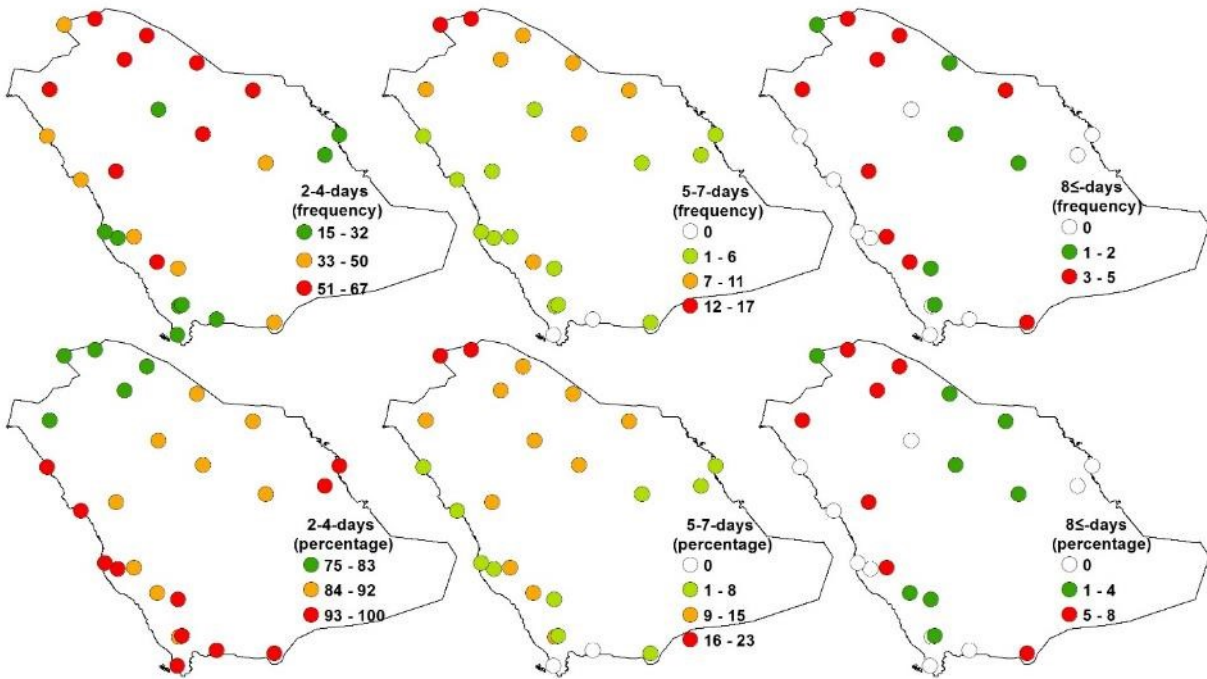


Figure 2.9. Number (upper) and percentage (bottom) of HWs based on three duration categories: 2-4-days, 5-7-days, and ≥ 8 -days. For stations names refer to Figure 2.1.

Relatively long and long-lived events (5-7-days and ≥ 8 -days) constituted a noteworthy number of events at stations in the north and at one station in the higher elevation area, Taif (4). Commonly, stations with frequent short-lived events (90%) tended to have a low frequency of long-lived events (e.g., Najran (5), Wejh (21), and Gizan (25)). Stations in northern Saudi Arabia tended to have infrequent short-lived events and notable and frequent long-lived events. A persistent atmospheric circulation pattern(s) could be responsible for these longer events at the northern stations.

2.3.2.3 Intensity

HW intensity, the Tmean of the warmest day during an event, showed no major patterns among months in relation to the length of events. HWs during July and August had higher intensities at a few stations, but consistent monthly patterns were not found across all stations. Although longer events were expected to have the higher intensities, shorter events (i.e., 2 and 3-

days) were often found to be the most intense (Figure 2.10). It should be noted that this comparison across stations is in terms of an absolute value since the intensity value (i.e., Tmean of the hottest day) depends on day-to-day temperature anomalies.

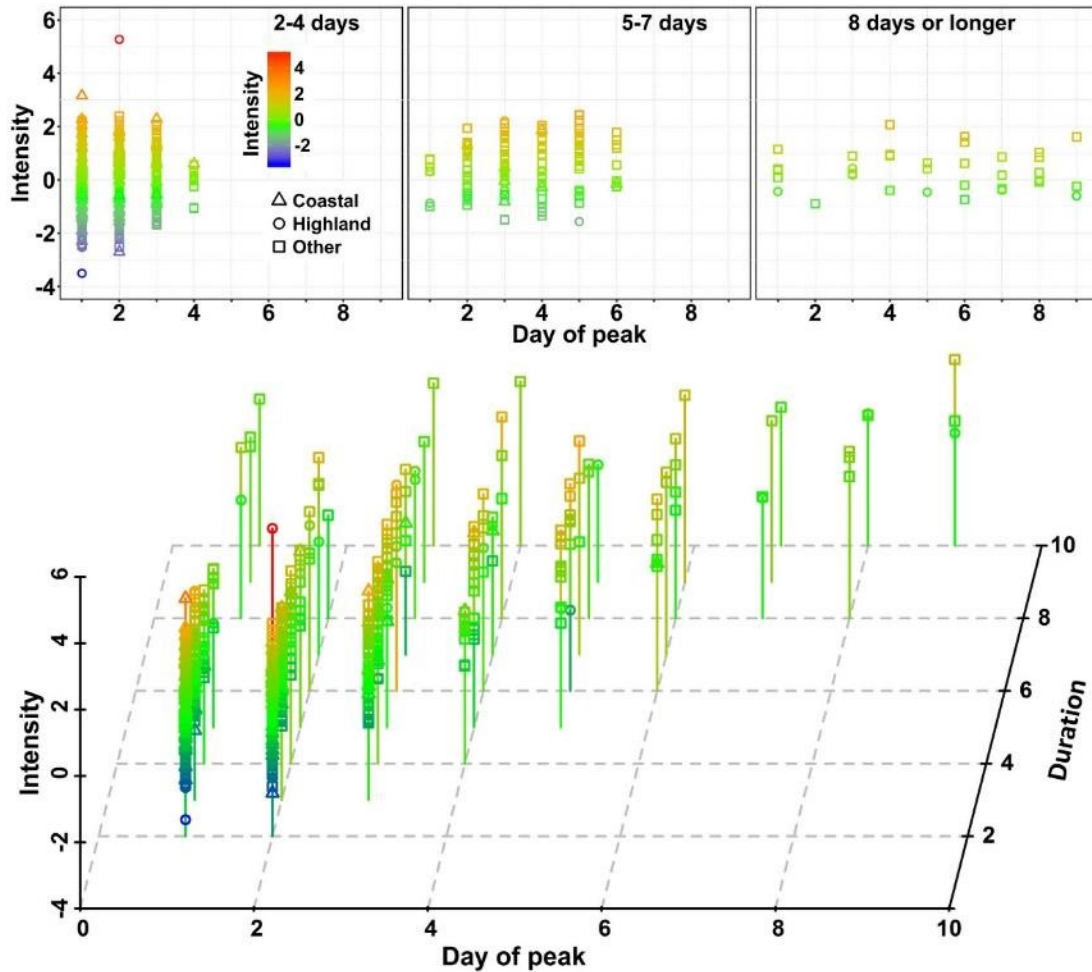


Figure 2.10. Two-dimensional (top) and three-dimensional (bottom) scatterplots of day of peak (highest Tmean), duration (in day) and intensity (standardized Tmean with zero mean and unit standard deviation at station level) at all the 25 stations. Coastal, Highland, and other categories include stations (IDs): 21:25, 1:6, and 7:19, respectively. Refer to Figure 2.1 for stations names and locations.

The intensity of a HW, was found to peak autonomously in relation to duration as highest temperatures were sometimes in the middle of the string of days; for other events, the peak occurred either after or before the middle of the event. However, short-lived HWs (2 to 4-day) tended to record maximum intensity a day before event end, whereas, maximum intensity was

observed a few days before event end of long-lived HWs (>5-day) (Figure 2.10). For events of 2-days duration, this aspect had a more random spatial distribution, suggesting differences in local and micro-climate factors. It also suggests that local and micro-climate factors could be more important than the effects of atmospheric circulation on the association between HW intensity and their duration.

2.3.3 Trend analyses

By design the decade-to-decade, long-term warming or cooling (i.e., shift in the mean climate) was relatively removed for this analysis of HWs in Saudi Arabia. Subsequent analysis for the remaining trend in the HW data for the 30-year period from 1985-2014 could be related to changes or variation in the upper-tail characteristics (i.e., variance and skewness). Figure 2.11 displays different temporal trend patterns across stations for the three HW characteristics. It is worth noting that the values of frequency and duration in Figure 2.11 are as percentages, so that a one-unit change per year corresponds to change in frequency or duration of one percent. Only Makkah (19), had significant upward trends in all the studied aspects (frequency, duration and intensity), suggesting that the station had experienced not only more frequent HWs put also longer and more intense events. At Makkah City, the Hajj (pilgrimage) takes place, raising a serious concern about coming years when the Hajj will be during the warm season.

Taif (4), Gassim (12), and Bisha (6) had significant upward trends in frequency, but an insignificant trend in duration (HWLD). Only one station had an insignificant decrease in intensity (Al-Jouf (11)), whereas 24% and 36% of the stations had decreases in HW frequency and duration, respectively. For HW intensity, an upward trend was found at 60% of stations, 36% of which had significant intensification trends. The geographical patterns of both frequency and intensity aspects (Figure 2.11) showed that coastal and high elevation stations had rising

trends in event frequency, with lower intensity trends.

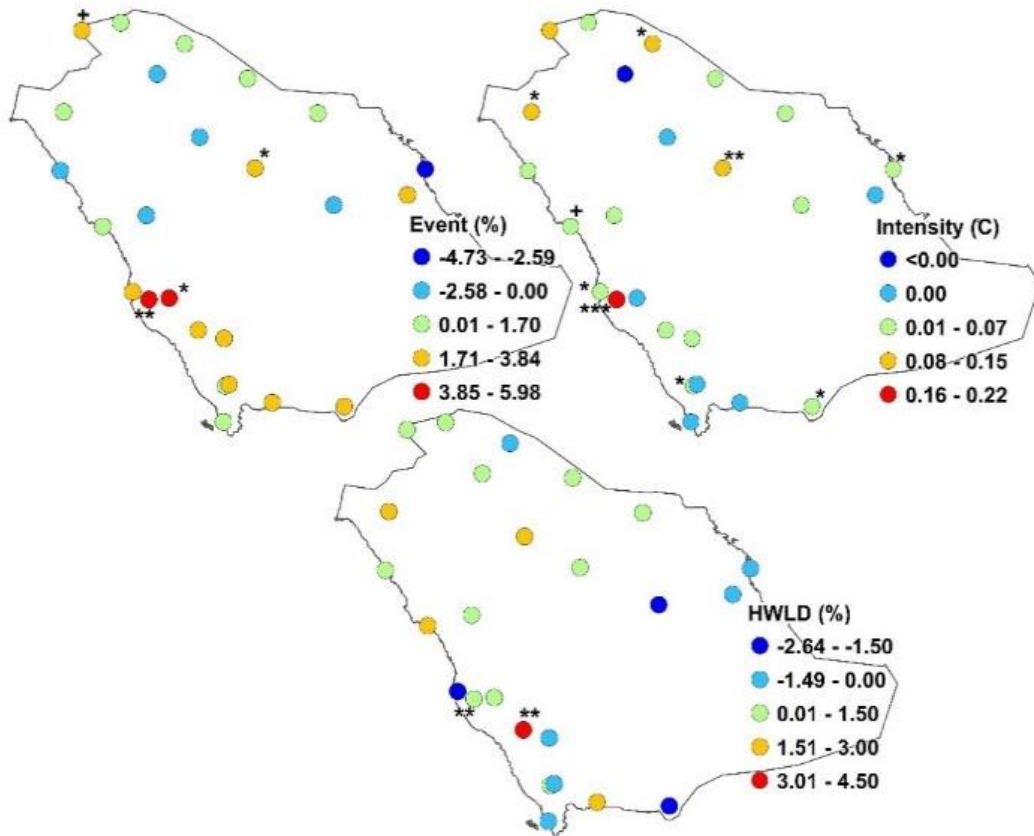


Figure 2.11. Temporal annual trends in frequency (left-top), intensity (right-top), and duration/HWLD (bottom) aspects. *, **, *, and + $\alpha = 0.001, 0.01, 0.05, 0.10$ level of significances respectively. For stations names refer to Figure 2.1.**

These findings suggest that local factors impact the regional effects of heat extremes. The patterns identified, and the time-sensitive criterion (i.e., decadal time-window), suggest that the trends in the intensity of HWs in Saudi Arabia are related to regional warming and local factors may play important roles in moderating or enhancing the regional trends. Although several stations had low trend magnitudes (either upward or downward), it is important to remember the time-sensitive criterion. Temporal trend analysis was not applied at the monthly level due to high (i.e., excess) number of zeros (no event observations). However, linking results from Figures 2.8A and 2.11 suggests that stations which tended to have frequent events during the early warm season (May) are those that recorded the greatest increase in frequency over time and had a

lower intensity trend. These stations were characterized by frequent short-lived HWs (Figure 2.9), where they experienced largely decreasing or small increasing trends in event duration (i.e., the HWLD indicator (Figure 2.11)), except Al-Baha (3)). Stations with frequent late warm season HWs (September) (e.g., Najran (5), Sharurah (10), Riyadh-New (14), Rafha (17), and Al-Qaysumah (18)) had low upward trends in intensity and different patterns in their HWLD (Figure 2.11). This could be due to differences in event duration and annual frequency aspects (Figures 2.8B and 2.9), which may be the result of differences in both regional and local factors.

2.4 Summary and Conclusions

The frequency, intensity, and duration aspects of HW events in Saudi Arabia were explored using data from 25 stations for 1985-2014. Data quality received careful attention and a regionally relevant HW definition was developed to account for any possible warming, cooling, and year-to-year variability. The importance and effect of different time bases for determining a HW threshold was examined and the importance of selecting an appropriate threshold and indices for different HWs aspects were addressed. Results reveal the need for careful consideration of HW indicators. HWs in the study area behave spatially and temporally differently at the station level, although common patterns were found with some grouping of stations, with local factors proposed to play an important role.

The geographic behavior of HWs was studied using traditional statistical classification methods (e.g., equal interval) to map different aspects of HWs. Less subjective methods (e.g., clustering analysis) could be used to provide further insights. Cluster analysis would help to better understand the spatial and temporal characteristics of HWs across a region. Understanding the spatial differences would not only help to recognize the geographic pattern(s) of change, but would also help in speculation about some of the possible factors that may have an important

influence on changes in extreme temperature and HWs such as topography, local water bodies, urbanization and surface cover/vegetation. This local knowledge also would provide insights into how spatial factors (e.g., topography and continentality) could relate to or influence the atmospheric circulation at different scales (e.g., micro- and meso-scales) that induce extreme temperatures (Kenawy et al., 2013).

Analyses of HWs were performed at the station level to unravel the intricacies of place-to-place differences and to provide detailed information. The study area contains several subclimate types (Almazroui et al., 2015) and it was thought that stations might show common patterns within these subclimate zones. However, the behavior of HWs within and among different subclimate zones was not clear, although some coherent spatial patterns were indicated with some of the results. The effects and roles of local factors and atmospheric circulation were discussed from a theoretical point of view and some suggestions were made. However, the interplay of regional and local factors is not clear, as some stations showed individual behavior (e.g., Bisha (6) and Turaif (8)) and local microclimate studies within Saudi Arabia are rare.

Percentiles were estimated using a decadal time-window, given the length of the available data record (30-years) and to balance between long and short climate variability. With the availability of longer and high-quality data, different time-windows could be used with different estimation techniques (e.g., moving window). The stability and effects of different methods in defining percentiles is an important aspect not only to model extreme temperature events, but also to better understand changes in climate variability. This methodological assessment was beyond the scope of this work and further studies are needed. Davis et al. (2003b) showed that heat-health outcomes in many of U.S. cities have experienced decadal variabilities and changes (decreases) and, thus, acclimatization processes and population

vulnerability may vary through time and space. Modeling and counting for acclimatization as a factor for HWs involves a substantial level of uncertainty and different methods has been developed (Sheridan et al., 2012). Accordingly, it is difficult to detect the time when populations get adapted/acclimatized (behaviorally and physiologically) to a changing climate. This uncertainty emerges from the non-linear relationship between adaptation and heat-related effects on other factors such as socio-economic conditions and demographic variables. It has been suggested that non-stationary models are more suitable for evaluating the outcome of adaptation to a changing climate (Gosling et al., 2009).

Although several stations showed no significant temporal changes in some of their HW characteristics (Figure 2.11), it does not imply that climate change is not taking place at these stations. In fact, significant changes were detected in the upper-tail percentiles at most of the studied stations (Figure 2.4). Consequently, results should be viewed comprehensively considering that our HW definition lessens (by detrending) any possible effects related to an overall warming or cooling trend. As we have discussed, climate change is usually accompanied by changes in the temperature trend and its distribution characteristics. Thus, any response would require fundamental changes/adaptation at different scales (locally, nationally, and globally) given the complexity and sensitivity of the changing climate. One of the main implications of this work is the importance of considering acclimatization in addressing the outcomes of climate change as several studies have showed the importance of these factors with respect to HWs (refer to Sheridan et al. (2012), Gosling et al. (2009), and Davis et al. (2003b) for additional reviews).

Chapter 3 - Trends and spatial pattern recognition of warm season hot temperatures in Saudi Arabia

Abstract

Temporal trends and spatial patterns of six warm season (May-September) hot temperature indicators (WSHTIs) were developed and explored for Saudi Arabia. The indicators focus on the frequency and intensity of hot days and nights, and heat waves. Systematic upward trends in maximum and minimum temperatures were found at most of the stations, suggesting on-going change in the climatology of the upper-tail of the frequency distribution. Taking into account the observed effects of climate change on the country's climate, hot temperature events were defined using a monthly and decadal, time-sensitive approach. Indicators of event frequency are count data; thus, different Poisson models were used for temporal analysis.

Further, a novel method of time-series clustering, was introduced to recognize spatio-temporal patterns of WSHTIs. Different patterns were observed over time and space not only across stations but also among WSHTIs. The overall results suggest that not only local and regional factors, such as elevation, latitude, and distance from a large body of water, but also large-scale factors such as atmospheric circulation patterns are likely responsible for the observed temporal and spatial patterns.

3.1 Introduction

Understanding the character of change in extreme hot temperature events is of critical importance for citizens of the Middle East (Pal and Eltahir 2015). An upward trend is the dominant pattern for thermal aspects of the climate and this warming has been accompanied by a positive shift for both minimum (T_{min}) and maximum (T_{max}) temperatures for the Arabian Peninsula, particularly, Saudi Arabia (Zhang et al., 2005; AlSarmi and Washington, 2011, 2013; Almazroui et al., 2012a, 2012b; Almazroui et al., 2013; Almazroui et al., 2014; Rehman and Al-Hadhrami, 2012; Athar, 2014; Donat et al., 2014; Islam et al., 2015). Studies of the area document that current hot temperature events (i.e., hot days, hot nights, and heat waves (HWs)) reached maximum frequencies during the last few decades, suggesting that such events may continue to become more common within the suite of local climate conditions. Almazroui et al. (2014) identified changes in the mean and variance in the distribution of air temperature over Saudi Arabia, which corresponded with decreases in the number of cold events and increases in the number of warm events. Almazroui et al. (2012b) also found that the warming/upward slope of the mean temperature trend is steeper for the summer season. Hansen and Sato (2016) reported a positive shift of 2.4 standard deviations in the distribution of summer temperature anomalies in the Mediterranean and the Middle East region compared to an increase of 0.87°C in winter. This shift has resulted in a larger annual variability and a more extended summer season. By the end of the century, the extreme warm temperature events of today are projected to become the norm and new rare extremely hot events will emerge in several places in the Arabian Gulf States (Pal and Eltahir, 2015).

Similar to the reported overall global warming trend with steeper rates since the 1990s (Bajat et al., 2015), the signal of warming of hot temperature events in the region started

gradually in the 1970s and a steeper upward trend was evident by the 1990s (Zhang et al., 2005). Several studies have shown that temperatures have risen across Saudi Arabia, largely during the latter part of the 20th and early part of the 21st centuries (AlSarmi and Washington, 2011, 2013; Almazroui et al., 2012a, b; Almazroui et al., 2014; Rehman and Al-Hadhrami 2012; Athar, 2014; Islam et al., 2015). From currently available literature, the overall findings are that the region has experienced substantial warming in mean annual temperature, annual mean Tmax and Tmin, and annual highest Tmax and Tmin for the last few decades.

Almazroui et al. (2014) compared trend slopes in several climatic extreme indices between two subperiods, 1981–1995 and 1996–2010, at the national level for Saudi Arabia and found that the latter period had greater upward slopes in the extremes and that the changes were accompanied by positive shifts in the frequency distributions of both Tmax and Tmin. During the latter period the rate of change in the frequency of warm days doubled whereas the frequency of warm nights increased more than ten times. Islam et al. (2015) used similar subperiods and detected significant changes in the frequency distributions of the average air temperature anomalies, where summer had the greatest positive shift. From these findings, it is plausible to suggest that there has been a change in the overall suite of climate conditions for Saudi Arabia and that what used to constitute a rare hot temperature event is now more common and will become increasingly frequent in the future.

Most of the existing literature about extreme temperature events and their trends for Saudi Arabia is based on a single set of climate indices, i.e., those developed by the Expert Team on Climate Change Detection and Indices (ETCCDI). In addition to the identified limitations of the ETCCDI indices (see Perkins and Alexander, 2013), results found using the indices could be affected by the observed changes in the mean and variance of the air temperature distribution

and, unfortunately, little attention has been paid to this potential issue. Event duration has been the dominant metric used for a good deal of the prior work examining HWs in Saudi Arabia and, as such, the intensity aspect of hot days and hot nights needs to receive more attention.

Previous studies document that the frequency of warm temperature events has increased, and that warming trends exist for T_{max} and T_{min} . However, it is highly possible that the upward trends in the frequency of warm temperature events are more due to the increases in the incidence of the exceedance using a constant threshold (static/fixed value), above which extremes are identified, for the period of record. An important implication of warming is the impact on evolving climatic conditions and related extreme temperatures (Perkins and Alexander, 2013; Alghamdi and Harrington, 2018). As the climate warms, its temperature frequency distribution shifts positively and thus new rare warm conditions emerge. Alghamdi and Harrington (2018) document a rationale and the value of using a time-sensitive approach to examine warm season extreme heat events for Saudi Arabia.

A warming climate is accompanied by large interannual variability (Hansen and Sato, 2016) and a decadal time-window can better reflect the influence of multi-year variations. The rate of warming or cooling could be different among years and months due to effects of external climate forcing such as ENSO or multi-year droughts. For instance, it has been shown that the long-term temporal trends of both hot days and HWs in the United States were affected by the multi-year droughts of 1930s and 1950s (Easterling et al., 2000). It is important to recognize that shifts in the distribution of mean temperature do not need to be that large to result in a substantial change in the probability of upper-tail events due to the nonlinear relationship between the mean and the extreme temperatures (Mearns et al., 1984; Katz and Brown, 1992). As an example, the 2003 European HW was very far off from the normal climate distribution (Schär et al., 2004).

For changes in climate extremes to be better understood, knowledge of the change in the mean climate needs to be supplemented by important changes in the variability and shape of the frequency distribution since the relationship between changes in mean climate and those of climate extremes are not always scaled (Seneviratne et al., 2012). In fact, the overall impacts of shifts in the average climate are less than those of the increasing climate extremes (Whan et al., 2015) and it has been established that short-term variations in extreme weather conditions can rapidly impact terrestrial ecosystem processes (Suseela et al., 2012). Heat-related mortalities, for instance, have been shown to increase with higher variability in warm season temperatures due to sudden changes in temperature (e.g., Braga et al., 2001; Medina-Ramón and Schwartz, 2007).

Dominance of extreme events/values during warmer months and the related impact on selecting extreme value thresholds (e.g., the 90th percentiles) for climatic analysis needs to receive more attention. By estimating percentiles over annual or seasonal time scales, warmer (cooler) months will dominate the estimation of the upper-tail (lower-tail) percentiles (Robeson, 2004). Consequently, hot events that occur early or late in the warm season months are less likely to be examined whereas warmer month events would dominate the analysis (Coelho et al., 2008). A time-sensitive approach defining threshold values on a monthly basis would enable documentation of the early and late season extreme heat events. Realistic estimates of changes in hot temperature events will help future planning efforts such as in managing changing demands for electricity and water resources in an arid environment.

Previous studies of Saudi Arabia have focused on temporal change using common climatic indices, with less attention given to the geography of extreme temperature events (i.e., spatial patterns). These efforts have not addressed in detail the effects of local and regional factors (e.g., urbanization and other land cover shifts or a coastal location), and the effects of

warming on the frequency of climatic extreme events. Identifying the spatial patterns of the temporal behavior of hot temperature events will help recognize the varying geographic patterns and influences of the local climate and will also help in the speculation and formulation of hypotheses about possible factors that have important control on the changes such as topography, distance from water bodies, and vegetation/land cover. Further identifying places/regions of similar warm/hot temperature behavior is beneficial for practical purposes including developing heat-warning systems and other policy-oriented planning.

Building on the previous research, the objectives of this study are to (1) detect temporal changes in the frequency and intensity in six warm season hot temperature indicators (WSHTIs) using a time-sensitive approach to account for the ongoing regional warming trend and (2) recognize the spatiotemporal character of warm season hot thermal events with an emphasis on event behavior through time and space using a time-series clustering approach.

3.2 Research Design and Methods

3.2.1 Study area and data

Saudi Arabia lies between the Red Sea and Arabian Gulf on the Arabian Peninsula (Figure 3.1). Using the Köppen climate classification, the study area has two main climate types. A large part of the study area is subtropical desert (BWh), which is characterized by hot and arid conditions. The southwestern mountain areas are subtropical steppe (BSh), which is characterized by hot and semi-arid climate conditions. Accordingly, most of the landscape is barren except for portions of the southwestern mountains. The latter area is characterized by high elevation with complex topography, moderate temperatures, a bit more precipitation and vegetation cover (Figure 3.1). Topography and the geographical location with respect to the Hadley circulation are the primary climate controls. Sinking air associated with the poleward

margin of the Hadley circulation is the dominant mechanism for limiting precipitation in the area.

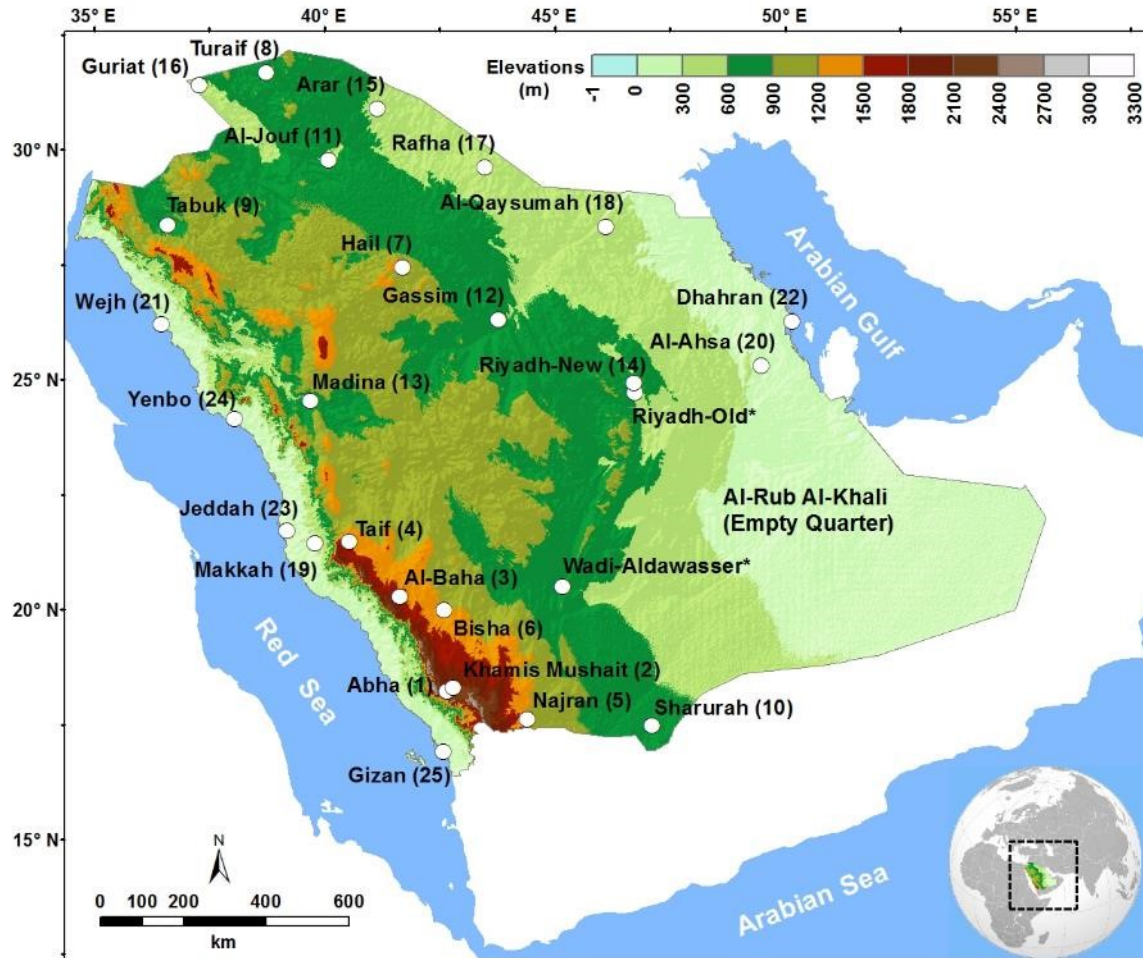


Figure 3.1. A map showing the study area and weather stations along with their names and IDs. Source: adapted from King Abdulaziz City for Science and Technology (KACST) and the GAMEP. * station was not included in this study.

Warm season hot temperature events were analyzed, for the period 1985-2014 for 25 meteorological stations using daily Tmax and Tmin data provided by the Saudi General Authority for Meteorology and Environmental Protection (GAMEP). The selected weather stations provide suitable spatial and temporal coverage, a homogeneous time series (AlSarmi and Washington, 2013; Almazroui et al., 2014), and a reasonable long-term dataset for spatial and temporal analyses. This study is focused on the behaviors of warm season hot temperature events

through space and time; thus the period of investigation begins in 1985, as six weather stations began recording in 1985.

Although a few stations in Saudi Arabia began recording observations earlier, direct temporal comparisons would be less efficient and some of these stations have issues in their metadata including missing data, and a limited time span prior to 1985 covered by some of their records. The study area is covered by 27 stations with more than 30 years of data, however, two were excluded in this study as those records have relatively large periods of missing data, 2011-2013 for Riyadh Old and 1985-1990 for Wadi-Aldawasser (Figure 3.1). Quality control (QC) procedures developed by Alghamdi and Harrington (2018) were applied to maximize the accuracy of the data used in the analysis. Application of the QC procedures improved the overall data quality by 3-5%, on average, at the station level (refer to Alghamdi and Harrington (2018) for details on the used QC procedures).

3.2.2 WSHTIs for subtropical arid climates under changing climate effects

Although Alghamdi and Harrington (2018) documents the rationale and the value of using a time-sensitive approach to examine warm season extreme heat events, some relevant information will be discussed briefly in this section to guide the process of WSHTIs development and to emphasize some important aspects. Given the nature of climate seasonality in study area (i.e., long warm season (Ali, 1994; Alkolibi, 1995) and the pronounced magnitudes and effects of early hot temperature events on heat-related morbidity and mortality (Hajat et al., 2002; Nasrallah et al., 2004), the warm season was defined for this study as May through September. The count statistics are limited by the number of days from May 1st to September 30th (154 days). Six WSHTIs (warm season hot temperatures indicators) were developed and explored (Table 3.1). To detect changes in these indicators of rare hot temperature events and to

account for different warming or cooling trends and variabilities among years and months (Figure 3.2), percentile thresholds were estimated using a time-sensitive, decadal (and on a month-by-month basis) approach (Robeson, 2004; Alghamdi and Harrington, 2018).

Table 3.1. The definition of warm season hot temperature indicators (WSHTIs). Percentile values were estimated using a decadal time-window on a month-by-month basis. Tmean, Tmax, and Tmin are mean, maximum, and minimum temperatures respectively.

Indicators	Name	Definition	Units
HD	Hot days	Annual count of days when daily Tmax \geq monthly 90th percentile of Tmax	Days
HDI	Hot day intensity	For selected days that exceed the 90 th percentile, the average difference between the daily Tmax and monthly 90th percentile of Tmax	°C
HN	Hot nights	Annual count of nights when daily Tmin \geq monthly 90th percentile of Tmin	Nights
HNI	Hot night intensity	For selected days that exceed the 90 th percentile, the average difference between the daily Tmin and monthly 90th percentile of Tmin	°C
HWE	Heat wave events	Annual count of events with two or more consecutive days with a daily Tmax and Tmin \geq monthly 90th percentile of the Tmax and 85th percentile of Tmin	Events
HWEI	Heat wave event intensity	For heat wave days, average of difference between the hottest day Tmean and monthly 88th percentile of Tmean	°C

The choice of a time-sensitive analysis minimizes the role of the hottest months in determining the relevant threshold values for both May and September. This time-sensitive approach (monthly and decadal) has been established to be more suitable for low-probability climate events that are impacted by a changing climate (e.g., Robeson, 2002a, 2002b, 2004; Robeson and Doty, 2005; Alghamdi and Harrington, 2018). The R8 method was used to estimate percentile thresholds as it delivers unbiased estimates and requires no distribution assumptions (Hyndman and Fan, 1996).

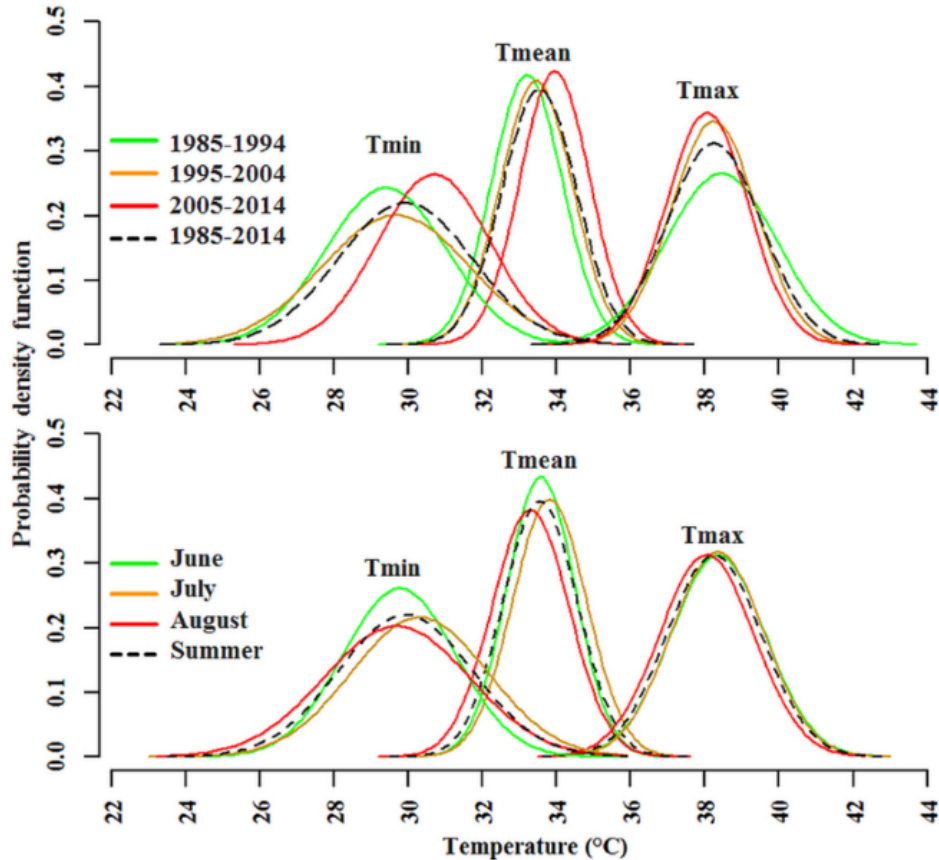


Figure 3.2. Distributions of the probability density function of daily temperatures at Gizan (25) for three decades using summer months (June-August) Tmean, Tmax, and Tmin (upper) and for 30-years summer season months Tmean, Tmax and Tmin (bottom). Gizan was selected as it exemplifies different temporal and shape changes found for many of the stations.

To allow direct comparison among the 25 stations through time and space, a relative indicators approach (i.e., use of the percentile technique for the data from each station) was applied for the WSHTIs. For the first 4 WSHTIs (hot days and nights and their intensity indices), the 90th percentile was used as the threshold. The 90th percentile was selected as it is commonly used for defining hot days and nights and it has been shown to optimize the balance of extreme versus other temperature events (Perkins and Alexander, 2013). However, for HW indices (HWE and HWEI) the percentile thresholds were reduced, since Tmin was built into both indicators. During periods with hot days, lower nighttime temperatures become necessary to allow for a period of relief by reducing the cumulative heat stress impact on organisms. Given the nature of

radiational cooling in an arid climate and the tendency of T_{min} to drop considerably (Oke et al., 1998) and the limited nighttime summer stress relief within such an arid climate type; the 85th percentile (i.e., warm nights) was selected as the T_{min} threshold for defining a HW event. For HW event intensity (HWEI), the 88th percentile of mean temperature (T_{mean}) was used to incorporate both T_{max} and T_{min} into the calculation. Since both T_{max} and T_{min} are used to define a HW, intensity of a HW was assessed by the T_{mean} of the hottest day, the peak of the HW (e.g., Perkins and Alexander, 2013; Alghamdi and Harrington, 2018). The 88th percent threshold could be critical for several sectors such as agricultural practices and energy generation.

3.2.3 Temporal trends analysis

Common statistical approaches for trend detection of climatic extreme indices are: rank-based tests for significance testing (e.g., Mann–Kendall and Spearman Rank Correlation) and slope-based tests for estimating the rate of changes (e.g., Least Squares Linear Regression and Sen’s Slope estimator). Indicators of intensity aspects (i.e., HDI, HNI and HWEI) are temperature values that can be rank ordered and thus the Mann-Kendall and Sen’s Slope methods were used, since they require no distribution related assumptions. However, the frequency of climatic extreme event indicators are count data (i.e., HD, HN and HWE) and thus event-count time series techniques are most suitable (Ryden, 2016; Alghamdi and Harrington, 2018).

In modeling event-count data, the occurrences of events are rare and commonly assumed to result from a Poisson process or density (Cameron and Trivedi, 1998; Chatterjee and Simonoff, 2013). Frequency of extreme climate events are count variables that can only have non-negative values (e.g., Alghamdi and Harrington, 2018); accordingly, use of a linear regression model is not appropriate as negative estimated mean responses are not possible

(Chatterjee and Simonoff, 2013). Further, the Poisson regression method relies on two critical assumptions that are fundamentally inline with the nature of extreme temperature events. The method assumes that the occurrences of events are independent and random. Unlike a linear regression model, a count regression model provides slope coefficients of the mean relative change (not the absolute change) in the expected response/occurrence associated with a unit change in the predictor variable.

By definition, extreme climate events are rare and thus variability in their counts is highly expected, which usually results in overdispersion (i.e., variance is greater than the mean) and with zero-inflation (an excess number of zeros or ‘no event’ observations). The Poisson regression model assumes that the mean and variance are equivalent (i.e., equidispersion) and uses a maximum-likelihood technique to estimate the Poisson mean parameter. Several techniques have been developed to correct for overdispersion, with the common approach being a Negative Binomial Estimator (Brandt et al., 2000), which also allows the presence of an excess number of zeros to be addressed by using a Zero-Inflated Negative binomial model (Chatterjee and Simonoff, 2013; Brandt et al., 2000). Table 3.2 presents the statistical frameworks used in this study to estimate temporal trends in HD, HN and HWE indicators. To select and compare models, the Vuong’s test (Vuong, 1989) was applied. For theory, mathematical terms and implementation, refer to Chatterjee and Simonoff (2013).

Table 3.2. Used framework for trend analysis of WD, WN, and HWE indicators. Modified after Yang et al. (2015).

Over-dispersion	Zero-inflation	Model
No	No	Poisson regression
Yes	No	Negative Binomial regression
No	Yes	Zero-inflated Poisson regression
Yes	Yes	Zero-inflation negative binomial regression

3.2.4 Spatial and temporal pattern recognition

The aim of this research component is to provide insight into how hot temperature events at the 25 stations behave through time and space. In other words, were there similarities among the time series for the stations? And if so, what were the spatial patterns? Previous studies have commonly used traditional statistical classification methods (e.g., equal interval and standard deviation) to map the temporal behaviors of climatic extreme events. These methods are one-value classification means; that is, stations with similar temporal statistics (e.g., average frequency or intensity) are grouped together. However, stations within groups do not necessarily behave similarly in time (i.e., across the 30 individual years).

Given the subjectivity in the use of such methods and the observed complexity of the HW events (e.g., Alghamdi and Harrington, 2018), less subjective and more advanced pattern recognition techniques are required. To explore the similarity and to detect common patterns in time, a time-series clustering (TSC) approach was applied. TSC aims to extract useful information to help recognize patterns and formulate hypotheses. Different TSC methods are available and a choice is based on the goal of the analysis. In clustering climate data, the hierarchical average-linkage (HAL) approach is commonly suggested when the goal is to recognize homogenous regions/stations (Robeson, 2004; Robeson and Doty, 2005). The method is among those commonly used in TSC particularly for short and small time-series datasets (Aghabozorgi et al., 2015). A primary goal of the spatial analysis in this study is to identify stations with similar time-series (homogeneous temporal behaviors) and thus, the HAL method was applied as it maximizes cluster homogeneity by minimizing (maximizing) within-cluster (between-cluster) variance (Unal et al., 2003).

One of the critical steps in TSC is the selection of similarity/dissimilarity measures. Different measurements are available and the choice is based on the objective of the analysis (Aghabozorgi et al., 2015; Liao, 2005). When the objective is to identify regions/stations with similar temporal patterns in time or shape, Euclidean distance or dynamic time warping (DTW) methods are recommended (Aghabozorgi et al., 2015). This approach, which conforms to the work (i.e., station level) in this study, is usually referred to as shape-based clustering that operates on the local patterns (Aghabozorgi et al., 2015). The Euclidean distance method is more suitable in TSC compared to DTW, particularly with short or moderate-length time-series with equal length and when the similarity in time is more important (i.e., the occurrence of events) (Wang et al. 2006; Aghabozorgi et al., 2015). Refer to Aghabozorgi et al. (2015) and Liao (2005) for further review and references on TSC and statistical distance measures.

To find reasonable grouping solutions and an appropriate number of clusters, three widely used and recommended cluster validity indices were used: Silhouette width, Dunn, and Calinski–Harabasz (CH) (Lord et al., 2017). For theory and mathematical terms, refer to Lord et al. (2017). Higher values are the goal in all the validity indices. Thus, they can help find a suitable solution that provides higher separation between clusters and more similarity within clusters. To evaluate the results from determining these indices and for further evaluation, the averages distances between and within clusters indices were used as well. Use of complementary validation methods is a highly recommended practice in finding reasonable grouping solutions (Handl et al., 2005). Cluster analysis was run for each of the hot temperature indicator time-series.

3.3 Results and Discussions

3.3.1 Evaluation of trends in the upper-limits of Tmax and Tmin

Temporal patterns of the 90th percentile of Tmax and Tmin determined on a yearly basis were explored. Trends in these percentile values were selected for evaluation due to possible unscaled relationship between changes in mean climate and the climate extremes and because hot temperatures and upper-tail variations in Tmax and Tmin are closely coupled (Seneviratne et al., 2012). Generally, warming trends were detected in thresholds for both Tmax and Tmin across the warm season months with a few surprising exceptions (Figure 3.3). Positive trends in annual Tmax and Tmin percentile values were found at most of the stations, with more pronounced increases for Tmin. These increases in the threshold for a hot temperature event suggest a change in the shape of the probability distribution and that a change in the climatology of the upper-tail conditions has occurred (i.e., rare warm events are getting hotter, and new norms are emerging). The positive trends at most stations support the methodological decision to use a decadal rather than period of record time window for determining extreme event thresholds. Thus, using the entire 30-year period to estimate the 90th percentile would violate the role of rarity and would result in miss detecting some possible rare events, particularly for short high-impact events. This could be a critical issue for stations with inconsistent monthly slopes.

As is expected with station level data, a few individual stations differ from the regional pattern and six of 25 stations had decreasing trends in some of their monthly Tmin values with more pronounced declines during either early or late warm season months. Gizan (25), on the Red Sea coast, had relatively constant negative trends for Tmax. This suggests the possible importance of local microclimatic conditions on changes in extreme events. Although some stations had either no sign of change or very small changes in the 90th percentile for their Tmaxs

and Tmins during different months, time-sensitive thresholds are still advantageous to account for possible variabilities; given the reported changes in the means and variances (e.g., Almazroui et al., 2014; Islam et al., 2015; Alghamdi and Harrington, 2018).

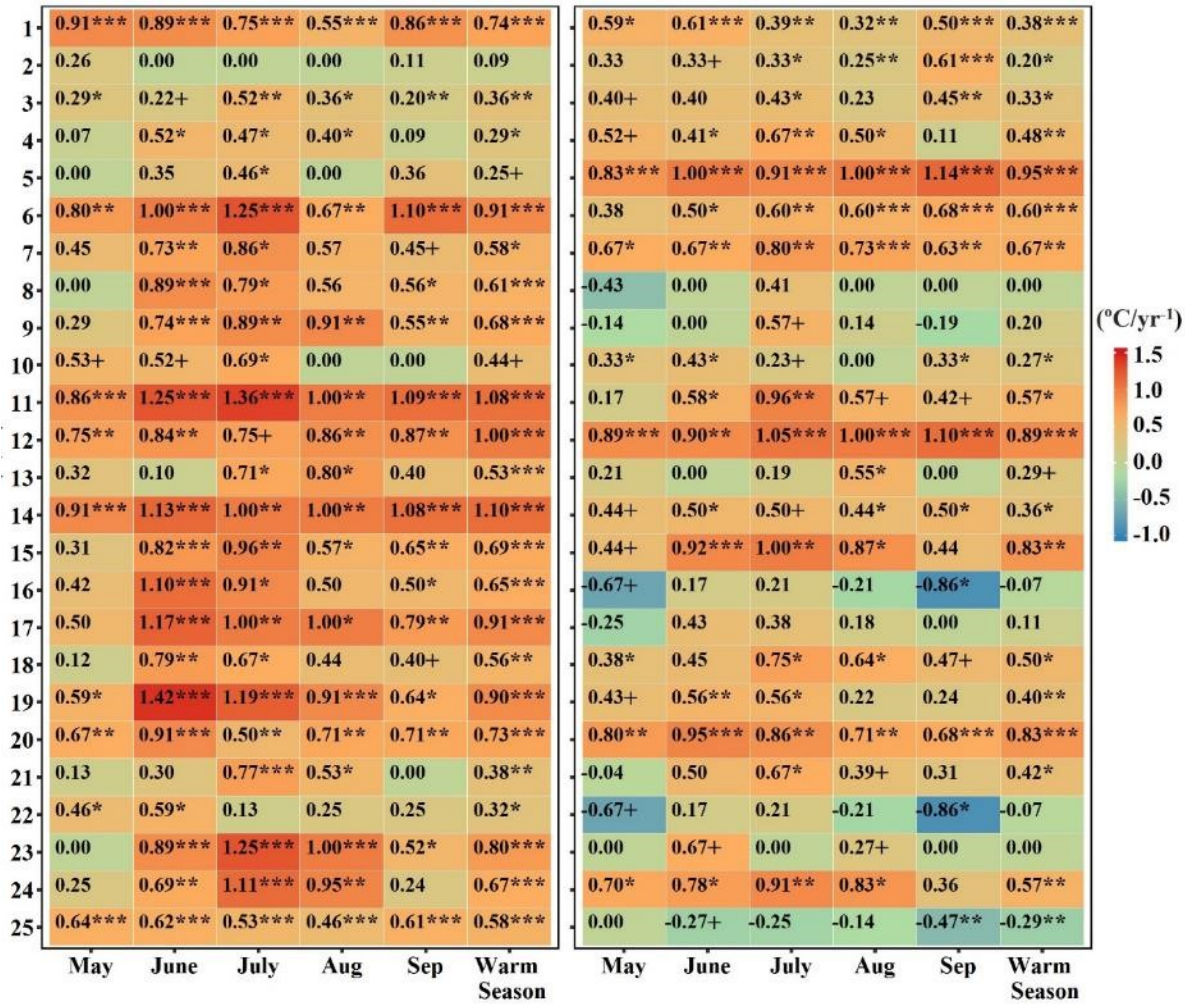


Figure 3.3. Heatmaps of decadal-based temporal trends in Tmin (left) and Tmax (right) 90th percentile values ($^{\circ}\text{C}/\text{yr}^{-1}$) at monthly and warm season (x-axis) time scale for each station (y-axis). *, **, *, and + $\alpha = 0.001, 0.01, 0.05, 0.1$ level of significances respectively. Trends were computed by Kendall-tau and Sen's slope estimator. For stations names and locations refer to Figure 3.1.**

It is also clear from Figure 3.3 that the magnitudes of slopes were different among warm season months. Months were not only under different trend magnitudes but also have different slope directions (i.e., positive or negative). Thus, use of a seasonal time scale (rather than monthly) will hide differences evident in individual monthly data. At Guriat (16), for example, if

the 90th percentile were estimated on a warm seasonal basis, hot events during months with upward trends would be over detected and less detected during months with downward trends. Downward trends largely suggest lower probability and intensity of hot temperature events but do not indicate an absence of extreme events.

From Figure 3.3 it is also clear that using a single atmospheric factor (e.g., just Tmax) would omit important aspects of the climatology of HWs, given the differences in the heatmap patterns for Tmax and Tmin. At a monthly scale, 59.2% of trends in Tmin were higher than those of Tmax, whereas 35.2% of Tmax trends were higher than those of Tmin. This suggests that any possible changes in the nature of a HWE at 59.2% of the studied stations are expected to be accompanied by more hazardous nighttime weather conditions (i.e., fewer periods of stress relief). At the 0.001 level of significance, 16 stations had significant positive trends in their Tmin 90th percentile, whereas only 9 stations had significant positive trends in Tmax 90th percentile. From these observations, it can be concluded that the impact of climate change on hot weather events was more pronounced at night for more of the stations in Saudi Arabia.

At the monthly scale, significant warming trends at the 0.001 level of significance were more frequent during September in the Tmax 90th percentile and during June for the Tmin 90th percentile. At the station level, Najran (5) had the highest significance level of an upward trend for Tmax 90th percentile in all months and for the entire warm season followed by Gassim (12). For the Tmin 90th percentile, Abha (1) and Gizan (25), which are both in the southwest part of the Kingdom but at very different elevations, had the highest significance level of upward trends across all months and for the entire warm season. Data analysis for Al-Jouf (11) in the north also suggests a strong upward signal for Tmin, especially in June and July. These examples indicate

the importance of using both Tmax and Tim in studying HWs and the important role of local complexity.

3.3.2 Temporal trends in WSHTIs

In contrast to the analysis done for Section 3.3.1, results presented herein used a decadal time window. Yearly totals of hot days and hot nights averaged more than 15 days per year and ranged considerably across the 30 years and among the 25 stations (see Table 3.4 in section 3.3.3). The frequency of HW events was also quite variable in time and space. Warm/hot temperature events largely result from physical processes at either regional (i.e., atmospheric circulation) or local levels (e.g., urban heat island). Accordingly, an event might be reported by adjacent stations depending on the spatial coverage of the event and the distance between stations. Distinguishing among events that occur at multiple stations and physical processes is beyond the scope of this statistical analysis which was performed at the station level.

Hot days (HDs) and hot nights (HNs) had statistically significant increasing trends only at two stations (Najran (5) and Gassim (12)) and one station (Jeddah (23)), respectively (Table 3.3). For both HD and HN, a majority of stations in Saudi Arabia have an upward trend. Analysis of Hot Day Intensity (HDI) produced a significantly rising trend at one station (Taif (4)) and a significant downward trend at Sharurah (10). Hot Night Intensity (HNI) had only a significant negative trend at Turaif (8). For the Heat Wave Event (HWE) indicator, four stations had a significant upward trend (Taif (4), Gassim (12), Guriat (16) and Makkah (19)), while only two stations had significant upward trends for Heat Wave Event Intensity (HWEI) (Sharurah (10) and Makkah (19)). It is worth mentioning that the slope coefficients of HD, HN and HWE are to be interpreted as one unit of change in the predictor variable (i.e., years) corresponds to mean relative change of one % in the expected response variable (i.e., HD, HN and HWE).

Table 3.3. Decadal-based temporal trends in annual warm season hot temperature indicators (WSHTIs). *, **, *, and + $\alpha = 0.001, 0.01, 0.05, 0.1$ level of significance respectively.**

ID	HD (% Days)	HDI (°C)	HN (%Nights)	HNI (°C)	HWE (%Event)	HWEI (°C)
1	10.60	0.03	10.59	-0.04	7.93	0.00
2	7.38	0.06	9.59	0.01	17.44	0.00
3	1.65	-0.01	9.98	0.06	21.40	0.08
4	18.40	0.08*	11.35	0.00	45.95*	0.00
5	24.66+	-0.03	3.66	-0.09	28.37	0.00
6	7.62	0.00	4.85	-0.07	23.83	0.00
7	3.15	-0.03	-1.65	0.04	-11.08	0.00
8	5.47	0.02	9.25	-0.21*	16.53	0.21
9	9.74	0.01	2.01	-0.08	14.26	0.24
10	6.63	-0.06+	2.72	-0.09	20.69	0.21*
11	-6.72	0.09	1.51	-0.13	-3.38	-0.18
12	30.18*	-0.07	7.32	-0.04	30.62*	0.02
13	6.97	0.04	-3.41	0.07	-4.58	0.00
14	-0.06	-0.03	0.34	-0.01	-0.59	0.00
15	-3.36	-0.04	-2.39	0.12	7.55	0.28
16	-3.64	0.07	0.85	-0.02	25.51+	0.32
17	-7.62	0.05	-3.26	0.10	0.50	0.23
18	5.52	-0.07	-4.08	0.03	3.31	-0.26
19	2.58	0.06	9.56	0.00	59.80**	0.85***
20	6.19	0.05	-0.20	0.01	20.35	0.00
21	4.20	0.19	2.93	0.01	-2.98	-0.09
22	3.05	-0.10	-0.15	-0.09	-47.34	0.00
23	3.68	0.01	8.03+	0.04	17.44	0.00+
24	9.48	0.02	5.47	0.03	14.53	0.00
25	-0.42	0.00	4.70	-0.04	8.95	0.00

Different slope patterns (i.e., both upward and downward) were found for all the indicators and few stations had statistically significant trends. In both HD and HWE indicators, 24% of stations had a negative slope value and 28% of the stations had a negative slope for the HN indicator. For their corresponding intensity indicators, 36%, 12% and 48% of stations had negative slopes, respectively. However, it is important to emphasize that the lack of significant slope values does not mean there are no changes/trends. Instead the analysis indicates the absence of enough evidence to conclude statistically significant changes/trends, since

significance statistics do not provide real quantitative confidence about the certainty of patterns (Ambaum, 2010).

Use of a decadal window to determine thresholds for temporal trends has an impact on data interpretation. Upward and downward trends identified here suggest that there were factors other than what a changing average climate might have contributed to the observed changes. In a relatively similar arid environment, Balling et al. (1990) showed that the warming trend in summer mean temperatures in Phoenix, Arizona, USA, had contributed more to an increased frequency of moderate Tmax events than of extreme Tmax events. In Phoenix, a considerable increase in the incidence of hot night events was observed. Differences could be due to urban growth impacts or to differences in the nature of changes in the shapes of the Tmax and Tmin probability distributions (Robeson, 2002b). Other factors could also have an influence. Urbanization has been reported not to provide a substantial contribution to the recent temperature warming in Saudi Arabia (Almazroui et al., 2013). Other potential contributing factors were reported to include changes in precipitation patterns, atmospheric circulation, or dew point temperature (AlSarmi and Washington, 2011, 2013). However, these factors have both spatial and seasonal differences, highlighting the importance of interpretation at the local scale.

There were no clear and consistent geographic patterns among HWs indicators (HWE and HWEI) and HD or HN indicators, suggesting that local factors might play more important roles than large-scale factors. Except for station 21, the HWE indicator frequently had a negative slope whereas there was only one negative slope for either HD or HN (Table 3.3). This could indicate that HWs at these stations are controlled more by the indicator with a negative slope. At 52% of stations, HD, HN, and HWI had similar slope directions, suggesting the possibility that hot days and nights had equal contributions to the frequency of HWEs at these stations. Although

Arar (15) and Rafha (17) had downward slopes in HD and HN indicators, the related HWE indicator showed an upward slope. This curious finding could suggest that the physical processes that induced a majority of the detected hot days and nights events were different from those that induced the detected HWs. Most of the negative slopes in both HD and HN indicators were at stations located in the northern part of the country suggesting hot events in this region are controlled by different physical processes or there has been a change in their controlling processes.

3.3.3 Spatial pattern recognition of WSHTIs

To find the suitable spatial grouping solution for each WSHTI, validity indices were carefully examined. Figure 3.4 shows the validity indices for the HD indicator (hot days). The Silhouette index suggested a 2-clusters solution as it had the highest value. However, the Dunn and CH indices did not support that solution. Dunn index results suggested either 6, 7, 8, 9 or 10 clusters. The 6-cluster solution was supported by the other indices. For instance, a closer look at the Dunn and CH indices shows that there are no substantial improvements between the 6 and 13 cluster solutions. When the number of clusters increased after 6, each new cluster had only one station until 12 clusters, where the additional new two clusters (12 and 13) had two stations in each, as shown in the cluster dendrogram Figure 3.4 This indicates a very low improvement in between and within cluster distances (i.e., separation and homogeneity) after 6 clusters.

Such a characteristic of clustering indexes was present for all the other WSHTIs, and it was more pronounced in the intensity indicators. This could be due to the distance measure used and/or the classifier, or the climatology of the study area and the selected stations. In a quick exploration, the Kendall correlation was used as a measure of similarity/dissimilarity and a similar case was still present for the intensity indicators. Thus, a 6 cluster solution was selected

for the HD indicator because it optimizes between generalization and individual station details. A similar procedure was followed to find suitable solutions for the other WSHTIs.

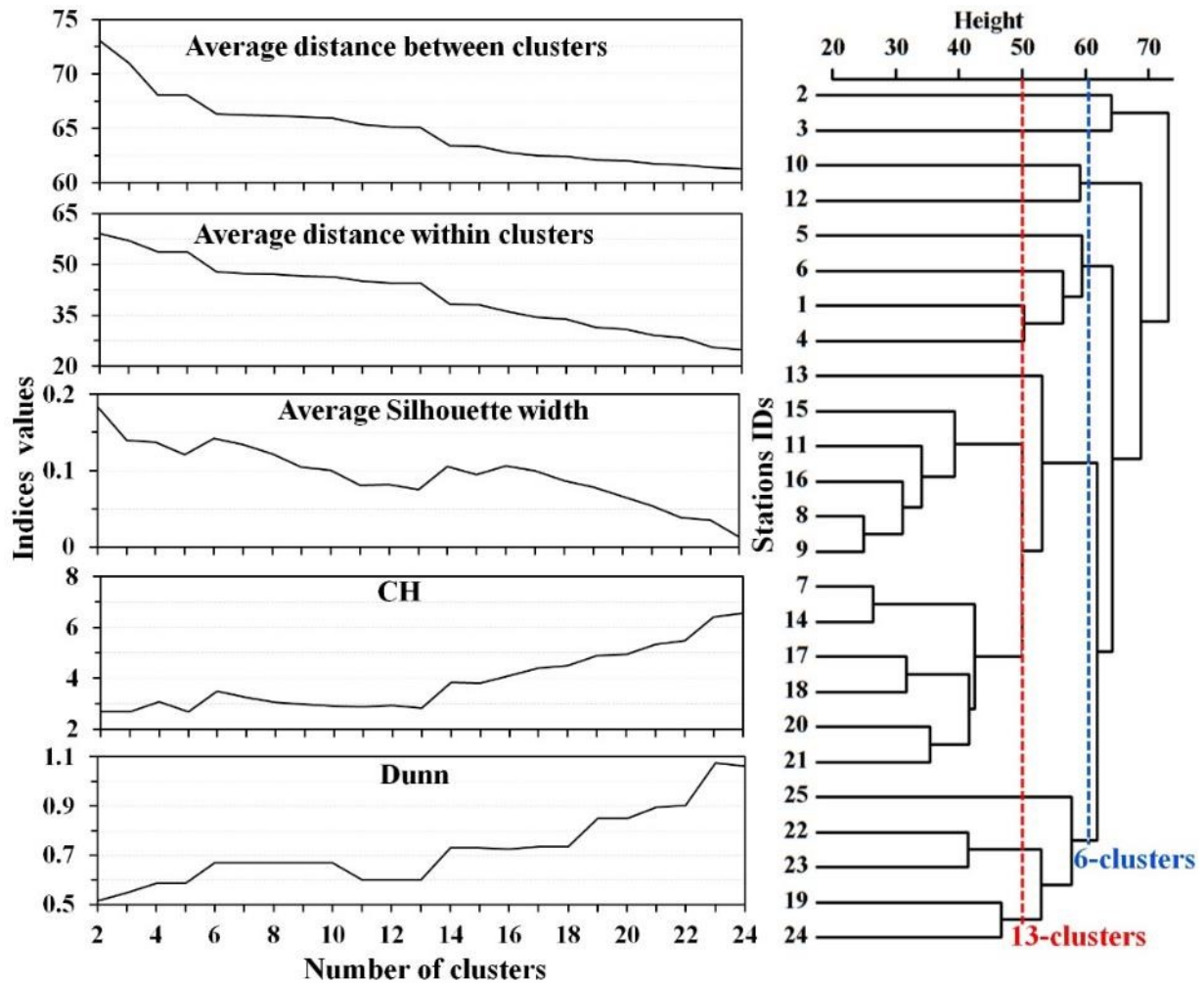


Figure 3.4. Validity indices for the HD indicator (left) and cluster dendrogram (right) along with stations IDs.

The spatiotemporal patterns of WSHTIs over the 30-year period using a time-sensitive approach are displayed in Figure 3.5. The general spatial patterns are different between the frequency and intensity of each indicator, which may suggest that the leading factors for each WSHTI are different. Except for a few stations, the northern part of Saudi Arabia showed similar HD and HN spatial behavior. The large areal coverage of cluster 4 in both indicators suggests that the frequency of hot days and nights were more related to large-scale factors (i.e., synoptic

atmospheric circulation patterns). Al-Ahsa (20), Wejh (21), Dhahran (22) and Yenbo (24) behaved differently in their HD and HN indicators, highlighting the possible effects of a nearby water body, which may have differing impacts during the day and night. Differences could be due to changes in wind pattern or the effects of other local factors (e.g., urban heat island). The corresponding intensity indicators (HDI and HNI) showed different spatial patterns. Thus, local factors could be more important in determining the event intensities. The effects and type of local factors may differ from daytime to nighttime, as in the case of Wejh (21) and Dhahran (22).

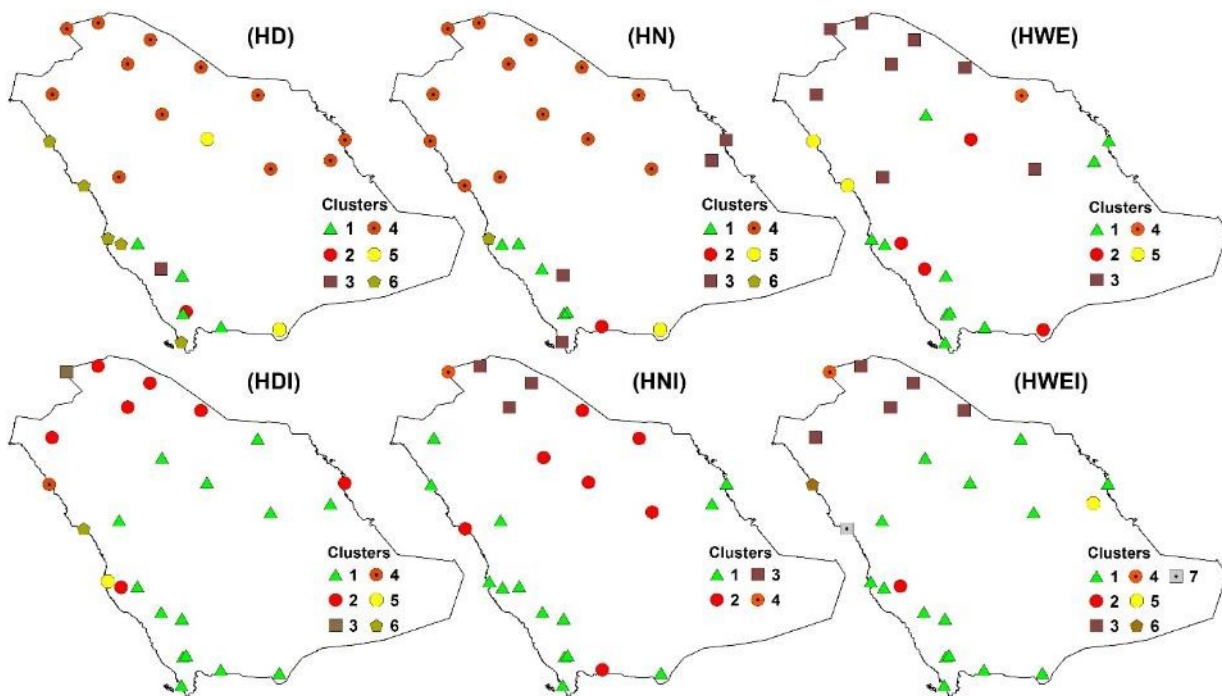


Figure 3.5. Maps showing the clustering of stations of WSHTIs. For stations names refer to Figure 3.1.

Stations in the southwestern part of Saudi Arabia showed relatively irregular cluster patterns for HN and HD (Figure 3.5). However, their corresponding intensity indicators, HDI and HNI, tended to cluster together. This region has higher elevations with complex mountain topography and more dense vegetation cover with higher relative humidity, and it is highly likely that these factors have different roles for each WSHTI aspect (frequency v. intensity). Although

stations in this region and several stations from the central part of the Kingdom were classified into similar HDI clusters, the cluster dendrograms showed these stations were not exactly similar in their temporal behaviors, suggesting differences in local factors. Similarly, HWE and HWEI indicators produced different spatial patterns. A large portion of stations in the HWE analysis was classified into cluster 1 and they are coastal and high elevated stations. This could indicate that relatively moist air is a major factor.

Although Al-Baha (3) and Taif (4) are at higher elevation, they were classified into a different cluster (cluster 2) with two internal stations (Sharurah (10) and Al-Jouf (11)), where other microclimate factors could be more important. These two highland stations had higher annual means and standard deviations compared to the other stations at high elevations. Interestingly, the HWEI indicator showed relatively similar spatial clustering patterns to those of the HDI indicator. Such a similarity could suggest that HW intensities patterns were related to the pattern of hot days. Throughout all the 6 indicators, few stations were classified independently, where they were found to have distinct patterns of either frequency or intensity compared to their neighboring stations. This is in support of the technique employed for spatiotemporal analysis.

To summarize the overall spatiotemporal patterns of all the 6 WSHTIs, one can use a dimensionality reduction technique (e.g., principal component analysis). However, two possible methods were proposed for simple and straight forward analyses (i.e., interpretations). Since the hierarchical average-linkage (HAL) method uses Euclidian distance to calculate similarity/dissimilarity among objects (i.e., time-series of stations) for each indicator, the resultant measurements could be used to epitomize all WSHTIs' classifications. The first possible method is to average the calculated Euclidian distances among stations of all 6

indicators and use that average as the similarity/dissimilarity input to the clustering algorithm (i.e., HAL). This measurement could be understood as the mean indicators' distances (MID), where station cluster membership is determined directly based on their overall memberships according to their individual distances for each WSHTI. The second possible method is to standardize and average WSHTIs for each station and use that average statistic to calculate the overall Euclidian distance among stations. Then the resulting distance is used as an input to the clustering algorithm, which can be understood as the distance of mean standardized indicators (DMSI). Here, the overall Euclidian distance is derived from the average stations' time series. In both methods, all indicators are standardized, zero mean and unit variance, and are weighted equally in the cluster analysis.

Using similar validation indices and procedures as in Figure 3.4, 6 and 8-clusters solutions were selected for DMSI and MID, respectively (Figure 3.6). Arar (15), Makkah (19), Dhahran (22), Jeddah (23), and Gizan (25) were classified differently by the two distance methods. To evaluate and measure the cluster goodness/degree of fit of both classifications, the cophenetic correlation coefficient (Sokal and Rohlf, 1962) was calculated for each hierarchical classification tree. The MID classification had a higher coefficient value of 0.74 compared with the DMSI classification method (0.68). Further, the correlations between each cluster's stations and their corresponding cluster averages were calculated for each WSHTI and each distance method (Figure 3.7). The MID solution tended to have higher median values and a lower range of correlations. Therefore, the MID solution (Figure 3.6B) was selected to summarize and describe the overall spatiotemporal patterns of WSHTs in the study area.

Overall clustering of the spatiotemporal behaviors of all WSHTIs (Figure 3.6B) suggested three large clusters/regions (1, 2 and 3) that showed coherent geographical patterns

(Table 3.4). In linking the results in Figure 3.6B with Table 3.4, Table 3.5 summarizes the main characteristics of WSHTI per cluster. Cluster 1 includes stations that are located in highland areas (southwest) and had higher HD frequency and variability and fewer intense events. Stations within clusters 2 and 3 are in dryer lands and were characterized by high HWE frequencies and higher intensities. Stations in Cluster 4 had low HW and HD frequency and variability, respectively. Clusters 5-8 are single-station clusters, and they are located along the Red Sea, highlighting the importance of local factors, such as more moisture and a sea breeze. However, WSHTIs showed differences among these clusters suggesting variation in the effects of local factors.

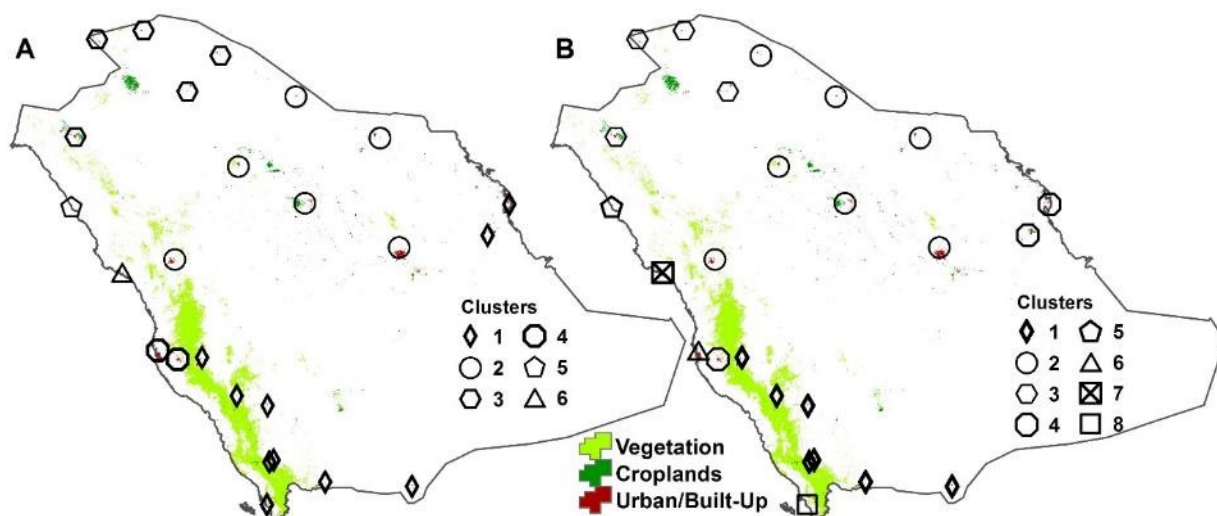


Figure 3.6. Clustering stations using Distance of Mean Standardized Indicators (DMSI), A and Mean Indicators' Distances (MID), B. Land cover data was obtained and modified after Broxton et al. (2014). For stations names refer to Figure 3.1.

It is clear that the clusters not only differ from one to another but also from indicator to indicator. Inverse time and space patterns between event frequency and their intensity were common for cluster 1 (Table 3.4). The effects of high elevation and vegetation cover could explain these patterns for cluster 1 (Figures 3.1 and 3.6). Another notable and common statistical pattern was that clusters with higher annual hot temperature event intensity tended to have higher

annual variabilities. Frequency aspects showed a relatively similar pattern but, were inconsistent. Stations within clusters did not experience similar temporal trends within and among WSHTIs (Table 3.3). This could be explained by the nature of the similarity/dissimilarity measure used for clustering, i.e., Euclidean distance. This cluster measure is based on similarity in time, i.e., occurrences, not in shape, i.e., change (Aghabozorgi et al., 2015).

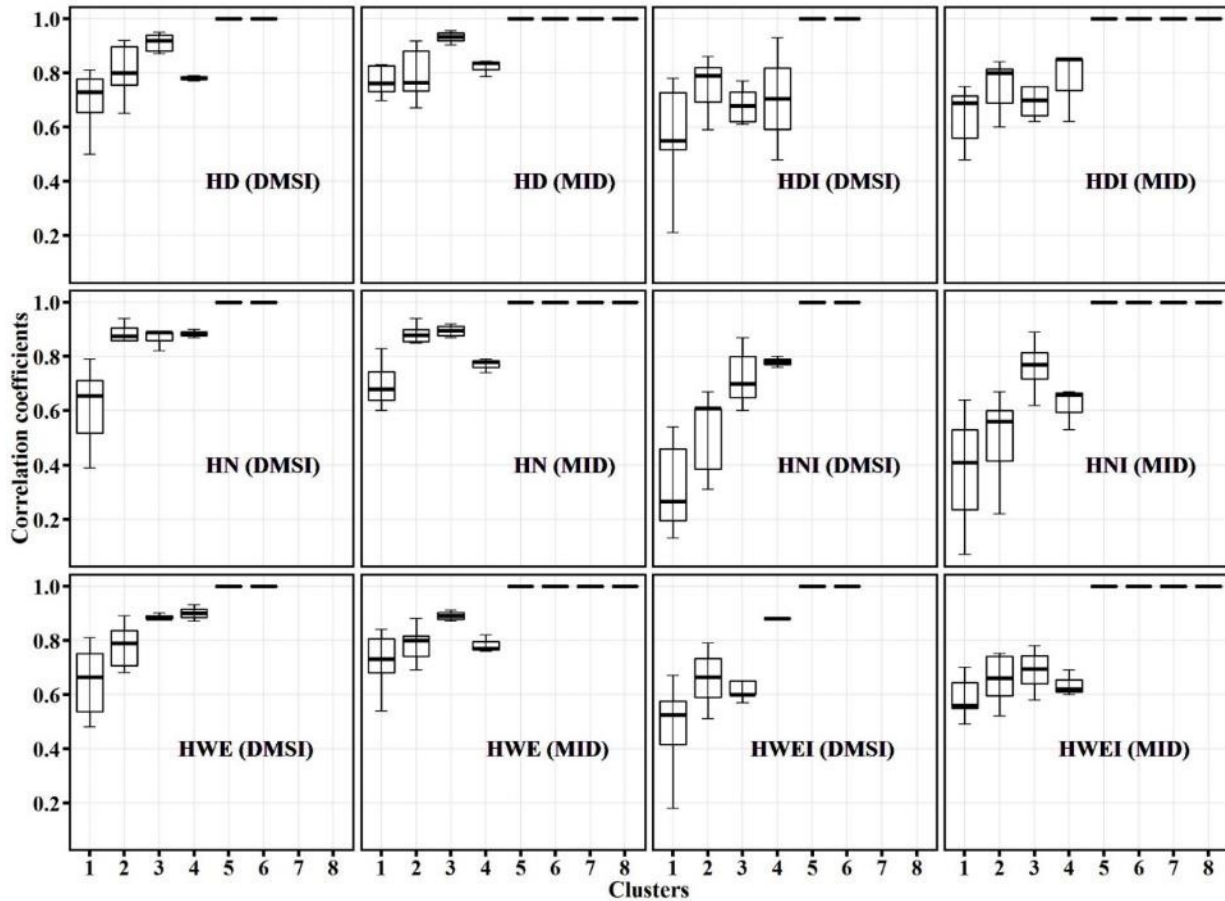


Figure 3.7. Boxplots of Pearson correlations between each cluster’s stations and cluster average for each WSHTI and each distance method. DMSI: Distance of Mean of Standardized Indicators, MID: Mean Indicators' Distances.

Table 3.4. Heatmaps of descriptive statistics based on annual totals for the 30-year period 1985-2014.

Cluster	Station ID	Average						Standard deviation					
		HD	HN	HWE	HDI	HNI	HWEI	HD	HN	HWE	HDI	HNI	HWEI
1	1	16.8	16.6	1.1	0.36	0.69	0.80	9.12	7.92	0.99	0.18	0.18	0.74
	2	17.07	16.97	1.13	0.34	0.65	0.49	15.4	7.72	1.59	0.17	0.26	0.67
	3	20.13	18.77	2.03	0.35	0.48	0.88	12.86	8.97	1.71	0.16	0.22	0.70
	4	18.73	17.97	1.43	0.39	0.62	0.94	9.97	9.2	1.57	0.18	0.20	1.34
	5	19.2	18.13	0.93	0.33	1.02	0.55	11.48	8.31	1.11	0.17	0.27	0.73
	6	17.33	16.97	1.2	0.35	0.82	0.65	12.71	9.6	1.4	0.21	0.29	0.71
	10	22.37	18.93	1.43	0.28	0.68	0.53	14.06	13.24	1.7	0.15	0.38	0.61
2	7	17.1	16.1	1.1	0.61	1.26	1.51	10.09	6.71	0.88	0.27	0.23	1.18
	12	20.17	17.6	1.97	0.56	1.03	1.23	11.08	11.5	1.77	0.27	0.36	0.85
	13	18.43	17.23	2.13	0.47	0.84	1.25	10.52	6.64	1.87	0.19	0.23	0.78
	14	17.27	16.13	1.53	0.63	1.02	1.39	9.94	8.22	1.85	0.25	0.33	0.99
	15	16.33	16.23	2.13	0.87	1.05	1.69	10.6	8.34	1.87	0.43	0.41	1.28
	17	16.2	15.9	2.23	0.89	1.22	1.70	6.91	9.53	1.61	0.37	0.31	1.06
	18	16.83	16.5	2.63	0.73	1.01	1.56	7.48	8.57	1.61	0.39	0.32	0.77
3	8	17.7	18.17	2.77	0.94	1.06	2.04	8.94	9.32	1.74	0.37	0.48	0.99
	9	18.3	17.37	2.33	0.81	0.82	1.83	7.8	9.61	1.6	0.29	0.39	0.80
	11	17.03	17.1	2.3	0.83	0.97	1.69	11.18	8.45	2.14	0.33	0.38	1.12
	16	16.3	16.47	2.17	1.20	1.28	2.65	9.06	8.11	1.72	0.45	0.48	1.42
4	19	16.83	18.07	1.03	0.87	0.72	1.20	8.63	8.73	1.25	0.29	0.23	1.16
	20	15.97	16.57	1.07	0.68	0.68	1.01	8.3	7.32	1.31	0.32	0.27	1.39
	22	16.3	16	0.53	0.96	0.79	0.73	7.11	8.44	0.86	0.35	0.25	1.00
5	21	16.5	17.33	1.57	1.98	0.73	2.04	7.42	8.07	1.19	0.83	0.30	1.40
6	23	19.5	22.13	0.63	1.33	0.60	0.79	8.15	9.62	0.93	0.71	0.25	1.18
7	24	16.43	17.73	1.73	1.27	0.89	2.46	7.11	7.98	1.44	0.46	0.26	1.54
8	25	17	19.4	0.6	0.53	0.38	0.39	10.13	9.45	0.81	0.21	0.17	0.48

Low Moderate High

Table 3.5. Summary of WSHTs main characteristics of clustering. -, *, and +: low, moderate, and high year-to-year variability, respectively, SID: station ID.

Cluster	Name	Land type	WSHTs main frequency characteristics		
			Low	Moderate	High
1	South	Highland	HDI-, HNI*, and HWEI-	HN*, and HWE*	HD+
2	North-East	Interior	HN-	HD*, HDI*, and "HD*"	HNI+, HWE+, HWEI*
3	North		---	HD- and HN*	HWE+, HDI+, HNI*, and HWEI+
4	Mixed	Highland (SID 19) Interior (SID 20), and Coastal (SID 22)	HD-, HN-, HWE-, HNI- and HWEI+	HDI*	---
5	North-West	Coastal	HD-, and HNI*	HN-, and HWE-	HDI+, and HWEI+
6	West		HWE-, HNI-, and HWEI+	---	HD-, HN+, and HDI+
7	West-North		HD-	HN-, HWE*, and HNI*	HDI+ and HWEI+
8	South-West		HWE-, HDI-, HNI-, and HWEI-	HD*	HN+

3.4 Summary and Conclusions

Decent temporal trends and spatial patterns in six hot temperature indicators in Saudi Arabia were explored for the warm seasons (May through September) of 1985-2014. The indicators studied focused on the frequency and intensity of hot days, hot nights and HWs. The definitions of these events were developed for use with a monthly and decadal time-sensitive approach to accommodate different individual station trends (i.e., warming or cooling) and variability. Trends in Tmax and Tmin percentiles were analyzed on a monthly time scale to examine the effects and importance of different time bases for determining the occurrences of hot temperature events. Further a novel method for time-series clustering was introduced to the

field of warm/hot temperature event analysis to detect and recognize spatiotemporal patterns of hot temperature events.

Different patterns were observed over time and space not only across stations, but also among indicators. Overall, the results suggest that synoptic-scale factors such as atmospheric circulation patterns and local and regional factors, such as elevation, latitude, and distance from a large body of water are likely responsible for the temporal and spatial patterns. Decadal and monthly time-sensitive approaches were used to capture any possible general changes or variations in the Tmax and Tmin probability distributions, however there is a need to use additional measurements (e.g., variance, kurtosis and skewness) to understand and account for the differences in the statistical characteristics of the extreme temperature climatology of Saudi Arabia, particularly for the upper probability events (i.e., high extremes).

As climate warming in the region is accompanied by high year-to-year temperature variability (e.g., Hansen and Sato, 2016) and changes occur in precipitation, atmospheric circulation, and dew point patterns (AlSarmi and Washington, 2011, 2013), the statistics of the upper probability events are highly expected to have notable variabilities if not changes. Extreme temperate events are more sensitive to year-to-year variability, since small changes in the distribution of mean temperatures could result in substantial changes in the statistical distribution of upper and lower-tails and their corresponding extremes (Mearns et al., 1984; Katz and Brown, 1992; Schär et al., 2004). This would also raise a challenging question as to whether or not mega-extreme events (e.g., the 2003 European or the 2010 western Russia HWs) should be included in defining the mean climates, from which thresholds of extremes are determined.

Given the nature of our climate system (sensitivity and nonlinearity) and as climate is projected to continue to warm with more hot temperature events (e.g., Pal and Eltahir, 2015;

Mora et al., 2017), one of the implications of this work is to establish baselines and appropriate methods for future efforts. This study shows the importance of using definitions that adjust for changes/variabilities in climate conditions. Adaptation, vulnerability, and future climate conditions are important for society and among a growing number of research interests. For these studies to help prepare us for future challenges with climate warming, changes in the features of climate conditions and possible effects of extraordinary climate or weather events (e.g., drought or major HWs— European 2003 HW) should be comprehensively considered and understood. Hot weather response measures, for instance, have been implemented in several cities and have resulted in notable reductions in heat-related health outcomes (e.g., Fouillet et al., 2008; Ebi et al., 2004). Mitigation of heat hazard effects relies on the implementation of effective warning systems and emergency responses plans (Bao et al., 2015), and requires a good understanding and detailed analyses not only of the adaptation dimension (i.e., the ability to cope with), but also with the hazard exposure dimension (i.e., hot temperature events).

Chapter 4 – A preliminary assessment on synoptic climatology and sea surface temperatures teleconnections for warm season heat waves in Saudi Arabia

Abstract

Little information is available about the synoptic patterns and physical factors contributing to the formation and intensity of heat waves (HWs) in Saudi Arabia. The research objectives were to identify the synoptic situations that are related to HW occurrence, to match different HW aspects (frequency and intensity) to different circulation types, and to examine the possible links/associations between HW days and the sea surface temperature (SST) anomalies of closely associated water bodies (i.e., Mediterranean Sea, Black Sea, Caspian Sea, Arabian Gulf, Arabian Sea, and Red Sea).

Using reanalysis data (1985-2014) three weather/circulation types were detected using Ward's cluster method. Together, weather Types 1 and 3 induced 57.5% of HW days and connected with negative anomalies in sea level pressure with lower heights and warmer temperatures at the 850 hPa level. Intensification of Indian Summer Monsoon Trough and Arabian heat lows were key atmospheric features related to weather Types 1 and 3. Weather Type 2 induced 42.5% HW days and it was related to positive anomalies at all heights. Anomalies of SSTs of the Red Sea, Arabian Gulf, Caspian Sea, Black Sea, and Mediterranean Sea were positive for both weather Types 1 and 3. SSTs anomalies seem to be a more important factor for HW day intensity. HWs in Saudi Arabia tend to occur during regional warming due to atmospheric circulation conditions and SST teleconnections.

4.1 Introduction

The climate of Saudi Arabia is warming, and extreme temperature events are becoming more frequent (e.g., Almazroui et al., 2014; Athar, 2014; Donat et al., 2014; Raggad, 2017a; Alghamdi and Harrington, 2018), as observed by the significant upward trend in the frequency of extreme temperature events in the last few decades (e.g., AlSarmi and Washington 2011, 2013; Almazroui et al., 2012a, 2012b; 2014; Rehman and Al-Hadhrami, 2012; Athar, 2014; Donat et al., 2014; Islam et al., 2015). Climate modeling studies suggest that the frequency, intensity, and duration of heat waves (HWs) are expected to increase as the global and local climate continues to warm (e.g., Lelieveld et al., 2012; Sharif, 2015; Pal and Eltahir, 2016; Almazroui et al., 2016). Changes in precipitation patterns, atmospheric circulation, dew point temperature, the Southern Oscillation (ENSO), the North Atlantic Oscillation (NAO), continentality and aridity conditions are some of possible contributing factors for the warming climate in the region (AlSarmi and Washington, 2011, 2013; Donat et al., 2014; Almazroui et al., 2014; Kenawy et al., 2016). However, available information is very scarce on the possible effects and the underlying mechanisms by which these factors contribute to the recent climate changes and extreme temperatures for Saudi Arabia.

It has been established in the literature that anomalies in atmospheric circulation, soil moisture and temperature, and sea surface temperatures (SSTs) are among the major factors linked to extreme HWs with respect to their formation and intensity (e.g., Black et al., 2004; Fischer et al., 2007a, 2007b; Feudale and Shukla, 2011; Perkins, 2015). High pressure synoptic systems have been reported to be the atmospheric circulation feature most closely associated with summer HWs at the global scale (Fischer et al., 2007b; Perkins, 2015). However, this may not be the case for summer HWs in Saudi Arabia, with its subtropical arid climate where thermal

lows are reported to be the predominant factor controlling the summer atmospheric circulation across the Arabian Peninsula (Bitan and Saaroni, 1992; Ziv et al., 2004; Almazroui, 2006).

Almazroui et al. (2015) showed that cyclonic weather types were the leading circulation conditions inducing hot days and warm nights on the annual timescale. Nevertheless, available detailed information about the synoptic patterns and physical factors contributing to the formation and intensity of HWs in Saudi Arabia is very scarce.

Atmospheric circulation alone has been suggested to not fully explain the formation and intensity of HWs as in the case of the 2003 European HW (e.g., Ferranti and Viterbo, 2006; Fischer et al., 2007a, 2007b; García-Herrera et al., 2010; Feudale and Shukla 2011). Positive feedbacks between land surface temperature and the atmospheric circulation were suggested to amplify the 2003 European HW through land surface-atmosphere interaction or coupling, low soil moisture (due to a precipitation deficit during the previous seasons, i.e., winter and spring) and a warm SSTs anomaly (e.g., in the North Atlantic and the Mediterranean) (Ferranti and Viterbo, 2006; Fischer et al., 2007a, 2007b; García-Herrera et al., 2010; Feudale and Shukla 2011). Surface temperatures are affected by low soil moisture as dryness decreases the latent heat flux and increases the sensible heat flux (Fischer et al., 2007b; García-Herrera et al., 2010).

The exact contributions of SSTs (global v. local patterns) to HW events (including their occurrence and intensity) are not entirely agreed upon due to the complexity of ocean-atmosphere coupling and related teleconnections (Fischer et al., 2007b; García-Herrera et al., 2010). However, the general contributions of SSTs to HWs could be summarized as: the warm SST anomaly heats the lower boundary layer of the atmosphere which limits the sea surface from cooling and the leading circulation condition is intensified (Feudale and Shukla, 2007; García-Herrera et al., 2010). For the 2003 European HW, global SSTs anomalies helped to set up the

ideal atmospheric circulation while local SSTs contributed more to local HW response (e.g., Feudale and Shukla, 2007; Fennessy and Kinter, 2011; Feudale and Shukla, 2011).

The research objectives of this study were to identify the general synoptic situations that cause warm season HW occurrence in Saudi Arabia, to match different HW aspects (frequency and intensity) to different circulation types, and to examine some possible links/associations between HWs and the SST anomalies of nearby large bodies of water (i.e., Mediterranean Sea, Black Sea, Caspian Sea, Arabian Gulf, Arabian Sea, and Red Sea).

4.2 Research Design and Methods

4.2.1 Study area and data

During the summer season Saudi Arabia is affected by different air masses and pressure systems (Takahashi and Arakawa, 1981; Alkolibi, 1995; Almazroui, 2006). While the southwestern region is under the influence of maritime Tropical air masses (mT) that migrate northward from the western Indian Ocean, the rest of the country is controlled by a continental Tropical air Mass (cT) that originates over the central Asia or the African Sahara and thus brings hot and dry air. The elevation of Saudi Arabia is generally low in the east and gradually increases toward the more mountainous southwest region (Figure 4.1).

Daily maximum and minimum air temperature data recorded at 25 weather stations across Saudi Arabia (Figure 4.1) over a 30-year period (1985–2014) were used to identify HWs. Data sets were obtained from the records of the Saudi General Authority for Meteorology and Environmental Protection (GAMEP). Data from 25 weather stations over 30-year period were selected as they allowed for a relatively long homogeneous time series with fewer gaps of missing records. Following the procedures described in Alghamdi and Harrington (2018), data

quality was assessed and improved by 3-5% at the station level.

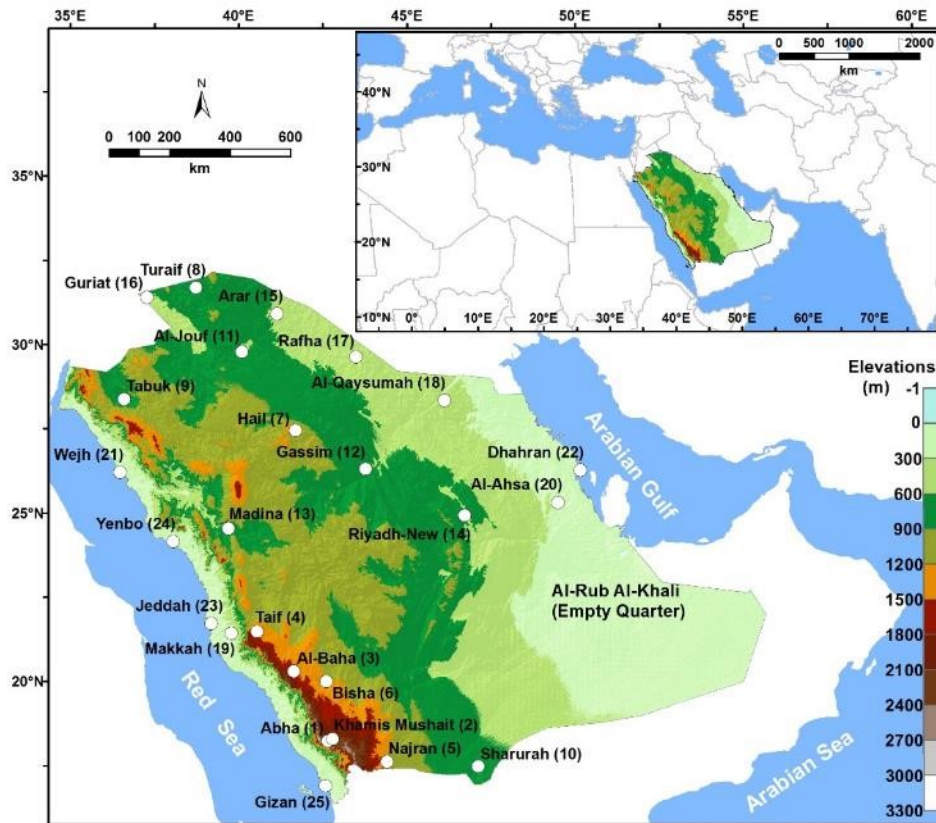


Figure 4.1. A map showing the study domain (upper-right) and the topography of Saudi Arabia along with the used weather stations. Source: adapted from King Abdulaziz City for Science and Technology and GAMEP.

For synoptic analysis, daily values of mean sea level pressure (MSLP), geopotential heights at 500-hPa, 850-hPa, and 850-hPa temperatures (T-850) were obtained from the records of the ERA-Interim reanalysis (Dee et al., 2011), at a grid resolution of $0.125^{\circ} \times 0.125^{\circ}$ latitude-longitude. The ERA-Interim dataset has been used for synoptic circulation analysis over the Middle East and it has been reported to be reliable (e.g., Vries et al., 2013; Almazroui et al., 2015; Zolina et al., 2017). The area of synoptic circulation analysis encompasses the region $10^{\circ}\text{N}–40^{\circ}\text{N}$ by $10^{\circ}\text{E}–75^{\circ}\text{E}$ (Figure 4.1), as it provides excellent synoptic resolution to account for essential circulation systems related to Mediterranean, Sudan, and the Indian Summer Monsoon thermal lows. From the ERA-Interim reanalysis dataset, daily means of SSTs values

were also obtained for the nearby water bodies including the Red Sea, Arabian Sea, Arabian Gulf, Caspian Sea, Black Sea, and Mediterranean Sea.

4.2.2 Heat Wave definition

Due to the diversity of impacts, HWs are of interest to diverse stakeholders, including health researchers, agricultural producers, energy providers, climatologists, and meteorologists (Smith et al., 2013). There is no single perfect standard method or definition for a HW that works for all applications (e.g., Perkins and Alexander, 2013; Smith et al., 2013). As discussed in Alghamdi and Harrington (2018) a HW was defined as a period of at least two consecutive days with a daily maximum temperature equal or higher than the 90th percentile of the monthly maximum and with a daily minimum temperature equal or higher than the 85th percentile of the monthly minimum for the decade in question (1985-1994, 1995-2004, and 2005-2014).

A decadal rather than period of record time window was used to determine the monthly percentile thresholds to account for the regional warming trend. A monthly and decadal time-dependent approach allows hot temperature events to have a better chance of being detected throughout the warm season since different decades could experience different patterns of changes. Raggad (2017a) suggested that non-stationary models are more suitable for analyzing extreme temperatures in the country. Alghamdi and Harrington (2018) demonstrated the value of using a time-sensitive approach (monthly and decadal time-windows) in studying extreme thermal events in Saudi Arabia due to the on-going change in the climatology of the upper-tail of the frequency distribution of maximum and minimum temperatures. To explore how station level HW intensity is responding to different weather types and SST anomalies, the intensities of HW days were assessed by their temperature departures from their warm season mean temperature climatology.

4.2.3 Synoptic analysis

A total of 1338 HW days were detected at the 25 stations for the warm seasons from the 30-year period (1985-2014). To eliminate events that could be induced by local factors (e.g., urban heat island) rather than regional factors (i.e., atmospheric circulation), the synoptic analysis was restricted to days where a HW was recorded at a minimum of 2 stations. The criterion of 2 stations reduced the number of days to 746 (Figure 4.2). A larger criterion (3 or 4 stations) could be used, but due to having just 25 stations and to maximize the sample size (across months and years), the 2 station criterion was selected (Figure 4.2). For example, the 4-station criterion resulted in a sum of 322 HW days where two years had no HW days (1993 and 1997) and five years had less than two HW days (1986, 1992, 2004, 2009, and 2014). Also, using the threshold of two stations (as compared with 3 stations) captured most of the HW days that constitute the onset or the ending days of long events. Two groups of stations (IDs: 1, 2, and 4 and 19 and 23) are somewhat questionable for use of the 2-station criterion as they have the shortest Euclidean distances among the 25 stations. However, most of their HW days (using the 2-station criterion) were found to be either the onset or ending day (or with a gap of one day) associated with long events.

Synoptic climatology analysis involves two general methods: circulation-to-environment (C-to-E) and environment-to-circulation (E-to-C) (Yarnal, 1993). The main difference between these methods is the dependency on the outcome (i.e., the resulting weather events such as flooding, sand storm, and HWs). In the C-to-E approach, the atmospheric flows are classified, using upper air measurements, into circulation patterns then an environmental phenomenon (i.e., outcome) is analyzed whereas in E-to-C, days of an outcome of atmospheric circulation are specified first then the atmospheric observations of these days are classified (Lee and Sheridan,

2015). Each approach has its advantages and disadvantages, and the selection is based on the aims of the investigation (Beck and Philipp, 2010; Lee and Sheridan, 2015; Philipp et al., 2016). For example, while the C-to-E approach provides readily available information that can be used for further studies, since all the atmospheric flows are classified, the E-to-C approach is more efficient in studying extreme weather events as it provides greater insights and understanding about the atmospheric circulation patterns that produce an extreme event occurrence for a specific area (Lee and Sheridan, 2015).

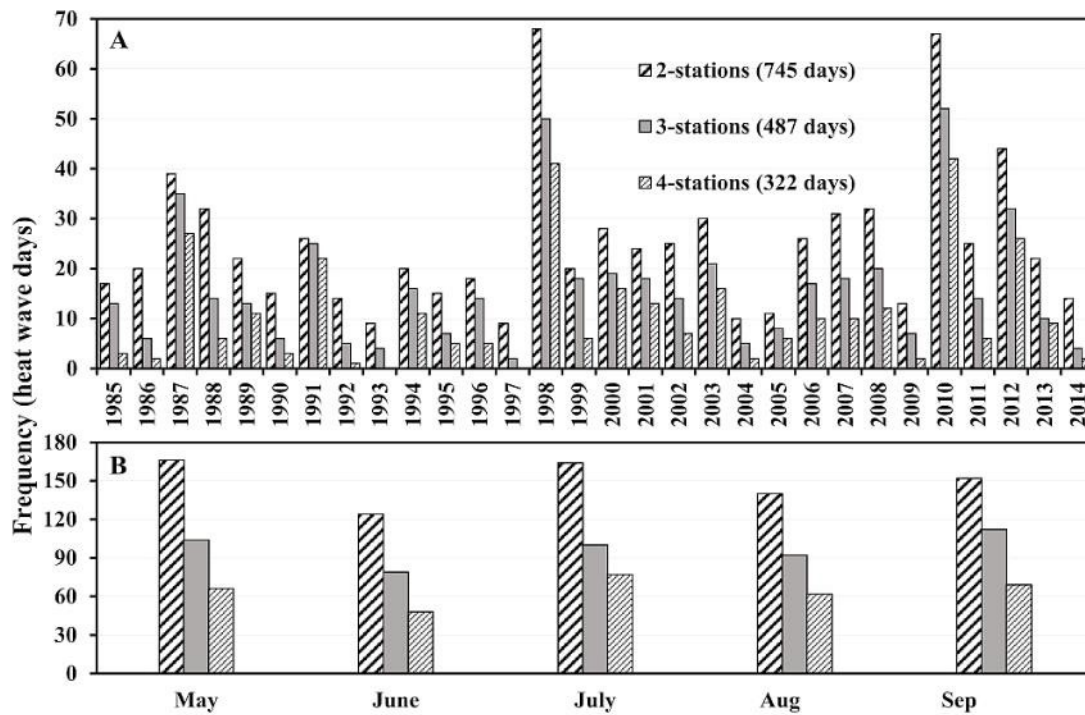


Figure 4.2. Annual (A) and monthly (B) heat wave days frequency using different minimum criterion.

Using an E-to-C approach, the synoptic analysis was applied in two stages including general synoptic assessment and clustering analyses. General synoptic analysis involved developing composites and anomalies maps for all the 746 HW days to examine the overall synoptic climatology. Since HWs could result from different daily atmospheric circulation types (Tomczyk and Bednorz, 2016), and to explore if different HW characteristics (i.e., frequency,

intensity, and spatial coverage) are related to different atmospheric circulation situations, clustering analysis was applied to the environmental data for the 746 days identified. Ward's (1963) minimum variance classification method was used as it one of the most commonly employed techniques not only in classifying atmospheric circulation patterns (e.g., Tomczyk and Bednorz, 2016; Tomczyk and Sulikowska, 2017), but also in hierarchical agglomerative clustering as a statistically-based technique (Vrac et al., 2007). The classification was based on the gridded pattern of daily MSLP data (10°N–40°N, 10°E–75°E) of the selected HW days, using Euclidean distance as a measure of similarity/dissimilarity among data objects. Prior normalization of the daily MSLP data was done as per Esteban's et al. (2005) recommendation.

4.2.4 Circulation types, Heat Wave days frequency, intensity, and SSTs

To explore if different circulation types would provide some insight into the frequency and intensity characteristics of the 746 HW days at the station level, correlation analysis (Pearson product-moment) was applied. The analysis was carried out on the anomaly of the frequency and intensity of each of the identified circulation types and the anomalies of frequency and intensity of HW days for each station. The intensity of each of the circulation types was defined as the mean intensity of its HW day temperature departures from their warm season (May-September) mean temperature climatology (1985-2014). Similarly, the intensity of a HW day was measured by its mean temperature departure from the warm season mean temperature climatology at station level. Correlation analyses were applied at the annual timescale.

To explore possible links between the selected HW days and the SSTs anomaly patterns of the selected water bodies, observational and correlation analysis approaches were used to help establish a baseline for future detailed studies. Correlation analysis (Pearson product-moment) was applied on the warm season anomaly of frequency and intensity of each of the identified

circulation type HW days and the warm season anomaly of corresponding SSTs. All the analyses were applied on the SST anomalies of HW days, since including previous observations (i.e., few days or weeks) of the onset of the HW might not provide essential differences (Boschat et al., 2016).

4.3 Results

4.3.1 Circulation conditions

4.3.1.1 General synoptic conditions

During the warm season, Saudi Arabia is influenced by a low-pressure system (Figure 4.3A), the Indian Summer Monsoon Trough (ISMT) or Persian Trough (Almazroui, 2006; Lelieveld et. al, 2016). This trough is a thermal low or heat low that can be distinguished clearly at the 850 hPa level (Bitan and Saaroni 1992) (Figure 4.3C). Temperatures at 850 hPa have higher values centered over the western parts of Saudi Arabia (Figure 4.3C). At a higher level (500 hPa), a subtropical ridge system dominates the area (Figure 4.3A) extending from Africa to the Arabian Gulf. The overall pattern confirms the findings of Blake et al. (1983), where the heat low over Saudi Arabia exists as a well-mixed layer within the lower levels of the atmosphere ($<\sim 850$ hPa). Dry convection and radiation in the near-surface mixed layer combined with the upper level subsidence motions ($>\sim 700$ hPa) to provide for the necessary conditions for the heat low to operate during the warm season (Mohalfi et al., 1998).

During HW days, the overall composite pressure and thermal patterns did not change substantially, but the composite patterns showed features of intensification and spreading to cover more territory (Figure 4.3B, D, E, and F). Associated with a HW day, most of the Arabian Peninsula is under lower surface pressure than the warm season average, with greater negative anomalies centered over Red Sea and west-central Saudi Arabia. The 850-hPa composite showed

a similar pattern of negative height anomalies with greatest departures over southwestern Saudi Arabia. At the 500 hPa level, a pattern with two areas of higher heights on the subtropical ridge was found, one over northwestern Africa and a closed high centered over northwest part of Saudi Arabia. Thermal anomalies were positive at both the 500 hPa and the 850 hPa levels (Figure 4.3F).

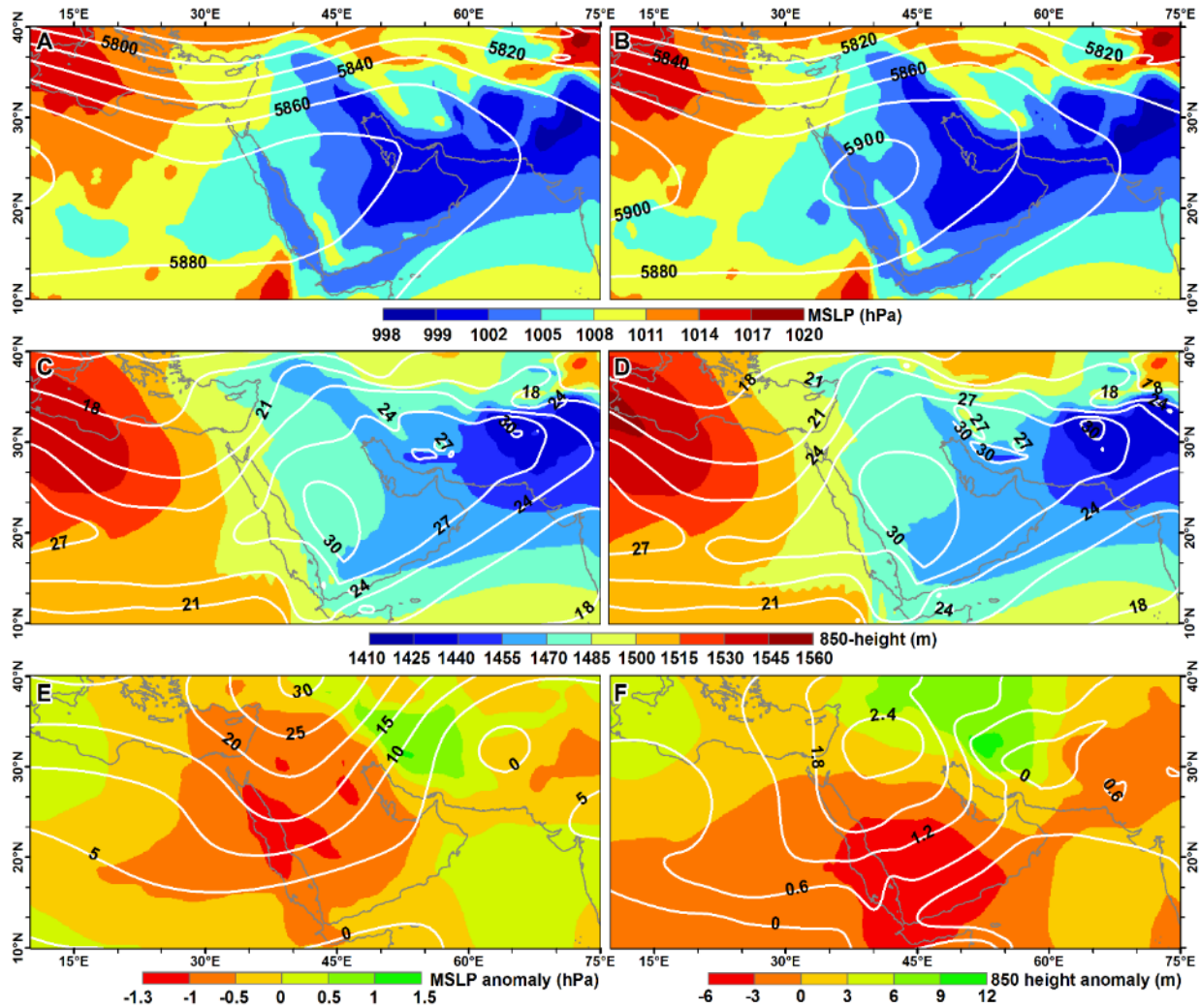


Figure 4.3. Composite maps for MSLP- hPa (A shaded), geopotential height at 500- hPa (A contour), geopotential height at 850- hPa (C shaded) and T-850 (C contour) during warm season. Heat wave days (746 days) composite maps for MSLP- hPa (B shaded), geopotential height at 500- hPa (B contour), geopotential height at 850- hPa (D shaded), T-850 (D contour) and their anomalies (E for MSLP, shaded, and 500- hPa, contour, and F for 850- hPa, shaded, and T-850, contour). Anomalies are departures from 1985–2014 climatology.

4.3.1.2 Clustering

The initial synoptic analysis was based on composite maps of 746 HW days, where individual events could be induced by slightly different atmospheric circulation patterns. Therefore, the Ward's clustering method was applied on the MSLP data for the 746 HW days. Using average distances between and within clusters indices, 3, 4, and 6-cluster solutions were suggested. Using the minimum number of clusters criteria (Carvalho et al., 2010), the three-cluster solution (Figures 4.4, 4.6, and 4.7) was selected. Three clusters provided a reasonable balance between minimizing the distances within clusters and maximizing the distances between clusters. In fact, the composite maps of 4, and 6-cluster solutions showed no substantial synoptic differences from those identified by 3-cluster solution.

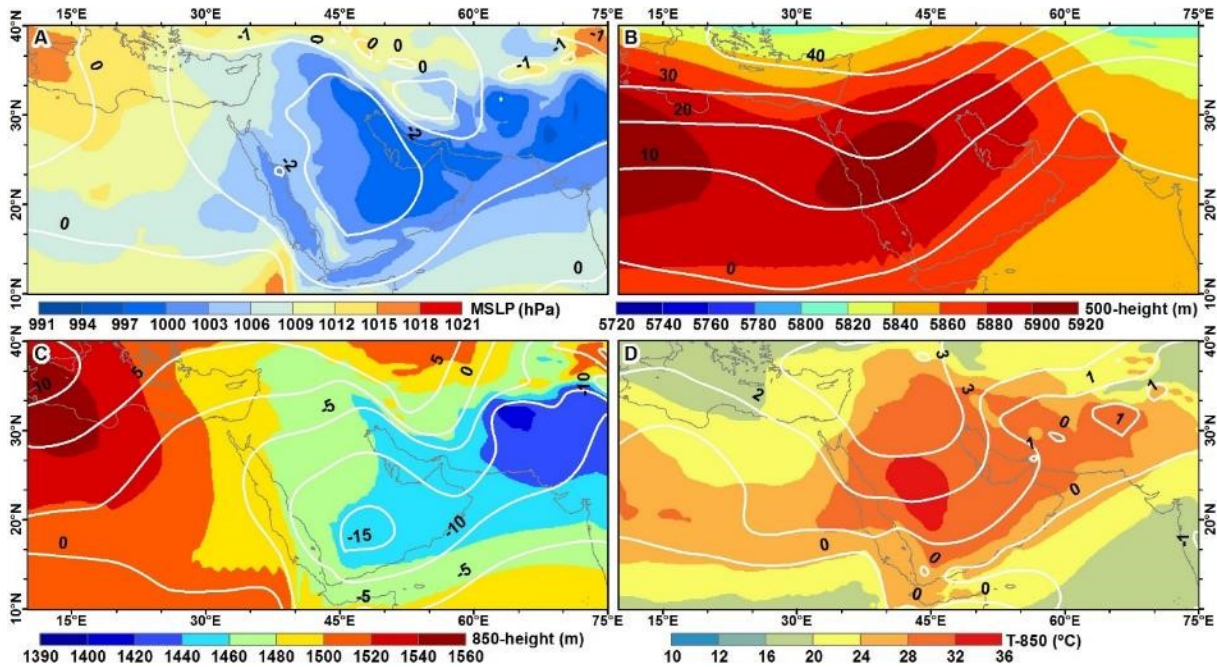


Figure 4.4. Weather Type 1 composites for MSLP (A shaded and contours for anomaly); geopotential height at 500-hPa (B shaded and contours for anomaly); geopotential height at 850-hPa (C shaded, contour for anomaly; and T-850 (D shaded and contour for anomaly). Anomalies are departures from 1985–2014 climatology.

For circulation Type 1 (Figure 4.4), 301 HWs days (40.3%) were classified into this cluster and it was more frequent during the mid-warm season (Figure 4.5). During HWs related

to this synoptic weather type (1), most of the Arabian Peninsula was under lower surface pressure (<999 hPa) than usual for the warm season, with an anomaly of -2 hPa situated over the Arabian Gulf and eastern parts of the Arabian Peninsula. Air mass subsidence helps create the features at the 500-hPa level, where a closed area of higher heights is centered over the west-north part of the Peninsula. Greatest height anomalies were to the north (Figure 4.4B). The subtropical ridge over the Mediterranean intensified (by an anomaly of about 10 m) at the 850-hPa (Figure 4.4C), with a negative height anomaly at 850-hPa of over 10 m in the ISMT region extending from Iran to most of Saudi Arabia. The negative anomaly for 850-hPa heights was accompanied by higher temperatures centered over Saudi Arabia with a warming anomaly pattern (Figure 4.4D) extending northward to Eastern Europe.

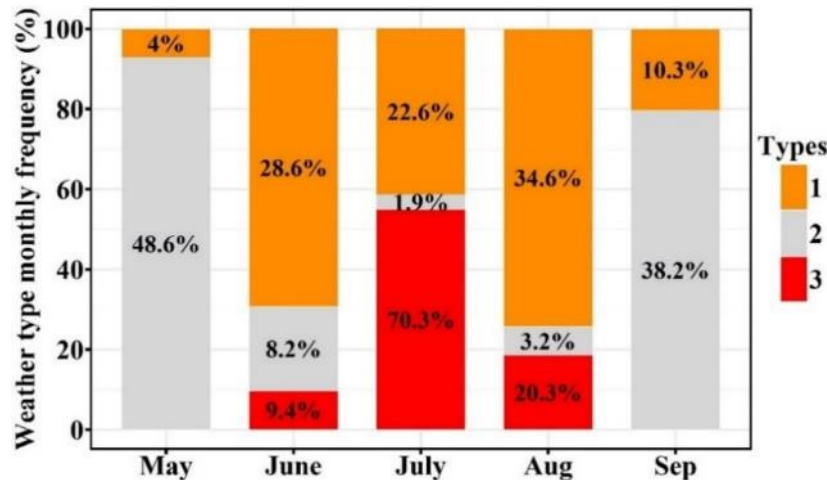


Figure 4.5. Monthly frequency of detected weather types during warm season months. Percentages inside bars are per weather type, that is 9.4%, 70.3%, and 20.3% of type 3 occurred in June, July, and August.

Circulation Type 2 (Figure 4.6) was comprised of 317 HW days (42.5) and it was most frequent during May (48.6% of Type 2 patterns) and September (38.2%) (Figure 4.5). Type 2 has a positive MSLP anomaly extending into Saudi Arabia from the north and east. The 500-height anomaly pattern showed a positive anomaly penetrating into the Arabian Peninsula from the east whereas negative heights were centered over the north-east and north-west (<10 m). A ridge with

higher heights can be clearly seen over the Arabian Gulf (Figure 4.6B). Unlike the pattern for Type 1, the subtropical ridge at 500-hPa over North Africa has shifted south. At the 850-hPa height level, most of the study domain was under positive anomalies (unlike Types 1 and 3) centered over Iran and Arabian Gulf. Thus, the ISMT is weaker at the lower level (850 hPa) and temperatures anomalies were not very pronounced (Figure 4.6D).

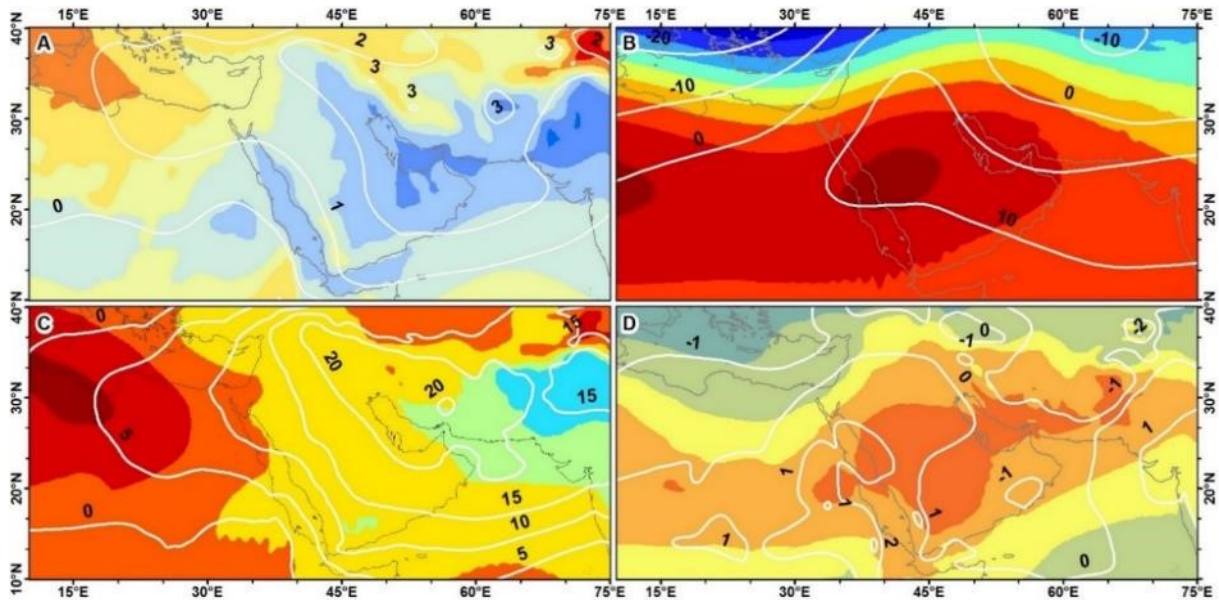


Figure 4.6. As in Figure 4.4 but for weather Type 2.

Circulation Type 3 (128 HW days or 17.2%) was more frequent during July (70.3% of type 3 events) and August (20.3%) (Figure 4.5). Type 3 has relatively similar anomaly patterns as Type 1, but with a greater magnitude of the anomalies (Figure 4.7A). The negative anomalies in MSLP (<-4 hPa) have shifted north-east compared with Type 1. The heights at the mid-tropospheric levels (500 hPa) increased over north (by 10 m) as the African subtropical ridge shifts slightly to the north and the Arabian subtropical ridge is reduced in size. In the lower levels (850 hPa), all the study domain was under lower heights and the ISMT was more active (Figure 4.7C). As a result, temperature at the 850-hPa height level had the warmest anomalies among all the three types (Figure 4.7D).

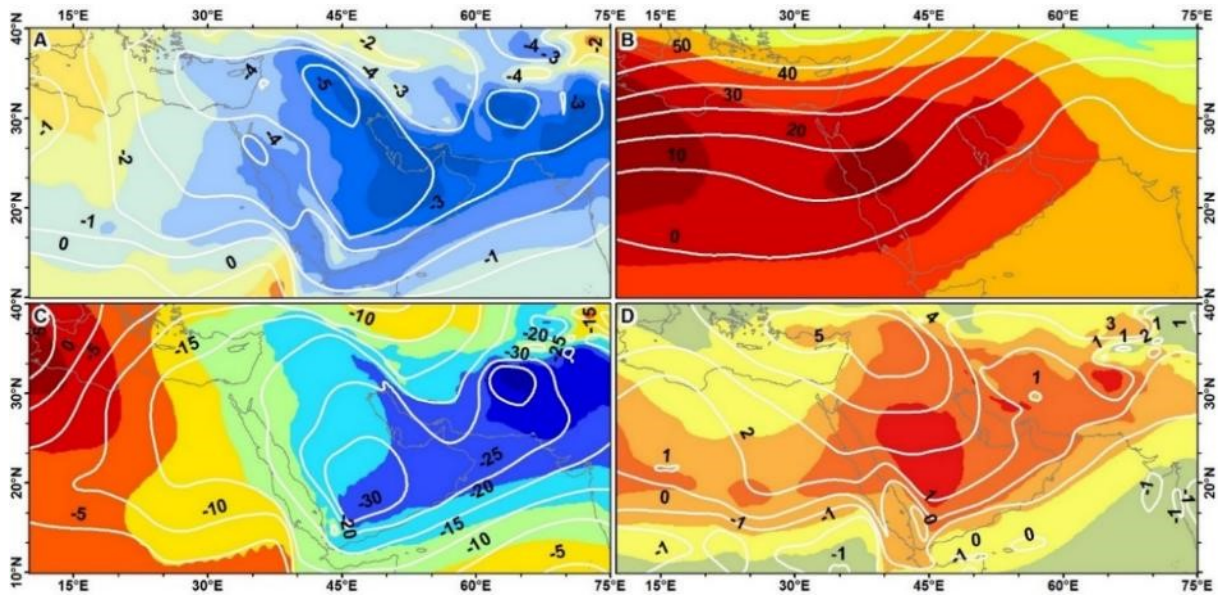


Figure 4.7. As in Figure 4.4 but for weather Type 3.

4.3.2 Heat Wave days frequency, intensity and circulation types

This section explores the question as to whether different circulation types provide some insights at the station level into the characteristics (frequency and intensity) of the 746 HW days. Correlation coefficients ranged from -0.22 to 0.67 (Figure 4.8). For HW frequency, circulation Types 1 and 3 had more significant positive correlations with HW days at most locations except a few stations on the west coast (Figure 4.8A and C). Circulation Type 2 was associated with lower statistical associations and only 5 stations had significant correlations (Figure 4.8B). For HW intensity, circulation Types 1 and 2 had fewer significant positive associations, compared to circulation Type 3 (Figure 4.8D-F).

Correlation coefficients and the variability in their spatial distributions suggest that the synoptic circulation patterns do not fully explain the patterns of the frequency and intensity of HW days in Saudi Arabia. This is in agreement with other previous studies which have reported that atmospheric circulation does not usually explain all HW characteristics (Ferranti and Viterbo, 2006; Fischer et al., 2007a, 2007b; García-Herrera et al., 2010; Feudale and Shukla,

2011). Low correlation coefficients here suggest that atmospheric circulation establishes the required conditions for a HW to form but additional factors, such as soil moisture, atmospheric humidity, antecedent land surface temperature, or the urban heat island effect, would play important roles for HW frequency and intensity. Although Type 3 had a lower frequency compared to Types 1 and 2, (since it composed of 128 HW days), most of stations showed more significant associations with this anomaly pattern. In examining the spatial aspect of these associations, it was found that HW days related to weather Type 2 tended to result in greater spatial coverage (11-16 stations). Medium spatial coverage (6-10 stations) was more related to Types 1 and 3, respectively.

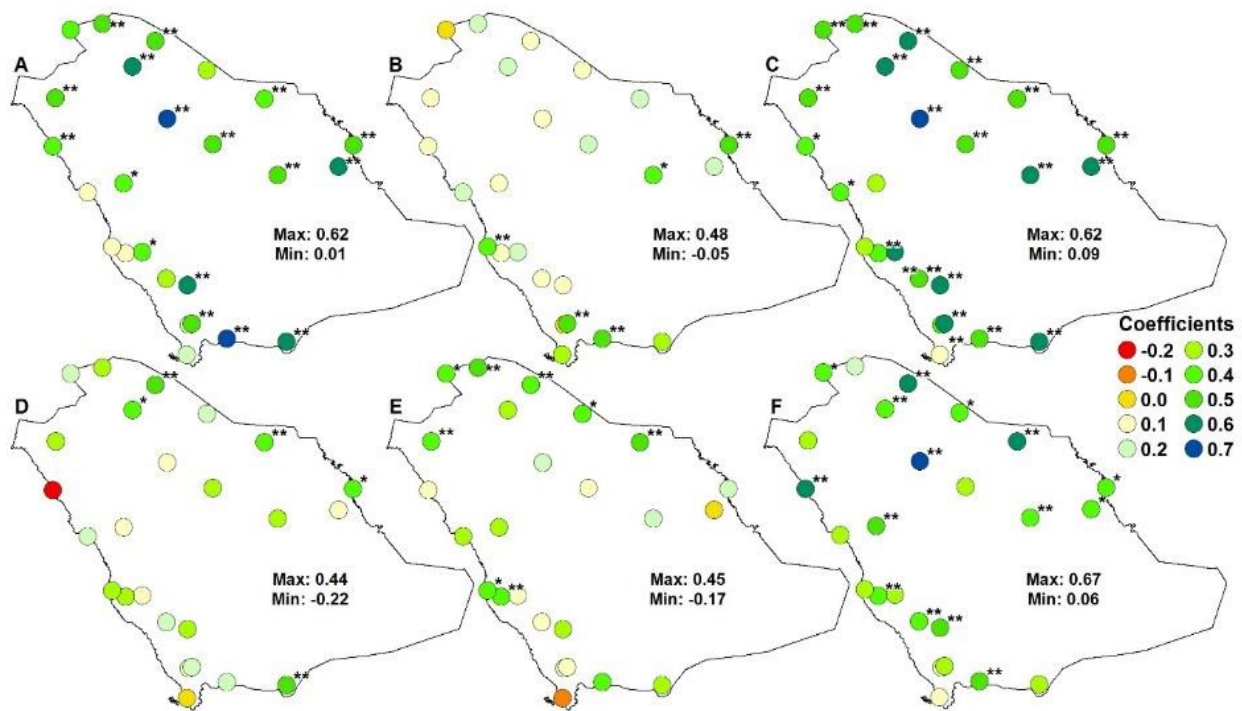


Figure 4.8. Correlation coefficients between anomalies of heat wave days frequency (A-C) and intensity (D-F) and anomalies of circulation Type 1 (A and D), 2 (B and E), and 3 (C and F). Refer to Figure 4.1 for station names. ** and * are statistically significant at the 95% and 90% levels, respectively.

4.3.3 Analysis of SST Teleconnections

For HW events classed in circulation Types 1 and 3, all seas showed positive surface temperature anomalies, except for the Arabian Sea (Figure 4.9). Among the water bodies analyzed, the Caspian Sea, Black Sea and northern Arabian Gulf had the highest SST warming anomalies with Types 1 and 3. These SST anomaly patterns corresponded to the general spatial features of 850 hPa temperature anomalies in both Types 1 and 3 (Figures 4.4C and 4.7C), suggesting interaction and some teleconnection with regional warming during HW days. On the other hand, HW days of circulation Type 2 were accompanying by warm anomalies only in the Arabian Sea (0.5-1.1°C) and negative anomalies in the other nearby seas (-0.1 to -1.5°C). The highest SSTs warm anomaly (3-5°C) was found for HW days of Type 3 over the Caspian Sea and the Black Sea.

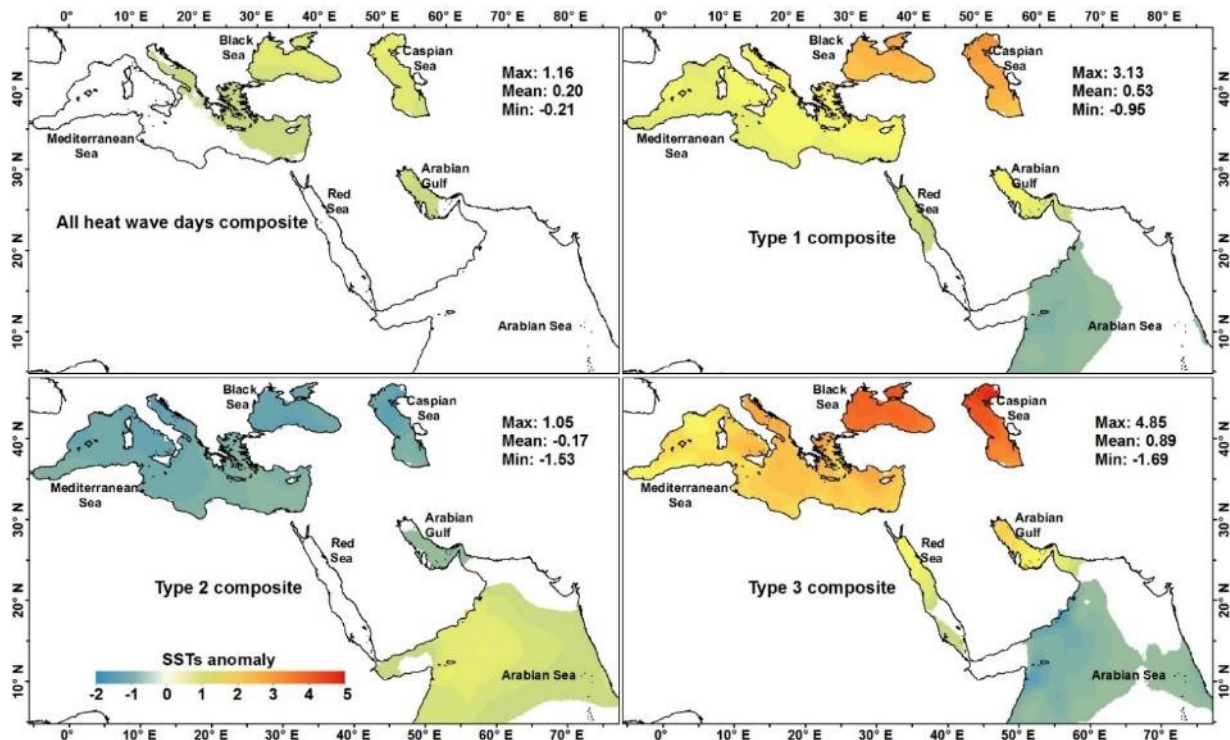


Figure 4.9. SSTs anomalies composites of all heat wave days (upper-left), and circulation Types: 1 (upper-right), 2 (bottom-left), and 3 (bottom-right). Anomalies are departures from 1985–2014 climatology.

These patterns suggest some possible links between HW events in Saudi Arabia and nearby SST anomalies. For further exploration, correlation analysis was applied on the warm season anomaly of frequency and intensity for each of the three HW circulation types and the SSTs anomalies. Correlation coefficient values ranged from -0.14 to 0.42 for event frequency and from -0.46 to 0.62 for intensity (Table 4.1). The frequency anomaly of HW days of weather Type 1 was linked to the sea surface temperature anomaly of the Black Sea (33%) and the Caspian Sea (42%) whereas the links for Type 3 were only with SSTs anomalies of the Black Sea (39%). Although the frequency anomaly of Type 2 HW events had negative correlation coefficients with all SSTs anomalies, except for the Arabian Sea and Red Sea, (as results in Figure 4.9 suggested), no statistically significant correlation was found.

Table 4.1. Correlation coefficients between anomalies of local SSTs and different heat wave days characteristics for three detected weather types. ** and * are statistically significant at the 95% and 90% levels, respectively.

	Frequency			Intensity		
	Type 1	Type 2	Type 3	Type 1	Type 2	Type 3
Arabian Gulf	0.30	-0.10	0.30	0.51**	0.26	0.45**
Arabian Sea	-0.08	0.23	0.28	-0.46**	-0.01	0.00
Black Sea	0.33*	-0.11	0.39*	0.58**	0.34*	0.51**
Caspian Sea	0.42**	-0.08	0.36	0.62**	0.33*	0.29
Mediterranean Sea	0.19	-0.14	0.27	0.44**	0.21	0.47**
Red Sea	0.25	0.09	0.28	0.54**	0.30*	0.38*

For intensity, correlation analysis suggested that the intensity aspect of HW days responded more to SSTs compared with frequency. The intensity anomaly of HW days in Types 1 and 3 displayed significant associations with all SSTs anomalies except for those for the Arabian Sea and the Caspian Sea for events in Type 3. Interestingly, the intensity of HW days for type 2 showed significant positive correlations with sea surface temperature in the Black Sea, Caspian Sea, and Red Sea.

4.4 Discussion

Cluster analysis suggested that HW days at two or more stations in Saudi Arabia could be summarized with three circulation/weather types (Figures 4.4, 4.6, and 4.7). Types 1 and 3 are similar in their general synoptic conditions and patterns (Figures 4.4 and 4.7), where Type 3 represents an intensification of Type 1. In all the three types, there were two primary surface pressure systems presented: low pressure over the east and high pressure over the northwest. The low pressure system is a thermal low that spreads west from India to near the central area of Saudi Arabia establishing a surface trough of lower pressure (i.e., the ISMT). During Type 3 the ISMT intensifies and the region experiences a negative 850-hPa height anomaly (-30 m) centered over the southwest area of the Arabian Peninsula. At 850 hPa, the high temperature anomaly documents the strength of the thermal low. Type 2, a synoptic pattern more frequent at the beginning and end of the warm season exhibited a different pattern where the ISMT disappears as the southwest subtropical high (Azores) extends to the southeast, as shown by higher heights at the 850 hPa pressure level (Figure 4.6C).

In both synoptic Types 1 and 3, two troughs of lower heights were observed at the 850 hPa level, one over the Arabian Gulf (i.e., ISMT) and one over the Al-Rub Al-Khali Desert (Empty Quarter). The latter is known as a substantial energy source contributing to some major climate characteristics of surrounding areas; it is commonly referred to as the Arabian heat low (Blake et al., 1983; Smith 1986a, 1986b; Mohalfi et al., 1998). Smith (1986a) reported that as the Arabian heat low intensifies, more moisture is transported into its area, which reduces sensible heat transport in the boundary layer. An increase in specific humidity associated with the Arabian heat low was observed in this study for HW days of Types 1 and 3 (Figure 4.10). Yet, as distance increases from the center of this heat low, sensible heat exchange increases (Smith

1986a). Such a feature and process can help explain the lower temperatures within the heat low over the Empty Quarter and the presence of higher temperatures northwest of the heat low for HW days of Types 1 and 3 (Figure 4.10).

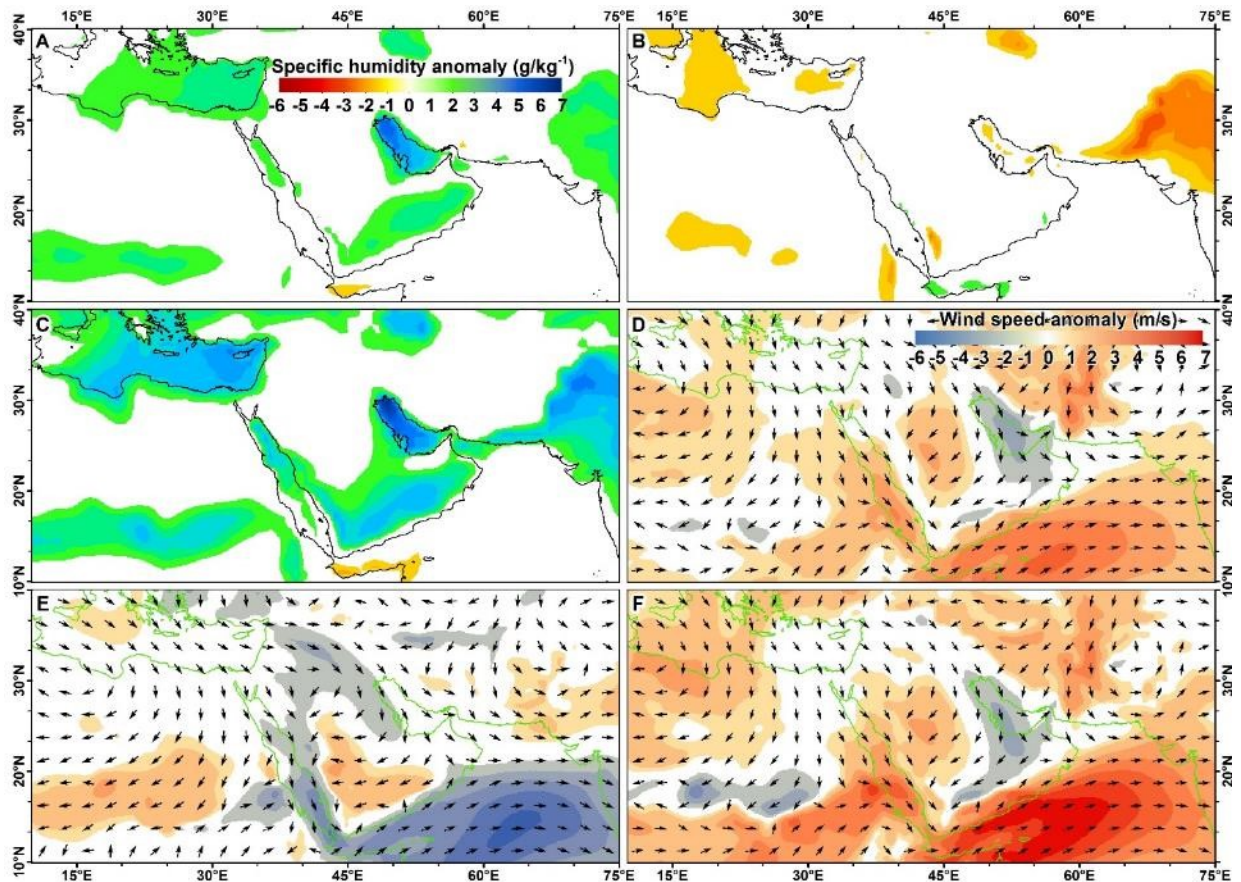


Figure 4.10. Specific humidity anomaly composites of circulation Type 1 (A), 2 (B), and 3 (C) and wind speed anomaly and mean direction composites of circulation Type 1 (D), 2 (E), and 3 (F). Anomalies are departures from 1985–2014 climatology.

It is clear from Figure 4.10 (D-F) that surface wind speeds did not deviate much from the mean during HW days over Saudi Arabia, particularly for Types 1 and 3. The areas of both heat lows experienced a slight reduction in the wind speed anomaly during HW days of Types 1 and 3 and a positive anomaly during HW days of Type 2. It was reported that the surface wind becomes almost calm when the Arabian heat low reaches its daily maximum intensity (Smith

1986a). In fact, Mohalfi et al. (1998) disclosed that slow northerly winds reduce air mixing, allowing the Arabian heat low to intensify.

Based on the findings of Smith (1986a, 1986b) and Mohalfi et al. (1998), the change in both wind speed and humidity could be factors explaining the nonappearance of the thermal low and the circulation conditions of Type 2. During HW days of Type 2 wind speeds were higher than the warm season average over most of the Al-Rub Al-Khali Desert. For synoptic Type 2, the region experiences average humidity levels (Figure 4.10). At the same time, the ISMT recedes with a shift to the north and most the Arabian Peninsula was under a higher 500 hPa height anomaly (Figure 4.6). The subtropical ridge at 850 hPa intensifies and moves to the southwest towards the Peninsula, transporting dry and warm air.

The 850 hPa temperature anomaly showed a similar spatial pattern in Types 1 and 3 and a different pattern for type 2 (Figure 4.4, 4.6, and 4.7). In Type 1 and 3, positive anomalies were over the eastern Mediterranean and the northern Arabian Peninsula and values decreased southward. Type 2 produced the opposite pattern, with northern areas exhibiting negative anomalies. These patterns can be explained by the large-scale circulation patterns related to Indian Summer Monsoon (ISM). While Type 2 was more frequent during the transitional periods of the ISM season (May and September), Types 1 and 3 were most frequent during periods of strong ISMs (Figure 4.5). It has been shown that when the ISM intensifies (strong-phase) the ascending motions over Mid-Asia (80-100°E) increase and result in greater descending motions over east-Asia and the eastern Mediterranean down to mid-tropospheric levels; this subsidence produces an increase in adiabatic warming (Ziv et al., 2004). In fact, Rodwell and Hoskins (1996, 2001) showed that the adiabatic subsidence in the North African and eastern Mediterranean regions are related to the ISM as it induces a Rossby wave like response.

This east-west oriented atmospheric teleconnection pattern could help explain the warming SSTs anomalies of Mediterranean Sea, Black Sea, and Caspian Sea during HW days of circulation Types 1 and 3, and the cooling anomaly during HW days of circulation Type 2. While the Arabian Sea showed cooler SSTs anomalies during HW days of Types 1 and 3, it had warm SSTs anomalies during HW days of Type 2 (Figure 4.9). During strong ISM years, the Arabian Sea usually experiences higher wind speeds and cooler SSTs compared to years with a weak monsoon, due to strong upwelling along the Somalia coast (Murtugudde et al., 2007). Southwesterly winds enhance the coastal upwelling and the spread of cooler water over the Arabian Sea (Vinayachandran, 2004). As shown in Figure 4.10, the Arabian Sea had higher wind speed anomalies in Types 1 and 3 and a negative wind speed anomaly for Type 2.

4.5 Summary and Conclusions

Atmospheric circulation patterns and conditions related to HWs at two or more stations in Saudi Arabia were analyzed using reanalysis data (1985-2014). Cluster analysis methods were used to distinguish among different circulation/weather conditions associated with different HWs and three distinct types were found. The presence of Indian Summer Monsoon Trough (ISMT) was related to two weather types (Types 1 and 3) and its absence was connected to one weather type (Type 2). HW days induced by atmospheric conditions for Types 1 and 3 caused higher temperatures on average, where the less frequent but strong Type 3 was related to a strong ISMT and accompanied by an intensification of the Arabian heat low. Further, SSTs anomalies during the different weather types were mapped and analyzed. HW weather Types 1 and 3 showed warm SSTs over all of the selected water bodies except the Arabian Sea, whereas weather Type 2 showed warm surface temperature only over the Arabian Sea. Generally, the intensity of a HW day showed a stronger correlation with SSTs anomalies.

The overall results show the importance of a few points for forecasting and analyzing HWs in Saudi Arabia. The ISMT and the Arabian heat low are responsible for 57.5% of the detected HW days over 1985-2014. The importance of both systems to the climatology of Saudi Arabia have been stated in the literature and there is a need for more information about their influences and connections to extreme temperature events in Saudi Arabia. This study provides some of the first preliminary explorations of synoptic patterns for HWs and should initiate further research. It seems that HWs in Saudi Arabia tend to occur during regional warming as suggested by SSTs values particularly over areas to the north. This may be due to increasing subsidence over the region linked by teleconnection with the ascending motions over Mid-Asia during ISMs (Ziv et al., 2004). Thus, further analysis is needed to address the aspects of the results that suggest that both the ISM and SSTs of nearby water bodies might help in forecasting and predicting HWs in Saudi Arabia.

It is important, however, to emphasize that the magnitudes of distinctions among the frequency and intensity of HW days and related atmospheric circulation types and SSTs were not that large. In most cases, small fractions of the total variance were explained. This finding suggests the importance of other local factors such as soil moisture, humidity, land surface temperature, and urban heat islands. More work on local microclimatic conditions at weather stations is needed. Correlation analyses were based on small samples (each variable was represented by one annual mean value), where the selected variables did not have a uniform spatial distribution. Thus, the results of this work should be viewed as a preliminary assessment and future research should consider using a larger sample (e.g., reanalysis temperature data) and more advanced analysis methods (e.g., data modeling). Such efforts would not only provide

insights into how the selected variables (HW days frequency and intensity, atmospheric circulations, and SSTs) are related, but also into feedbacks and underlying mechanisms.

Chapter 5 - Summary and Conclusions

This dissertation aimed to advance our understanding of the climatology of heat waves (HWs) in Saudi Arabia using data for 1985 to 2014. Analyses addressed the frequency, intensity, and duration characteristics of warm season extreme temperature events. Several issues associated with commonly used indices and methods are addressed and new definitions and methods help advance specific assessment practices. A new locally relevant and time-sensitive definition to detect HWs is examined. A HW event is defined as a period of two or more consecutive days (i.e., at least 48 hours) with a daily maximum and a minimum temperature exceeding the 90th and 85th percentiles of the maximum and minimum, respectively. Threshold percentiles were calculated on a monthly basis and adjusted for each decade of analysis. In addition, HW temporal changes, spatiotemporal, and atmospheric patterns were assessed.

Chapter 2, *Time-sensitive analysis of a warming climate on heat waves in Saudi Arabia: Temporal patterns and trends*, establishes the importance and impact of changes/variabilities in the mean climate for determining a HW threshold. Further, the importance of selecting indices for different HWs aspects and trend analysis techniques are addressed. Different and noteworthy results were revealed regarding the temporal behaviors of different characteristics of HWs in Saudi Arabia (i.e., frequency, intensity, and duration). Although different geographical and temporal behaviors were found at the station level, the overall results suggested that regional and local factors, such as elevation, latitude, and distance from a large body of water, may play important roles.

Chapter 3, *Trends and spatial pattern recognition of warm season hot temperatures in Saudi Arabia*, took a further step by using time-series clustering analysis to recognize spatiotemporal patterns and related frequency and intensity of HWs and an additional four hot

temperature indices (frequency and intensity of hot days and nights). First, the chapter reemphasized the importance of the on-going change in the climatology of the upper-tail of the frequency distribution of the temperature regime. Then, the spatiotemporal characters of six warm season hot temperature indices were analyzed with an emphasis on event behavior through time and space. A time-series clustering approach was used. A method was proposed to summarize the overall geographical behavior of warm season hot thermal events and eight clusters were suggested. Local and regional factors, such as elevation, latitude, and distance from a large body of water, helped explain some the clusters of HW locations. The analyses also revealed the importance of large-scale factors such as the atmospheric circulation.

Chapter 4, *Circulation conditions and sea surface temperatures observations of warm season heat waves in Saudi Arabia: A preliminary assessment*, explores how synoptic circulation patterns and sea surface temperature (SST) anomalies are related to frequency and intensity of HW days. Cluster analysis was used to identify and distinguish among different atmospheric circulation types that induce HWs. Three weather types were identified. Two of which (Types 1 and 3) were related to 57.5% of the occurrences of HW days and were connected with negative anomalies in sea level pressure and in the height of the 850 hPa level. Synoptic Type 2 was responsible for 42.5% of occurrences of HW days and was related to positive anomalies at all atmospheric heights. The Indian Summer Monsoon Trough and the Arabian Heat Low were key surface pressure features related to HWs days. Anomalies of surface temperatures of the Red Sea, Arabian Sea, Arabian Gulf, Caspian Sea, Black Sea, and Mediterranean Sea displayed different anomaly patterns and associations during different weather types. SST anomalies seem to be a more important factor for the intensity of HW days. However, the effects of synoptic conditions and SST anomalies produced some spatial variabilities and did not explain large

fractions of variances in individual station conditions, suggesting the importance of both large-scale and microclimate factors.

A main conclusion that can be derived from this dissertation about HWs in Saudi Arabia using a time-sensitive definition is that HWs could not be completely explained by one factor. Results from chapters 2-4 showed that local-, meso-, and regional or synoptic scales factors all have important impacts on the behavior of HWs in time and space. This highlights a local complexity aspect of HWs and a need to examine conditions at the station level. Thus, the main suggestion this dissertation makes is that HWs in Saudi Arabi are not to be understood fully by one atmospheric variable (e.g., maximum temperature) nor by one spatial factor (e.g., vegetation cover). Forecasting and prediction of HW should be carried out considering such complexity. In fact, through the literature review it was noted that microclimate studies of HWs are mostly focused on impacts and little work has been done on the local physical meteorological aspects.

This dissertation provided a detailed investigation of HWs across Saudi Arabia, and several themes have emerged, as the results in each chapter have highlighted. A main theme is the need to consider on-going changes or variabilities in the “normal” climate and acclimatization. A decadal time-window was used to account for these two factors. Although, a different length time window could be used depending on the length of the period of record and/or the rate of climatic warming. In order to determine the most appropriate window, detailed statistical analysis for the nature of changes/variabilities in a temperature regime is required. Raggad (2017a, 2017b) recently addressed some aspects of such an analysis and showed the importance of non-stationary models in analyzing extreme temperatures for the country. However, information about changes in the temperature distribution and its shape parameters (e.g., variance and skewness) and how extreme temperature events would respond to such

changes/variabilities is not available as of yet for the study area. Availability of such information would help document climate change as an important factor and more suitable ways to examine extreme temperature events could be determined. With such consideration, planning and management efforts could be more effective with respect to an emergency and enable an improved response related to impacts of extreme events under a changing climate.

The time-sensitive approach developed for this research does not imply climate change is not taking place. As shown in Figures 2.4 and 3.3, the climate of Saudi Arabia is warming with considerable multi-decade variations in the shape parameters of T_{min} and T_{max} distribution (i.e., variance and skewness, Appendix B- Figures 1-4). The time-sensitive approach acknowledges the on-going change in the climatology of the upper-tail of the frequency distribution of T_{min} and T_{max} by accounting for emerging new rare warm conditions. It also accounts for changes/variabilities in the population's ability to acclimatize to heat over time. The approach establishes a novel baseline for understanding past and future change. By accounting for changes and variabilities, more realistic estimates of hot temperature events will help future planning and adaptation efforts such as in managing the changing demands for electricity and water resources, development of heat-warning systems, and other policy-oriented planning in an arid environment.

References

- Aghabozorgi S, Shirkhorshidi AS, Wah TY. 2015. Time-series clustering—A decade review. *Information Systems*. *Information Systems* 53:16–38.
- Alexander LV, et al. 2006. Global observed changes in daily climate extremes of temperature and precipitation. *Journal of Geophysical Research: Atmospheres*, 111(D5).
- Alghamdi AS, Harrington Jr. 2018. Time-sensitive analysis of a warming climate on heat waves in Saudi Arabia: Temporal patterns and trends. *International Journal of Climatology*. DOI: 10.1002/joc.5489.
- Alghamdi AS, Moore TW. 2014. Analysis and Comparison of Trends in Extreme Temperature Indices in Riyadh City, Kingdom of Saudi Arabia, 1985–2010. *Journal of Climatology*. ID 560985.
- Alghamdi AS, Moore TW. 2015. Detecting temporal changes in Riyadh City’s urban heat island. *Papers in Applied Geography* 1: 312–325.
- Ali A .1994. Wind Regime of the Arabian Gulf. In: *The Gulf War and the Environment*, El-Baz F, Makharita RM (ed) *The Gulf War and the Environment*, Switzerland. pp. 31–48.
- Alkolibi FM. 1995. Mid-Tropospheric geopotential height patterns as related to temperature and precipitation in Saudi Arabia, ETD collection for University of Nebraska-Lincoln. Paper AAI9604395.
- Almazroui M, Dambul R, Islam MN, Jones PD. 2015. Atmospheric circulation patterns in the Arab region and its relationships with Saudi Arabian surface climate: a preliminary assessment. *Atmospheric Research* 161: 36–51.
- Almazroui M, Islam MN, Athar H, Jones PD, Rahan MA. 2012a. Recent climate change in the Arabian Peninsula: Annual rainfall and temperature analysis of Saudi Arabia for 1978–2009. *International Journal of Climatology* 32: 953–966.
- Almazroui M, Islam MN, Athar H, Jones PD, Rahan MA. 2012b. Recent climate change in the Arabian Peninsula: Seasonal rainfall and temperature climatology of Saudi Arabia for 1978–2009. *Atmospheric Research* 111: 29–45.
- Almazroui M, Islam MN, Dambul R, Jones PD. 2014. Trends of temperature extremes in Saudi Arabia. *International Journal of Climatology* 34: 808–826.
- Almazroui M, Islam, MN, Jones, PD. 2013. Urbanization effects on the air temperature rise in Saudi Arabia. *Climatic Change* 120: 109–122.
- Almazroui M, Saeed F, Nazrul M, Alkhalaf A. 2016. Assessing the robustness and uncertainties of projected changes in temperature and precipitation in AR4 Global Climate Models over the Arabian Peninsula. *Atmospheric Research* 182: 163–175.

- Almazroui, M., Dambul, R., Islam, M.N. and Jones, P.D., 2015. Atmospheric circulation patterns in the Arab region and its relationships with Saudi Arabian surface climate: A preliminary assessment. *Atmospheric research* 161: 36–51.
- Alrashed F, Asif M. 2012. Prospects of renewable energy to promote zero-energy residential buildings in the KSA. *Energy Procedia* 18: 1096–1105.
- AlSarmi S, Washington R. 2011. Recent observed climate change over the Arabian Peninsula. *Journal of Geophysical Research: Atmospheres* 116: D11109. doi:10.1029/2010JD015459.
- AlSarmi S, Washington R. 2013. Changes in climate extremes in the Arabian Peninsula: Analysis of daily data. *International Journal of Climatology* 34: 1329–1345.
- Ambaum, MHP. 2010. Significance Tests in Climate Science. *Journal of Climate* 23: 5927–5932.
- Athar H. 2014. Trends in observed extreme climate indices in Saudi Arabia during 1979–2008. *International Journal of Climatology* 34: 1561–1574.
- Bajat, B. et al., 2015. Spatial analysis of the temperature trends in Serbia during the period 1961–2010. *Theoretical and Applied Climatology* 121: 289–301.
- Balling RC, Skindlov JA, Phillips DH. 1990. The Impact of Increasing Summer Mean Temperatures on Extreme Maximum and Minimum Temperatures in Phoenix, Arizona. *Journal of Climate* 12: 1491–1494.
- Bao J, Li X, Yu C. 2015. The Construction and Validation of the Heat Vulnerability Index, a Review. *International Journal of Environmental Research and Public Health* 12: 7220–7234.
- Beck C, Philipp A. 2010. Evaluation and comparison of circulation type classifications for the European domain. *Physics and Chemistry of the Earth, Parts A/B/C* 35: 374–387.
- Bishop-Williams KE, Berke O, Pearl DL, Hand K, Kelton DF. 2015. Heat stress related dairy cow mortality during heat waves and control periods in rural Southern Ontario from 2010–2012. *BMC Veterinary Research* 11: 291.
- Bitan A, Saaroni H. 1992. The horizontal and vertical extension of the Persian Gulf pressure trough. *International Journal of Climatology* 12:733–747.
- Black E, Blackburn M, Harrison G, Hoskins B, Methven J. 2004. Factors contributing to the summer 2003 European heatwave. *Weather* 59:217–223.
- Boschat, G, Simmonds I, Purich A, Cowan T, Pezza AB. 2016. On the use of composite analyses to form physical hypotheses: An example from heat wave–SST associations. *Scientific reports* 6: ID:29599.

- Braga ALF, Zanobetti A, Schwartz J. 2001. The time course of weather-related deaths. *Epidemiology* 12: 662–667.
- Brandt PT, Williams JT, Fordham BO, Pollins B. 2000. Dynamic Modeling for Persistent Event-Count Time Series. *American Journal of Political Science* 10: 823–843.
- Broxton PD, Zeng X, SullaMenashe D, Troch PA. 2014. A Global Land Cover Climatology Using MODIS Data. *Journal of Applied Meteorology and Climatology* 53: 1593–1605.
- Cameron AC, Trivedi PK. 1998. Introduction. In: *Regression Analysis of Count Data*. Cambridge: Cambridge University Press, pp. 1–17.
- Carril AF, Gualdi S, Cherchi A, Navarra A. 2008. Heatwaves in Europe: areas of homogeneous variability and links with the regional to large-scale atmospheric and SSTs anomalies. *Climate Dynamics* 30: 77–98.
- Carson C, Hajat S, Armstrong B, Wilkinson P. 2006. Declining vulnerability to temperature-related mortality in London over the 20th century. *American journal of epidemiology* 164: 77–84.
- Carvalho A, et al. 2010. High ozone levels in the northeast of Portugal: Analysis and characterization. *Atmospheric Environment* 44: 1020–1031.
- Changnon SA, Kunkel KE, Reinke BC. 1996. Impacts and responses to the 1995 heat wave: A call to action. *Bulletin of the American Meteorological society* 77: 1497–1506.
- Chatterjee S, Simonoff JS .2013. Count Regression. In: *Handbook of regression analysis*. Hoboken, NJ: Wiley, pp 191–213.
- Coelho CAS, Ferro CAT, Stephenson DB, Steinskog DJ. 2008. Methods for Exploring Spatial and Temporal Variability of Extreme Events in Climate Data. *Journal of Climate* 21: 2072–2092.
- COPA-COGECA. 2003. Assessment of the impact of the heat wave and drought of the summer 2003 on agriculture and forestry. Fact sheets of the Committee of European heatwave – impacts Agricultural Organisations in the European Union and the General Committee for Agricultural Cooperation in the European Union. http://www.unisdr.org/files/1145_ewheatwave.en.pdf. Accessed 02/03/2018.
- Cowan T, Purich A, Perkins S, Pezza A, Boschat G, Sadler K. 2014. More frequent, longer, and hotter heat waves for Australia in the twenty-first century. *Journal of Climate* 27: 5851–5871.
- Davis RE, Knappenberger PC, Michaels PJ, Novicoff WM. 2003a. Changing heat-related mortality in the United States. *Environmental health perspectives*, 111: 1712–1718.
- Davis RE, Knappenberger PC, Novicoff, WM, Michaels PJ. 2003b. Decadal changes in summer mortality in US cities. *International Journal of Biometeorology* 47:166–175.

- Dayan U, Ziv B, Margalit A, Morin E, Sharon D. 2001. A severe autumn storm over the middle-east: Synoptic and mesoscale convection analysis. *Theoretical and applied climatology* 69: 103–122.
- Dee DP, et al. 2011. The ERA-Interim reanalysis: configuration and performance of the data assimilation system. *Quarterly Journal of the royal meteorological society* 137: 553–597.
- Donat MG, et al. 2014. Changes in extreme temperature and precipitation in the Arab region: long-term trends and variability related to ENSO and NAO. *International Journal of Climatology* 34: 581–592.
- Easterling DR, Meehl GA, Parmesan C, Changnon SA, Karl TR, Mearns LO. 2000. Climate extremes: observations, modeling, and impacts. *science*, 289: 2068–2074.
- Ebi KL. et al. 2004. Heat watch/warning systems save lives: Estimated costs and benefits for Philadelphia 1995–98. *Bulletin of the American Meteorological Society* 85: 1067–1073.
- Esteban P, Jones PD, Martin-Vide J, Mases M. 2005. Atmospheric circulation patterns related to heavy snowfall days in Andorra, Pyrenees. *International Journal of Climatology* 25: 319–329.
- Fennessy MJ, Kinter III JL. 2011. Climatic feedbacks during the 2003 European heat wave. *Journal of Climate* 24: 5953–5967.
- Ferranti L, Viterbo P. 2006. The European summer of 2003: sensitivity to soil water initial conditions. *Journal of Climate* 19: 3659–3680.
- Ferreira Braga AL, Zanobetti A, Schwartz J. 2001. The Time Course of Weather-Related Deaths. *Epidemiology* 12: 662–667.
- Feudale L, Shukla J. 2007. Role of Mediterranean SST in enhancing the European heat wave of summer 2003. *Geophysical Research Letters* 34. doi:10.1029/2006GL027991.
- Feudale L, Shukla J. 2011. Influence of sea surface temperature on the European heat wave of 2003 summer. Part I: an observational study. *Climate Dynamics* 36: 1691–1703.
- Fischer EM, Seneviratne SI, Lüthi D, Schär C. 2007a. Contribution of land-atmosphere coupling to recent European summer heat waves. *Geophysical Research Letters* 34: 1–6.
- Fischer EM, Seneviratne SI, Vidale PL, Lüthi D, Schär C. 2007b. Soil moisture–atmosphere interactions during the 2003 European summer heat wave. *Journal of Climate* 20:5081–5099.
- Folland CK, et al. 1999. Workshop on Indices and Indicators for Climate Extremes, Asheville, NC, USA, 3–6 June 1997 Breakout Group C: Temperature Indices for Climate Extremes. *Climatic Change* 42: 31–43.

- Fouillet A, et al., 2008. Has the impact of heat waves on mortality changed in France since the European heat wave of summer 2003? A study of the 2006 heat wave. *International Journal of Epidemiology* 37: 309–317.
- García ROC, Martínez AT, Ostos EJ. 2010. Heat waves and heat days in an arid city in the northwest of México: current trends and in climate change scenarios. *International Journal of Biometeorology* 54: 335–345.
- García-Herrera R, Díaz J, Trigo RM, Luterbacher J, Fischer EM. 2010. A review of the European summer heat wave of 2003. *Critical Reviews in Environmental Science and Technology* 40: 267–306.
- Gosling SN, Lowe JA, McGregor GR, Pelling M, Malamud BD. 2009. Associations between elevated atmospheric temperature and human mortality: a critical review of the literature. *Climatic Change* 92: 299–341.
- Guirguis K, Gershunov A, Tardy A, Basu, R. 2014. The impact of recent heat waves on human health in California. *Journal of Applied Meteorology and Climatology* 53:3–19.
- Habeeb D, Vargo J, Stone B. 2015. Rising heat wave trends in large US cities. *Natural Hazards* 76: 1651–1665.
- Hajat S, Kovats RS, Atkinson RW, Haines A. 2002. Impact of hot temperatures on death in London: a time series approach. *Journal of Epidemiology and Community Health* 56: 367–372.
- Hajat S, Kovats RS, Atkinson RW, Haines A. 2002. Impact of hot temperatures on death in London: A time series approach. *Journal of Epidemiology and Community Health* 56: 367–372.
- Handl J, Knowles J, Kell DB. 2005. Computational cluster validation in post-genomic data analysis. *Bioinformatics* 21: 3201–3212.
- Hansen J, Sato M. 2016. Regional climate change and national responsibilities. *Environmental Research Letters* 11: 034009.
- Harman JR, Winkler JA. 1991. Synoptic climatology: themes, applications, and prospects. *Physical Geography* 12: 220–230.
- Hyndman RJ, Fan Y. 1996. Sample Quantiles in Statistical Packages. *The American Statistician* 50: (4):361–365.
- IPCC (Intergovernmental Panel on Climate Change). 2001. Climate change: the scientific basis. In Contribution of Working Group I to the Third Assessment Report of the Intergovernmental Panel on Climate Change, Houghton JT, Ding Y, Griggs DJ, Noguer M, van der Linden PJ, Xiaosu D (eds). Cambridge University Press: Cambridge, UK, 944.

- IPCC. 2014. Climate Change 2014: Synthesis Report. Contribution of Working Groups I, II and III to the Fifth Assessment Report of the Intergovernmental Panel on Climate Change, Core Writing Team Pachauri RK, Meyer LA (eds.). IPCC, Geneva, Switzerland. pp 2.
- Karl TR, Knight RW. 1997. The 1995 Chicago heat wave: How likely is a recurrence?. *Bulletin of the American Meteorological Society* 78: 1107–1119.
- Katz RW, Brown BG. 1992. Extreme events in a changing climate: Variability is more important than averages. *Climatic Change* 21: 289–302.
- Kenawy AE, López-Moreno JI, Vicente-Serrano SM. 2013. Summer temperature extremes in northeastern Spain: spatial regionalization and links to atmospheric circulation (1960-2006). *Theoretical and Applied Climatology* 113: 387–405.
- Kenawy AM, McCabe M, Vicente-Serrano SM, Robaa SM, Lopez-Moreno JI. 2016. Recent changes in continentality and aridity conditions over the Middle East and North Africa region, and their association with circulation patterns. *Climate Research* 69: 25–43.
- Kent ST, McClure LA, Zaitchik BF, Smith TT, Gohlke JM. 2014. Heat Waves and Health Outcomes in Alabama (USA): The Importance of Heat Wave Definition. *Environmental Health Perspective*: DOI:10.1289/ehp.1307262.
- Klein Tank AMG, Zwiers FW, Zhang X. 2009. Guidelines on analysis of extremes in a changing climate in support of informed decisions for adaptation. *Climate data and monitoring WCDMPNo 72, WMO-TD No 1500*, 56.
- Kousky C. 2014. Informing climate adaptation: A review of the economic costs of natural disasters. *Energy Economics* 46: 576–592.
- Kyselý J, Plavcová E. 2012. Declining impacts of hot spells on mortality in the Czech Republic, 1986–2009: adaptation to climate change?. *Climatic change* 113: 437–453.
- Lee C, Sheridan S. 2015. Synoptic Climatology: An Overview. Reference Module in Earth Systems in Environmental Sciences. doi: 10.1016/B978-0-12-409548-9.09421-5.
- Lee TP, Silberberg SR, Boseart LF. 1988. A case study of a severe winter storm in the Middle East. *Quarterly journal of the Royal Meteorological Society* 114: 61–90.
- Lelieveld J, et al. 2012. Climate change and impacts in the Eastern Mediterranean and the Middle East. *Climatic Change* 114: 667–687.
- Lelieveld J, Proestos Y, Hadjinicolaou P, Tanarhte M, Tyrlis E, Zittis G. 2016. Strongly increasing heat extremes in the Middle East and North Africa (MENA) in the 21st century. *Climatic Change* 137: 245–260.
- Lioubimtseva E. 2004. Climate change in arid environments: revisiting the past to understand the future. *Progress in Physical Geography* 28: 502–530.

- Lord E, Willems M, Lapointe FJ, Makarenkov V. 2017. Using the stability of objects to determine the number of clusters in datasets. *Information Sciences* 393: 29–46.
- Mearns L, Katz R, Schneider S. 1984. Extreme high-temperature events: changes in their probabilities with changes in mean temperature. *Journal of Climate and Applied Meteorology* 23: 1601–1613.
- Medina-Ramon M, Schwartz J. 2007. Temperature, temperature extremes, and mortality: a study of acclimatisation and effect modification in 50 US cities. *Occupational and Environmental Medicine* 64: 827–833.
- Meehl GA, Tebaldi C. 2004. More intense, more frequent, and longer lasting heat waves in the 21st century. *Science* 305: 994–997.
- Met Office. 2013. European Heatwave (August 2003). <http://www.metoffice.gov.uk/education/teens/case-studies/heatwave>. Accessed 02/03/2018.
- Mohalifi S, Bedi HS, Krishnamurti TN, Cocke SD. 1998. Impact of shortwave radiative effects of dust aerosols on the summer season heat low over Saudi Arabia. *Monthly weather review*: 126: 3153–3168.
- Mora, C. et al., 2017. Global risk of deadly heat. *Nature Climate Change* 7: 501–506.
- Murtugudde R, Seager R, Thoppil P. 2007. Arabian Sea response to monsoon variations. *Paleoceanography* 22:1–17.
- Nairn JR, Fawcett RJB. 2015. The Excess Heat Factor: A Metric for Heatwave Intensity and Its Use in Classifying Heatwave Severity. *International Journal of Environmental Research and Public Health* 12: 227–253.
- Nasrallah HA, Nieplova E, Ramadan E. 2004. Warm season extreme temperature events in Kuwait. *Journal of Arid Environments* 56: 357–371.
- National Oceanic and Atmospheric Administration (NOAA): National Centers for Environmental Information (NCEI). <https://www.ncdc.noaa.gov/cdo-web>. Accessed 12 Nov 2016.
- Nazrul Islam, M. et al., 2015. Long-term changes in seasonal temperature extremes over Saudi Arabia during 1981-2010. *International Journal of Climatology* 35: 1579–1592.
- Oke TR, Grimmond CS, Spronken RA. 1998. On the confounding role of rural wetness in assessing urban effects on climate. *Preprints 2nd Second Urban Environment Symposium, AMS*: 59–62.
- Pal JS, Eltahir E A. 2015. Future temperature in southwest Asia projected to exceed a threshold for human adaptability. *Nature Climate Change* 6: 197–200.

- Perkins SE, Alexander LV. 2013. On the Measurement of Heat Waves. *Journal of climate* 26: 4500–4517.
- Perkins SE. 2015. A review on the scientific understanding of heatwaves—their measurement, driving mechanisms, and changes at the global scale. *Atmospheric Research* 164: 242–267.
- Pezza AB, Van Rensch P, Cai W. 2012. Severe heat waves in Southern Australia: synoptic climatology and large scale connections. *Climate Dynamics* 38: 209–224.
- Philipp A, Beck C, Huth R, Jacobeit J. 2016. Development and comparison of circulation type classifications using the COST 733 dataset and software. *International Journal of Climatology* 36: 2673-2691.
- Pielke, R. A. et al., 2002. Problems in evaluating regional and local trends in temperature: An example from eastern Colorado, USA. *International Journal of Climatology* 22: 421–434.
- Radinovic D, Curic M. 2012. Criteria for heat and cold wave duration indexes. *Theoretical and Applied Climatology* 107: 505–510.
- Raggad B. 2017a. Statistical assessment of changes in extreme maximum temperatures over Saudi Arabia, 1985–2014. *Theoretical and Applied Climatology*: 1–19.
- Raggad, B., 2017b. Stationary and Non-stationary Extreme Value Approaches for Modelling Extreme Temperature: the Case of Riyadh City, Saudi Arabia. *Environmental Modeling & Assessment*, pp.1–18.
- Rehman S, Al-Hadhrami LM. 2012. Extreme temperature trends on the west coast of Saudi Arabia. *Atmospheric and Climate Sciences* 2: 351–361.
- Rehman S, Al-Hadhrami LM. 2012. Extreme Temperature Trends on the West Coast of Saudi Arabia. *Atmospheric and Climate Sciences* 3: 351–361.
- Rehman S. 2010. Temperature and rainfall variation over Dhahran, Saudi Arabia (1970 to 2006). *International Journal of Climatology* 30: 445–449.
- Robeson SM, Doty JA. 2005. Identifying rogue air temperature stations using cluster analysis of percentile trends. *Journal of Climate* 18: 1275–1287.
- Robeson SM. 2002a. Increasing growing-season length in Illinois during the 20th century. *Climate Change* 52: 219–238.
- Robeson SM. 2002b. Relationships between mean and standard deviation of air temperature: Implications for global warming. *Climate Research* 22: 205–213.
- Robeson SM. 2004. Trends in time-varying percentiles of daily minimum and maximum temperature over North America. *Geophysical Research Letters* 31. doi:10.1029/2003GL019019

- Robinson PJ. 2001. On the Definition of a Heat Wave. *Journal of applied Meteorology* 40: 762–775.
- Rodwell MJ, Hoskins BJ. 1996. Monsoon and the dynamics of deserts. *Quarterly Journal of the Royal Meteorological* 122: 1385–1404.
- Rodwell MJ, Hoskins BJ. 2001. Subtropical anticyclones and summer monsoons *Journal of Climate* 14: 3192–3211.
- Russo S, et al. 2014. Magnitude of extreme heat waves in present climate and their projection in a warming world. *Journal of Geophysical Research: Atmospheres*, 119: 12500–12512.
- Russo S, Sillmann J, Fischer EM. 2015. Top ten European heatwaves since 1950 and their occurrence in the coming decades. *Environmental Research Letters* 10: 124003.
- Ryden J. 2016. A Statistical Analysis of Trends for Warm and Cold Spells in Uppsala by Means of Counts. *Geografiska Annaler: Series A, Physical Geography* 97: 431–436.
- Saudi General Authority for Meteorology and Environmental Protection. 2016. Environmental situation report: Kingdom of Saudi Arabia.
<https://www.mewa.gov.sa/ar/InformationCenter/Researchs/Reports/GeneralReports/%D8%AA%D9%82%D8%B1%D9%8A%D8%B1%20%D8%AD%D8%A7%D9%84%D8%A9%20%D8%A7%D9%84%D8%A8%D9%8A%D8%A6%D8%A9.pdf>. Accessed 24 April 2018.
- Saudi General Authority for Statistics. General Information about The Kingdom of Saudi Arabia.
<https://www.stats.gov.sa/en/page/170>. Accessed 24 April 2018
- Saudi Geological Survey. 2012. Kingdom of Saudi Arabia: facts and figures. Saudi Geological Survey, Jeddah, Saudi Arabia.
- Schär, C. et al., 2004. The role of increasing temperature variability in European summer heatwaves. *Nature* 427: 332–336.
- Seneviratne, S.I., et al. 2012: Changes in climate extremes and their impacts on the natural physical environment. In: *Managing the Risks of Extreme Events and Disasters to Advance Climate Change Adaptation* [Field, C.B., et al. (eds.)]. A Special Report of Working Groups I and II of the Intergovernmental Panel on Climate Change (IPCC). Cambridge University Press, Cambridge, UK, and New York, NY, USA, pp. 109–230.

- Sharif M. 2015. Analysis of projected temperature changes over Saudi Arabia in the twenty-first century. *Arabian Journal of Geosciences* 8: 8795–8809.
- Sheridan SC, Allen MJ, Lee CC, Kalkstein LS. 2012. Future heat vulnerability in California, Part II: projecting future heat-related mortality. *Climatic Change* 115:311–326.
- Smith EA. 1986a. The structure of the Arabian heat low. Part I: Surface energy budget. *Monthly Weather Review* 114: 1067–1083.
- Smith EA. 1986b. The structure of the Arabian heat low. Part II: Bulk tropospheric heat budget and implications. *Monthly weather review* 114: 1084–1102.
- Smith TT, Zaitchik BF, Gohlke JM. 2013. Heat waves in the United States: definitions, patterns and trends. *Climatic Change* 118: 811–825.
- Sokal RR, Rohlf FJ. 1962. The comparison of dendrograms by objective methods. *Taxon* 11:33–40. 10.2307/1217208.
- Souch C, Grimmond CSB. 2004. Applied Climatology: ‘heat waves’. *Progress in Physical Geography* 28: 599–606.
- Suseela V, Conant RT, Wallenstein MD, Dukes JS. 2012. Effects of soil moisture on the temperature sensitivity of heterotrophic respiration vary seasonally in an old-field climate change experiment. *Global Change Biology* 18: 336–348.
- Tebaldi C, Hayhoe K, Arblaster J, Meehl G. 2006. Going to the extremes: an intercomparison of model-simulated historical and future changes in extreme events. *Climatic Change* 79: 185–211.
- Teskey R, Wertin, T, Bauweraerts I, Ameye M, McGuire MA, Steppe K. 2015. Responses of tree species to heat waves and extreme heat events. *Plant, cell & environment*, 38:1699–1712.
- Tomczyk AM, Sulikowska A. 2017. Heat waves in lowland Germany and their circulation-related conditions. *Meteorology and Atmospheric Physics*: 1–17.
- Tsvieli Y, Abraham A. 2005. Synoptic climatology analysis of ‘wet’ and ‘dry’ Red Sea Troughs over Israel. *International Journal of Climatology* 25: 1997–2015.
- Unal Y, Kindap T, Karaca M. 2003. Redefining the climate zones of Turkey using cluster analysis. *International Journal of Climatology* 23: 1045–1055.
- Vautard et al. 2006. Summertime European heat and drought waves induced by wintertime Mediterranean rainfall deficit. *Geophysical Research Letters* 34. doi: 10.1029/2006GL028001.
- Vinayachandran PN. 2004. Summer cooling of the Arabian Sea during contrasting monsoons. *Geophysical Research Letters* 31: 1–4.

- Vrac M, Hayhoe K, Stein M. 2007. Identification and intermodel comparison of seasonal circulation patterns over North America. *International Journal of Climatology* 27: 603–620.
- Vries AJ, Tyrlis E, Edry D, Krichak SO, Steil B, Lelieveld J. 2013. Extreme precipitation events in the Middle East: dynamics of the Active Red Sea Trough. *Journal of Geophysical Research: Atmospheres* 118: 7087–7108.
- Vuong QH. 1989. Likelihood ratio tests for model selection and non-nested hypotheses. *Econometrica* 57: 307–333.
- Wang X, Smith K, Hyndman R. 2006. Characteristic-based clustering for time series data. *Data Mining and Knowledge Discovery* 13: 335–364.
- Warren Liao T. 2005. Clustering of time series data - A survey. *Pattern Recognition* 23: 1857–1874.
- Whan, K. et al., 2015. Impact of soil moisture on extreme maximum temperatures in Europe. *Weather and Climate Extremes* 9: 57–67.
- WMO (World Meteorological Organization). WMO examines reported record temperature of 54°C in Kuwait. <https://public.wmo.int/en/media/news/wmo-examines-reported-record-temperature-of-54%C2%B0c-kuwait>. Access 30 Jan 2017.
- Yang M, Cavanaugh JE, Zamba GK. 2015. State-space models for count time series with excess zeros. *Statistical Modelling* 15: 70–90.
- Yarnal B, Comrie AC, Frakes B, Brown DP. 2001. Developments and prospects in synoptic climatology. *International Journal of Climatology* 21: 1923–1950.
- Yarnal, B. 1993. Introduction to synoptic climatology. In: *Synoptic climatology in environmental analysis: a primer*. London: Belhaven Press, pp. 1-18.
- Zeileis A, Kleiber C, Jackman S. 2008. Regression models for count data in R. *Journal of Statistical Software* 27: 1–25.
- Zhang X, et al. 2005. Trends in Middle East climate extreme indices from 1950 to 2003. *Journal of Geophysical Research Atmospheres* 110: 1–12.
- Ziv B, Saaroni H, Alpert P. 2004. The factors governing the summer regime of the eastern Mediterranean. *International Journal of Climatology* 24: 1859–1871.
- Zolina O, Dufour A, Gulev SK, Stenchikov G. 2017. Regional Hydrological Cycle over the Red Sea in ERA-Interim. *Journal of Hydrometeorology* 18: 65–83.

Appendix A – Examples of different measurements and indices for extreme temperatures and heat waves

Table A.1. List of commonly used extreme temperature indices of ETCCDI. Modified after Athar at al. (2013).

Index ID	Index name	Index definition	Unit
FD0	Frost days	Annual (January 1–December 31) count when TN (daily minimum temperature) $<0^{\circ}\text{C}$	Day
SU25	Summer days	Annual count when TX (daily maximum temperature) $>25^{\circ}\text{C}$	Day
SU35	Summer days	Annual count when TX $>35^{\circ}\text{C}$	Day
ID0	Ice days	Annual count when TX $<0^{\circ}\text{C}$	Day
TR20	Tropical nights	Annual count when TN $>20^{\circ}\text{C}$	Day
TR25	Tropical nights	Annual count when TN $>25^{\circ}\text{C}$	Day
TXx	Max TX	Annual maximum value of TX	$^{\circ}\text{C}$
TNx	Max TN	Annual maximum value of TN	$^{\circ}\text{C}$
TXn	Min TX	Annual minimum value of TX	$^{\circ}\text{C}$
TNn	Min TN	Annual minimum value of TN	$^{\circ}\text{C}$
TXmean	Mean TX	Annual mean value of TX	$^{\circ}\text{C}$
TNmean	Mean TN	Annual mean value of TN	$^{\circ}\text{C}$
DTR	Diurnal temperature range	Monthly mean difference between TX and TN	$^{\circ}\text{C}$
TX10p	Cool days	Percentage of days when TX <10 th percentile	%
TX90p	Warm days	Percentage of days when TX >90 th percentile	%
TN10p	Cool nights	Percentage of days when TN <10 th percentile	%
TN90p	Warm nights	Percentage of days when TN >90 th percentile	%
WSDI	Warm spell duration indicator	Annual count of days with at least 6 consecutive days when TX >90 th percentile	Day
CSDI	Cold spell duration indicator	Annual count of days with at least 6 consecutive days when TN <10 th percentile	Day

Table A.2. Definitions of heat wave indices (HI). ^b Apparent temperature is a function of air temperature, humidity, wind speed, and solar radiation. ^c The HI is a function of air temperature and humidity, parameterized to take account of other environmental factors. Modified after Kent et al. (2014).

HI	Definition
HI01	Mean daily temperature > 95th percentile for ≥ 2 consecutive days
HI02	Mean daily temperature > 90th percentile for ≥ 2 consecutive days
HI03	Mean daily temperature > 98th percentile for ≥ 2 consecutive days
HI04	Mean daily temperature > 99th percentile for ≥ 2 consecutive days
HI05	Minimum daily temperature > 95th percentile for ≥ 2 consecutive days
HI06	Maximum daily temperature > 95th percentile for ≥ 2 consecutive days
HI07	Maximum daily temperature ≥ 81 st percentile every day, ≥ 97.5 th percentile for ≥ 3 nonconsecutive days, and consecutive day average ≥ 97.5 th percentile
HI08	Maximum daily apparent temperature ^b > 85th percentile for ≥ 1 day
HI09	Maximum daily apparent temperature ^b > 90th percentile for ≥ 1 day
HI10	Maximum daily apparent temperature ^b > 95th percentile for ≥ 1 day
HI11	Maximum daily temperature > 35°C (95°F) for ≥ 1 day
HI12	Minimum daily temperature > 26.7°C (80.1°F) or maximum daily temperature > 40.6°C (105.1°F) for ≥ 2 consecutive days
HI13	Maximum daily heat index ^c > 80°F for ≥ 1 day
HI14	Maximum daily heat index ^c > 90°F for ≥ 1 day
HI15	Maximum daily heat index ^c > 105°F for ≥ 1 day
HI16	Maximum daily heat index ^c > 130°F for ≥ 1 day

Table A.3. Definitions of heat wave indices (HI). Modified after Smith et al. (2013).

HI	Temperature metric	Threshold	Duration	Type
HI01	Mean daily temperature	>95th percentile	2+ consecutive days	Relative
HI02	Mean daily temperature	>90th percentile	2+ consecutive days	Relative
HI03	Mean daily temperature	>98th percentile	2+ consecutive days	Relative
HI04	Mean daily temperature	>99th percentile	2+ consecutive days	Relative
HI05	Minimum daily temperature	>95th percentile	2+ consecutive days	Relative
HI06	Maximum daily temperature	>95th percentile	2+ consecutive days	Relative
HI07	Maximum daily temperature	T1: >81st percentile T2: >97.5th percentile	Every day, >T1; 3+ consecutive days, >T2; Mean Tmax>T1 for whole time period	Relative
HI08	Maximum daily apparent temperature	>85th percentile	1 day	Relative
HI09	Maximum daily apparent temperature	>90th percentile	1 day	Relative
HI10	Maximum daily apparent temperature	>95th percentile	1 day	Relative
HI11	Maximum daily temperature	>35°C	1 day	Relative
HI12	Minimum & maximum daily temperature	Tmin>26.7°C Tmax>40.6°C	≥1 threshold for 2+ consecutive days	Absolute
HI13	Maximum daily heat index	>80°F	1 day	Absolute
HI14	Maximum daily heat index	>90°F	1 day	Absolute
HI15	Maximum daily heat index	>105°F	1 day	Absolute

Appendix B – Statistical characteristics of maximum and minimum temperatures

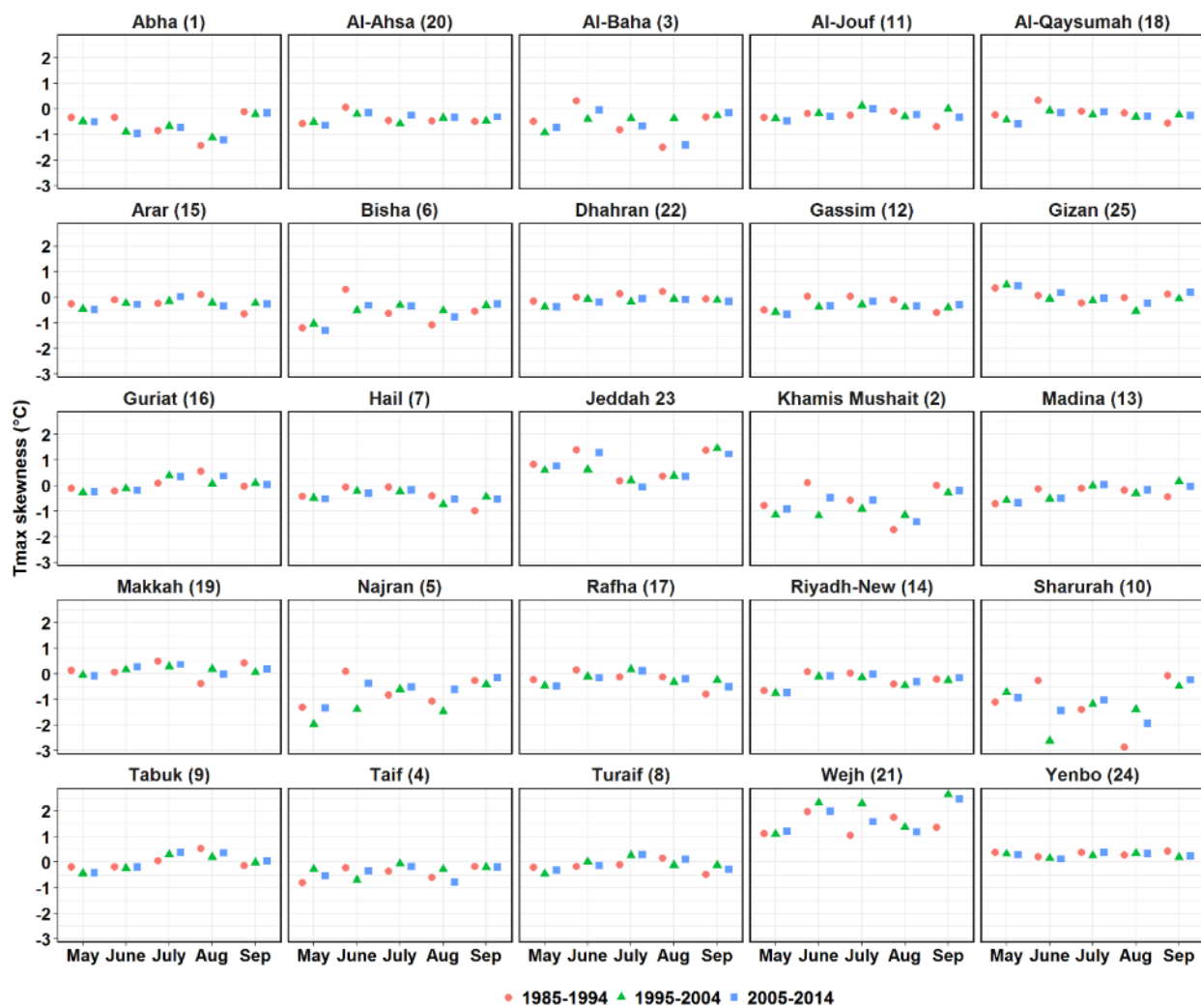


Figure B.1. Multi-decadal variation in Tmax skewness at warm-season-monthly time scale.

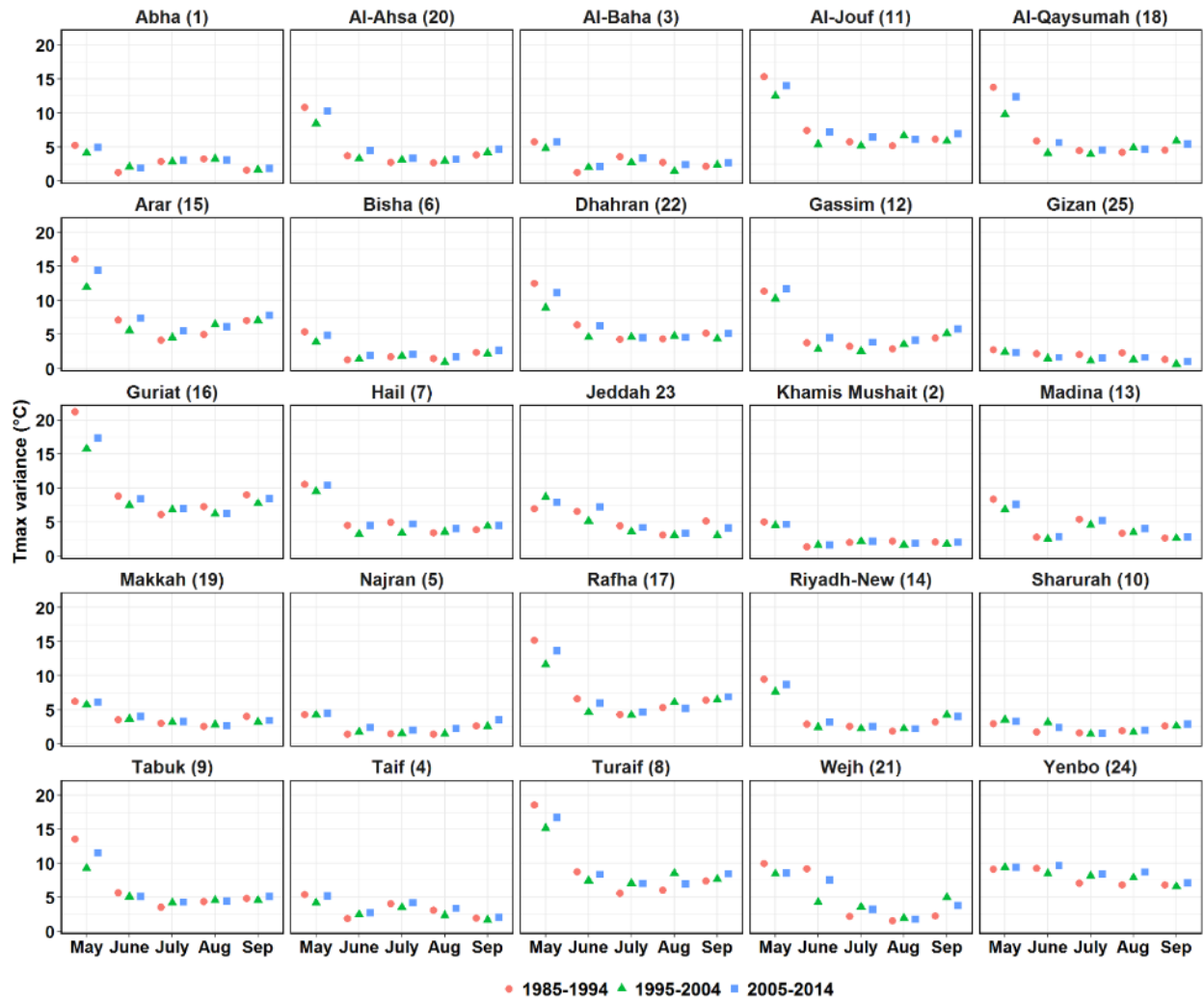


Figure B.2. Multi-decadal variation in Tmax variance at warm-season-monthly time scale.

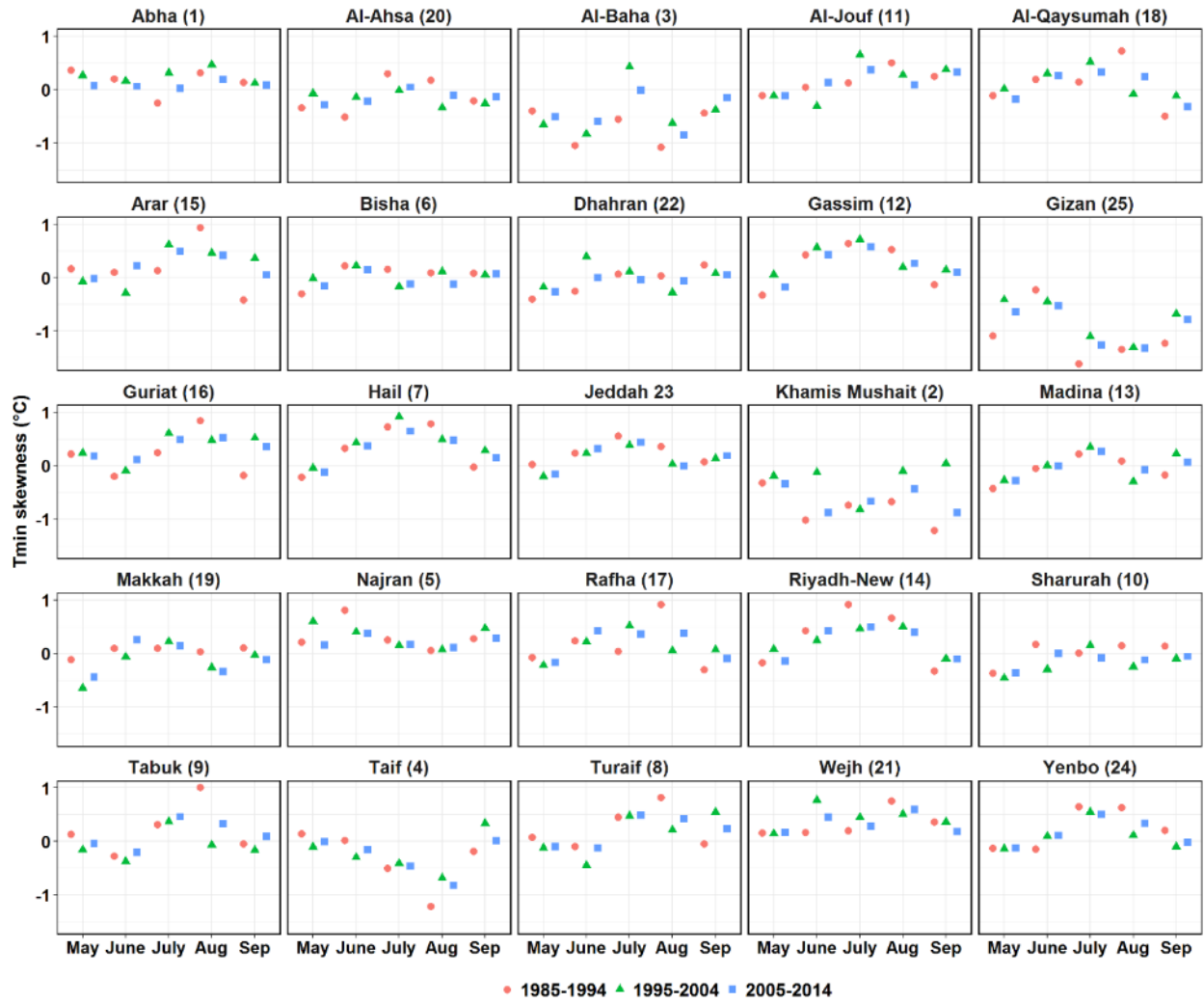


Figure B.3. Multi-decadal variation in Tmin skewness at warm-season-monthly time scale.

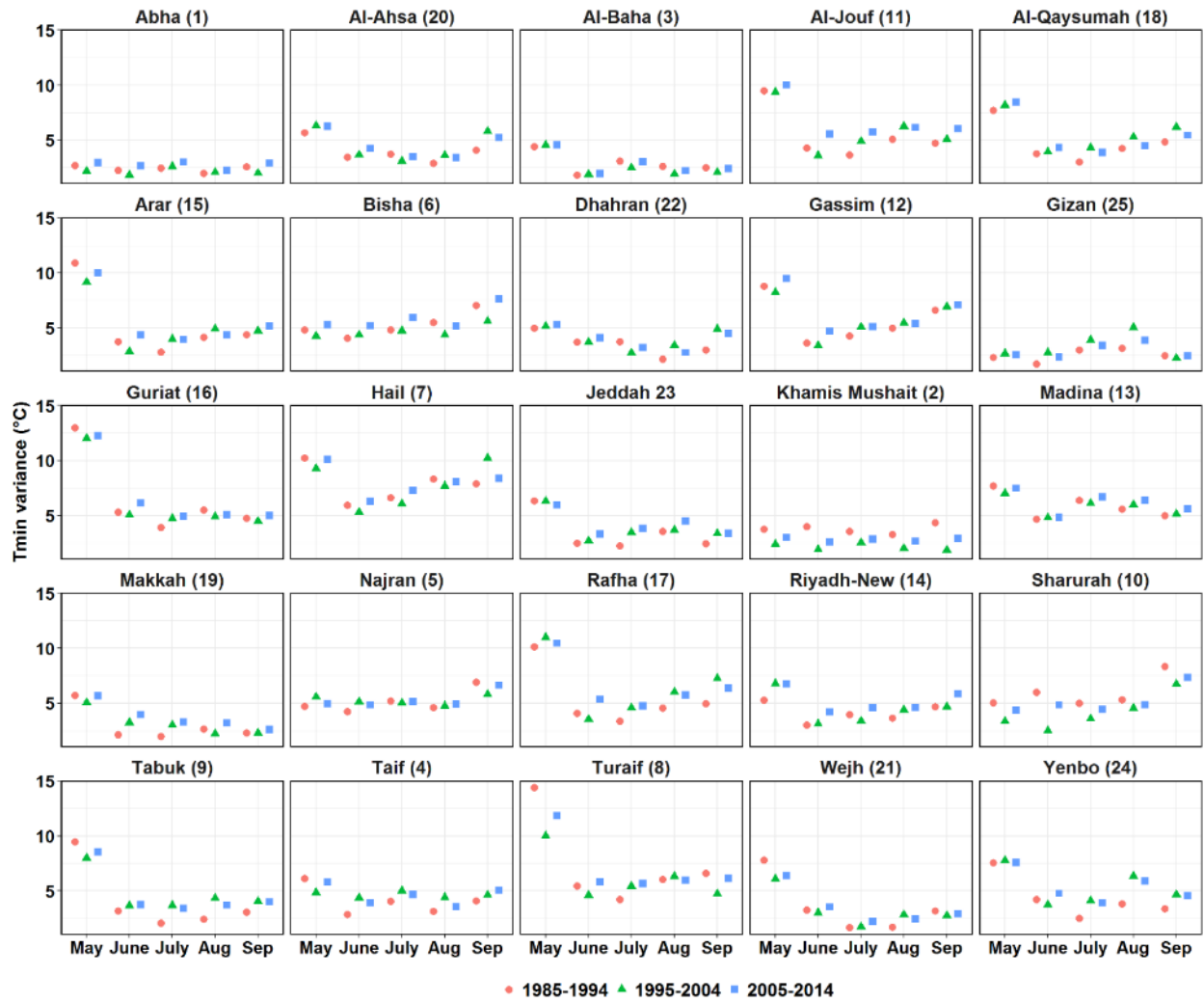


Figure B.4. Multi-decadal variation in Tmin variance at warm-season-monthly time scale.